Physiological and cell biological characterisation of two novel membrane proteins in *Arabidopsis thaliana*

by

Maria Papanatsiou

Thesis submitted in fulfillment of the requirements for the Degree of Master of Science (by research)

Institute of Molecular, Cell and Systems Biology
School of Life Sciences
University of Glasgow
April 2011

Abstract

This thesis describes the characterisation of *AtPQL4* and *AtPQL6*, two members of a hitherto uncharacterized gene family of *A. thaliana* with six members, *AtPQL1-6*. As their counterparts in other species and kingdoms *At*PQL proteins contain seven transmembrane domains and two copies of the so-called 'PQ-loop' domain. *At*PQL4 and *At*PQL6 show high amino acid sequence identity between each other and they are the closest *A. thaliana* homologues of the mammalian LEC35/MPDU1 protein, which has been shown to be required for all types of Man-P-Dol dependent glycosylation in the ER.

To address the functional homology between the two *At*PQL proteins and MPDU1, the sub-cellular localisation of *At*PQL4-GFP and *At*PQL6-GFP fusion proteins was investigated. Confocal laser scanning microscopy analysis of *Nicotiana tabacum* leaf cells expressing *At*PQL4-GFP or *At*PQL6-GFP showed fluorescence patterns typical for ER. ER localisation of *At*PQL4 and AtPQL6 was further confirmed by co-expression with the ER marker, YFP-HDEL.

A second set of experiments employed YFP-fusion proteins of AtSYP121, a plasma membrane SNARE protein, and AtTIP2, a tonoplast aquaporin. Confocal microscopy confirmed plasma membrane/tonoplast localisation of the YFP proteins when expressed on their own in tobacco leaf cells. However, both proteins were found to be retained in the ER when co-expressed with *At*PQL4-GFP or *At*PQL6-GFP fusion proteins. These new findings point to a role of *At*PQL4 and *At*PQL6 in protein processing in the ER thereby enforcing previous results from microarray experiments indicating ER-stress in *At*PQL4 and *At*PQL6 mutants.

Finally, a number of *AtPQL4* and *AtPQL6* knockout and *AtPQL6* overexpressor lines were tested under a variety of environmental stresses to investigate the function of the two *At*PQLs at whole-plant level. Low sucrose conditions resulted in growth inhibition of mutants compared to wild type plants. Considering previous findings that (a) *At*PQL4 and *At*PQL6 are localised in the ER (b) ATPQL mutants show differential expression of genes involved in the unfolded protein response (UPR) and (c) over-expression of *At*PQL4 and *At*PQL6 impacts on the targeting of other proteins, the observed phenotype could be linked to the unfolded protein response and autophagy that occurs during sugar starvation..

In conclusion, it is proposed that *At*PQL4 and *At*PQL6 proteins function in retaining membrane proteins for sufficient time in the ER to allow ER-quality control and related processes to take place. Further experiments to investigate such function are discussed.

Table of Contents

List of Figures and Tables

Author's declaration

I declare that, except where explicit reference is made to the contribution of others, that this dissertation is the result of my own work and has not been submitted for any other degree at the University of Glasgow or any other institution.

Maria Papanatsiou, April 2011

Acknoweledgments

I am grateful to my supervisor, Dr. Anna Amtmann, whose guidance, advice as well as expertise added considerably to all the levels of this project. I am also greatly thankful to all members of the Stevenson lab whose help and friendship is invaluable to me. Especially, I want to thank Naomi Donald for her assistance in general laboratory issues. Dr. Christopher Grefen and Cornelia Eisenach for their advice on cloning and plant transformation, Amparo Ruiz-Prado for collecting seeds and Annegret Honsbein for her patience and the thorough discussions.

I am also thankful to my family for supporting me and helping me financially with my studies. Finally, I want to thank Aris who has given me constant emotional and moral support for the last seven years, and especially for his patience during this project.

Abbreviations

ALG3	Asparagine-linked glycosylation 3
AKT1	Arabidopsis K^+ transporter 1
Asn	Asparagine
ATG	Autophagy
ATP	Adenosine triphosphate
BiFC	Bimolecular fluorescent complex
BiP	Binding protein
CaMV	Cauliflower mosaic virus
CHO	Chinese hamster ovary
CNX	Calnexin
Col0	Columbia 0
ConA	Concanavalin A
COP	Coat proteins
CRT	Calreticulin
Cs	Castanospermine
CTNS	Cystinosin
Cys	Cysteine
DTT	Dithiothreitol
Dedol-P-P	Dehydrodolichol pyrophosphate
DEPC	Diethyl pyrocarbonate
DNA	Deoxyribonucleic acid
dNTP	deoxyribonucleotid triphosphate
Dol	Dolichol
Dol-P	Dolichol monophosphate
DPS	Dehydrodolichol pyrophosphate synthase
EFR	EF-Tu receptor
elf18	Elfin 18
ER	Endoplasmic reticulum
ERAD	ER associated degradation
ERD2	ER retention defective 2
ERES	ER exit sites
ERS1	*erdΔ* suppressor 1
FACE	Fluorophore-assisted carbohydrate electrophoresis
fls22	flagellin 22
FLS2	Flagellin sensitive 2
FPP	Farnesyl diphosphates
GAG	Glycosaminoglycans
Gal	Galactose
GalNAc	N-acetylgalactosamine
gDNA	genomic DNA
GDP	Guanosine diphosphate
GDP-Man	Guanosine diphosphate-mannose
GFP	Green fluorescent protein
Glc	Glucose
GlcA	Glucuronic acid
GlcNAc	N-acetylglucosamine
Glc-P-Dol	Glucose-phosphate-dolichol
GPCR	G-protein coupled receptor
GPI	Glycophosphatidylinositol
GPP	Geranyl diphosphates
G-protein	Guanine nucleotide binding protein
GPT	GlcNAc phosphotransferase
GT	UDP-Glc:glycoprotein glycosyltransferase
GTP	Guanosine triphosphate
HPLC	High performance liquid chromotography
IPP	Isopentenyl diphosphates
Ire1	Inostol-required 1
KAT1	K^+ transporter of *Arabidopsis thaliana* 1
KC1	K^+ rectifying channel 1
LB	Luria Bertani
LEW1	Leaf wilting 1
LLO	Lipid-linked oligosaccharide
LTP	Lipid transfer proteins
Man	Mannose
Man-P-Dol	Mannose-phosphate-dolichol
Memb11	Membrin 11
MIP	Membrane intrinsic proteins
MPDU1	Man-P-Dol utilisation defect 1
mRNA	messenger RNA
MS	Murashige and Skoog
OD_{600}	Optical density at 600 nm
OST	OligoSaccharylTransferase
p35S	CaMV 35S promoter
PAS	Pre-autophagosome
PCR	Polymerase chain reaction
PDI	protein disulfide isomerase
PI	Phosphatidylinositol
PMM	phosphomannomutase
PQ	proline-glutamine
PQL	PQ-loop repeat
PR	Pathogenesis related
pUBQ10	*Ubiquitin10* promoter
QC	Quality control
qPCR	Quantitative polymerase chain reaction
rDNA	Ribosomal deoxyribonucleic acid
RNA	Ribonucleic acid
RNase	Ribonuclease

SAR	Systemic-acquired resistance
Sec22	Secretion 22
Ser	Serine
SNAP33	Soluble N-ethylmaleimide-Sensitive factor Adaptor Protein 33
SNARE	Soluble N-ethylmaleimide-Sensitive fusion proteins Attachment protein receptor
ST	α-2,6-sialyltransferase
STM1	Seven transmembrane 1
SYP121	Syntaxin of Plants 121
Sw	swainsonine
T-DNA	transferred DNA
Thr	Threonine
TIP	Tonoplast intrinsic proteins
Trp	Tryptophan
UDP	uridine diphosphate
UDP-Glc	Uridine diphosphate-glucose
UDP-GlcNAc	Uridine diphosphate-N-acetylglucosamine
UDP-Man	Uridine diphosphate-mannose
UGGT	UDP-glucose:glycoprotein glucosyltransferase
UPR	Unfolded protein response
UTR	Untranslated Region
Utr1	UDP-glucose/galactose transporter 1
VAMP722	Vesicle-associated protein 722
XET	xyloglucan endotransglycosylase
YFP	Yellow Fluorescent Protein

Chapter 1: General introduction

A novel family of *Arabidopsis thaliana*, named "PQ-loop repeat" (PQL) was characterised by Richard Pattison (PhD thesis, 2008, University of Glasgow). The *At*PQL gene family consists of six members, *At*PQL1-6, and is characterised by the presence of the PQ-loop domain. The objective of this project was the functional characterisation of two of the *At*PQL proteins, *At*PQL4 and *At*PQL6. In this chapter I will describe what is known for the *At*PQL family from the work carried out by Pattison (2008). In addition, I will review existing literature on yeast and mammalian PQL proteins that show high sequence identity and/or potential functional similarity with *At*PQL proteins, especially with *At*PQL4 and *At*PQL6.

1.1 Structural features of *At*PQL proteins

Six genes encoding *At*PQL proteins are present in the *Arabidopsis* genome, *AtPQL1* (At4G20100), *AtPQL2* (At2g41050), *AtPQL3* (At4g36850), *AtPQL4* (At5g59470), *AtPQL5* (At5g40670) and *AtPQL6* (At4g07390). The *At*PQL proteins have two copies of the defining PQ-loop domain. The PQ-loop domain is a region of 40-60 amino acids including the highly conserved proline-glutamine (PQ) motif. Hydropathy analysis of each *At*PQL protein showed that they are integral membrane proteins with seven transmembrane domains and a N-terminus facing the non-cytoplasmic side of the membrane. The seven transmembrane domains are a common characteristic of all PQL proteins identified so far (Hardwick and Pelham, 1990; Anand *et al*., 2001; Chung *et al*., 2001; Kalatzis *et al*., 2001). In addition, hydropathy analysis showed that the PQ-loop domain usually spans two transmembrane domains and consists of two hydrophobic regions surrounding a hydrophilic core. The significance of PQ-loop is not yet clear, but it is suggested to constitute a way of forming the transmembrane domains of proteins. All *At*PQL proteins contain a conserved PQ motif at position 22-23 of the PQ-loop domain. It was found that the PQ motif is close to the transition region of the transmembrane and non-transmembrane domain. It might facilitate the change in direction of the polypeptide chain, as proline has the ability to bind the amino acid chain twice (Betts and Russell, 2003). Nevertheless, mutations in residues within the PQ-loop have suggested an additional role for the PQ-loop (discussed below). The alignment of full-length *At*PQL amino acid sequences with other known non-plant PQL proteins led to the separation of *At*PQL proteins into three sub-groups. Figure 1.2 represents a phylogenetic tree showing the

relationship between the *At*PQL and PQL proteins from other species and the domain organization of each of the proteins. Sub-group 1 contains *At*PQL1, *At*PQL2 and *At*PQL3, sub-group 2 contains *At*PQL4 and *At*PQL6 and sub-group 3 is defined by *At*PQL5. The *AtPQL* genes are found throughout the genome, with *AtPQL2* being on chromosome 2, *AtPQL1*, *AtPQL3* and *AtPQL6* on chromosome 4 and *AtPQL4* and *AtPQL5* on chromosome 5. The *AtPQL* genes also differ in intron-exon organisation, *AtPQL1* contains no introns while its closest homologues *AtPQL2* and *AtPQL3* have 11 and 10 introns, respectively.

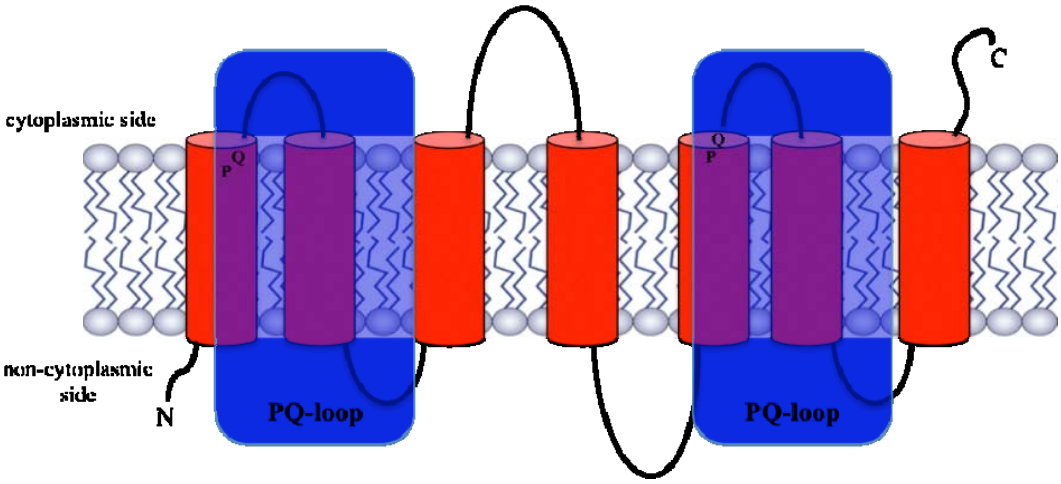

Figure 1.1: Predicted topology of PQL proteins.

PQL proteins are integral membrane proteins. They contain seven transmembrane domains and two PQ-loop domains. The PQ-loop domains typically span two transmembrane domains with the conserved PQ situated at the interface between the cytoplasmic loop and the second transmembrane domain.

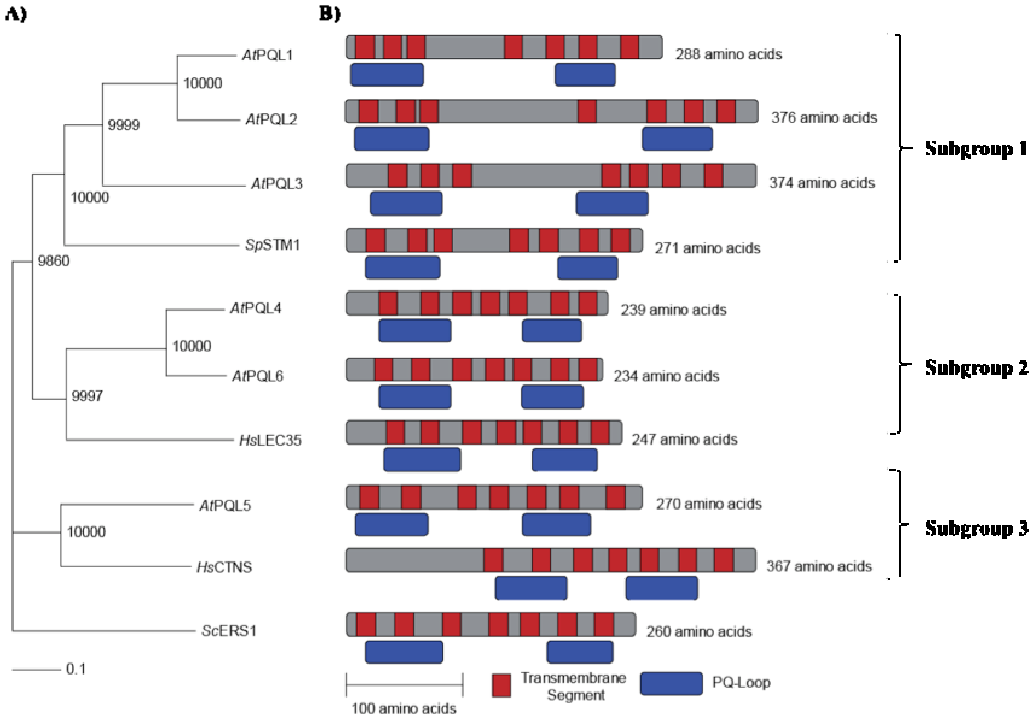

Figure 1.2: Classification of *At*PQL proteins in three different subgroups.

A) Phylogenetic tree shows the relationship between the *At*PQL1-6 proteins and PQL proteins characterised in other eukaryotes. The tree was created from full-length sequence alignements of selected PQL proteins. Node numbers indicate bootstrap values. **B)** The distribution of the domains for each PQL protein and number of amino acids is also shown. Transmembrane domains are shown in red color, while PQ-loop domains are shown blue color (Figure taken form Pattison, 2008).

1.2 *At*PQL1, *At*PQL2, *At*PQL3 and *STM1*

The sub-group 1 proteins *At*PQL1-3 show high sequence identity with a PQL protein, STM1, from the fission yeast *Schizosaccharomyces pombe*. STM1 has been proposed to act as a G-protein coupled receptor (GPCR) and was implicated in the control of cell cycle under nitrogen-deficient conditions. It is suggested that nitrogenous signals may bind to STM1 resulting in its activation through structural changes and therefore facilitating its interaction with heterotrimeric protein Gpa2. Gpa2 is involved in sexual differentiation in response to poor nutritional conditions (Chung *et al.*, 2001). This interaction occurs through the C-terminal region of STM1 that contains a putative Gpa2 binding site of 7-8 residues within the second PQ-loop. Site-directed mutagenesis in the binding site revealed a lysine residue at position 199 to be important for the function of STM1. A Gpa2 binding site is absent in the *At*PQL1-3 proteins.

Transcriptional profiling by Pattison (2008) showed that *AtPQL1* and *AtPQL2* have similar expression patterns and were strongly expressed in floral tissues. *AtPQL2* was also found

in rosette leaves and roots, though in much lower amounts. In contrast, *AtPQL3* showed higher mRNA levels than *AtPQL1* and *AtPQL2*, with highest expression in root tissues. Despite the overlapping expression profiles of *AtPQL1* and *AtPQL2*, both genes exhibited temporal differences of expression. *AtPQL1* showed peak expression in developing pollen whereas *AtPQL2* was more strongly expressed in mature pollen. Transient expression of *At*PQL1-GFP fusion protein in epidermal cells of *Nicotiana tabacum* indicated localisation to the tonoplast. No co-localisation data were obtained for *At*PQL2 and *At*PQL3 proteins. Pattison (2008) argued that a tonoplast localisation might not exclude a GPCR function of *At*PQL1 as its N-terminus faces the vacuolar lumen where it could interact with the only identified *Arabidopsis* Ga subunit, GPA1. Such interaction could take place at points where the tonoplast and plasma membrane are in close contact. Huang *et al*. (2006) reported interaction of GPA1 with THF1, a plastid localised protein, at points where the plastid membrane is in very close proximity to the plasma membrane. GPA1 is expressed throughout development in almost all tissues, with the exception of mature seeds and mature pollen (Weiss *et al*., 1993). It is therefore unlikely that *At*PQL2, which is highly expressed in mature pollen, interacts with GPA1. Single knockout lines of *AtPQL1* and *AtPQL3* and overexressors of *AtPQL1*, *AtPQL2* and *AtPQL3* did not show a phenotype different from wild type (Col0) when grown on soil or in different nutrient conditions (Pattison, 2008).

1.3 *At*PQL5 and cystinosin

Human cystinosin (*CTNS*) is the closest homologue of *AtPQL5* with 29.9% sequence identity at the amino acid level. CTNS is the only member of the PQL protein for which a function has been established at the molecular level. CTNS is a human H^+-driven transporter, mediating the efflux of cystine from lysosomes (Kalatzis *et al*., 2001). Cystine is the disulfide form of the amino acid cysteine (cys) and is a by-product of lysosomal protein hydrolysis. Cystine is exported into the cytosol, where it is reduced to cys (Gahl *et al*., 2002). Mutations in *CTNS* result in cystinosis, an inherited lysosomal storage disease. Defective cystine efflux leads to cystine accumulation inside lysosomes where reduction to cys cannot take place (Kalatzis *et al*., 2004). CTNS is one of the PQL proteins that is affected in its function by mutations in the PQ-loop. 16 different point mutations leading to clinical symptoms have been shown to fall within the two PQ-loops of CTNS (Attard *et al*., 1999; Kalatzis *et al*., 2001; Kalatzis *et al*., 2004). Most of these mutations affected the cys transport activity of CTNS and not its localisation.

Based on expression profiling (Pattison, 2008) *AtPQL5* appears to be the most strongly expressed member of the *At*PQL family. Expression was apparent in all tissues, with highest transcript levels occurring in open flowers. In addition, *AtPQL5* showed diurnal changes in expression, as transcript level was highest in the middle of the day, in both short and long days. This finding might argue against a function of *At*PQL5 in cys production, as other genes involved in the cys production are more expressed at the end of the night to provide sufficient cys for sulfur metabolism in the morning (Saito *et al*., 2004). Similar to what was observed for the subgroup 1 PQL proteins, *AtPQL5* was highly expressed in pollen and exhibited strong changes in expression level during pollen development. Sub-cellular localisation experiments suggested that *At*PQL5 also localises to the tonoplast (Pattison, 2008). This is in agreement with a similar function to CTNS, which is localized to the lysosome. Lysosomes are small organelles containing a plethora of hydrolytic enzymes and they are responsible for the degradation macromolecules derived from extracellular environment through endocytosis or from the cytosol through autophagy (Sun-Wada *et al*., 2003). In plants, the vast majority of hydrolytic activity resides inside the vacuoles. However, vacuoles have additional functions such as storage of ions and various metabolites, control of osmotic pressure and detoxification (Marty, 1999). Given the localisation of *At*PQL5, a CTNS-like function of *At*PQL5 could be possible. In plants, the reduction of cystine to cys is essential, as cys is a key intermediate for sulfur metabolism (Saito *et al*., 2004). However, *AtPQL5* knockout mutants did not show a phenotype when grown in low sulphur conditions (Pattison, 2008). The *ers1Δ* mutant disrupted in the yeast PQL gene *ERS1*, is sensitive to hygromycin (Gao *et al*., 2005). Expression of CTNS in the *ers1Δ* mutant resulted in increased hygromycin tolerance. However, functional complementation was not observed for any of the *At*PQL proteins expressed in *ers1Δ*, suggesting either a function different from CTNS or a loss of function due to heterologous expression.

1.4 AtPQL4, AtPQL6 and MPDU1

An alignment of *At*PQL4 and *At*PQL6 full amino acid sequence showed 74% identity between the two proteins. *AtPQL4* and *AtPQL6* genes displayed similar expression patterns with little variation in transcript level between different tissues (Pattison, 2008). *AtPQL4* was more strongly expressed in open flowers, while *AtPQL6* showed peak expression in floral buds. In addition, *AtPQL4* and *AtPQL6* genes showed diurnal changes

in expression. In both short and long days, the transcript levels were increased throughout the course of the day and reached a maximum at the end of the day. Experiments using green fluorescent protein (GFP)-tagged *At*PQL4 and *At*PQL6 suggested localisation to the endoplasmic reticulum (ER), as GFP fluorescence was observed in net-like structures (Pattison, 2008).

Transcriptional profiling of mutant lines for *AtPQL4* and *AtPQL6* genes as well as an overexpressor line for *AtPQL6* gene showed differential expression of genes in the mutant lines compared to wild type. The differentially expressed genes could be classified into three main groups. The first group includes pathogenesis related (*PR*) genes and genes involved in cell-wall modification, such as lipid transfer proteins (LTPs), xyloglucan endotransglycosylase (XET) and glycosylphosphatidylinositol (GPI) anchored proteins. *PR* genes are induced in response to pathogen infection and encode proteins with various functions (Van Loon *et al*., 2006). *PR-1* was up-regulated in both knockout and overexpressor lines for *AtPQL6*. *PR-2* was up-regulated in all knockout lines, while down-regulated in the *AtPQL6* overxpressor line. Opposite changes in knockout and oxerexpressor lines were also observed for several LTPs the cell-wall modification associated gene *XTR7*. Members of the COBRA family were up-regulated in *AtPQL6* knockout plants. All 12 members of the COBRA family encode GPI anchored proteins with a regulatory role in the deposition of cellulose microfibrils thus controlling the direction of cell wall expansion (Roudier *et al*., 2002). The second group of differentially expressed genes consists of lipid metabolism and ER stress-related genes. Several genes involved in lipid metabolism were differentially regulated in *AtPQL4* and *AtPQL6* mutants. The most interesting observation was the down-regulation in the *AtPQL4* knockout of a *DPS*-like gene, which encodes for a dehydrodolichol pyrophosphate (dedol-P-P) synthase that is responsible for the synthesis of dedol-P-P (Cunillera *et al*., 2000). Dedol-P-P is a precursor molecule of dolichol-pyrophosphate (Dol-P-P), which is the lipid acceptor of sugars in the synthesis of lipid-linked oligosaccharides (LLO) during N-glycosylation in the ER. ER stress results from accumulation of unfolded proteins in the ER and is accompanied by increased expression of a number of genes implicated in the unfolded protein response (UPR) (Liu and Howell, 2010), such as the binding protein (*BiP*), the protein disulfide isomerase (*PDI*), calnexin (*CNX*) and calreticulin (*CRT*). *BiP3*, one of the three *A. thaliana BiP* genes, was up-regulated in both *AtPQL6* knockout and overexpressing lines. The *UTr1* gene was also up-regulated in the *AtPQL6* overexpressing line. UTr1 is a UDP-glucose transporter that supplies glucose to the CNX/CRT cycle for the making of incorrectly folded proteins (Reyes *et al*., 2009). The third group contains

genes encoding N-glycoproteins and proteins targeted to the secretory pathway. Such proteins were over-represented among the differentially expressed genes in the *AtPQL* knockout lines, and under-represented in the *AtPQL6* overexpressor line.

Full-length alignments of amino acid sequence showed 29.3% and 30.4 % identity of *AtPQL4* and *AtPQL6* respectively with the mannose-phosphate-dolichol utilisation 1 (*MPDU1*) gene from humans. The three proteins show similar organisation of the seven transmembrane and the PQ-loop domains. LEC35/MPDU1 has been shown to be required for the utilization of dolichol-phosphate (Dol-P) linked sugars in different types of glycosylation processes (Anand *et al*., 2001, see below). Mutations in *MPDU1* and similar genes cause congenital disorders of glycolsylation (Kranz *et al*., 2001; Schenk *et al*., 2001; Koiwa *et al*., 2003).

1.5 Synthesis of Dol-P linked sugars

Glycosylation is a post-translational modification of proteins that is highly conserved in all eukaryotes. There are five different types of glycosylation, N-glycosylation, O-glycosylation, P-glycosylation, C-mannosylation and GPI anchoring, differing in the sugar-amino acid bond formed, all of which are initiated in the ER and Golgi. The first steps of N-glycosylation, C-mannosylation and GPI in the ER depend on mannose-phosphate-dolichol (Man-P-Dol) and glucose-phosphate-dolichol (Glc-P-Dol) (Spiro *et al*., 2002). In addition, a special type of O-glycosylation, known as O-mannosylation, is dependent on Man-P-Dol. In this chapter I will describe only those types of glycosylation that are dependent on Man-P-Dol.

Dolichols are long-chain polyisoprenoid lipids comprising 15 to 23 isoprenic units depending on the organism. Biosynthesis of dolichols involves formation of geranyl (GPP) and farnesyl (FPP) diphosphates through the mevalonate pathway (Swiezewskaa and Danikiewiczb, 2005). Elongation of the polyisoprenoids is catalyzed by *cis*-prenyltransferases that add isopentenyl diphosphates (IPPs) onto FPP. The *lew1* mutant of *A. thaliana* is defective in a gene encoding a *cis*-prenyltranferase. *lew1* plants show a hypersensitive response to tunicamycin and have altered levels of glycosylation (Zhang *et al*., 2008). Newly synthesized Dol-P is available for synthesis of Man-P-Dol and Glc-P-Dol that are required for glycosylation. This process takes place on the cytoplasmic side of the ER and is mediated by Dol-P- mannosyltransferase and Dol-P-glusosyltransferase

using the nucleotide sugar donors, UDP-Man and UDP-Glc, respectively (Helenius *et al*., 2002). Both Man-P-Dol and Glc-P-Dol require re-orientation in the ER membrane to be available for glycosylation-associated enzymes residing in ER lumen. Experiments using water-soluble analogues of Man-P-Dol and Glc-P-Dol suggested that translocation into ER sealed vesicles requires the involvement of so-called flippases (Schenk *et al*., 2001a). However, this remains to be identified.

1.6 Protein glycosylation in the ER

N-glycosylation of proteins is catalysed by the oligosaccharyltransferase (OST) complex in the ER lumen, where the LLO synthesized in the ER membrane is transferred to asparagine (Asn) residues of a strict consensus sequence Asn-X-Ser/Thr, with X being every amino acid except proline (Spiro *et al*., 2002, Koiwa *et al*., 2003). Several mutants defective in this process have been identified in plants. For instance, knockout of *STT3a* but not *STT3b* results in a salt sensitive phenotype in *A. thaliana* (Koiwa *et al*., 2003). The genes are homologues of yeast STT3 subunit of OST enzyme. Although single mutants are viable, double mutants of *stt3a/stt3b* show a gametophytic lethal phenotype. It was suggested that the two genes are redundant. At least the STT3a is involved in glycosylation, as *stt3a* mutants display decreased levels of glycosylation of proteins (Koiwa *et al*., 2003).

A schematic representation of all the steps of the LLO biosynthesis along with the known mutations in *A. thaliana* and chemical inhibitors affecting this process is displayed in Figure 1.3 from Pattison and Amtmann, 2009. Biosynthesis of LLO requires the sequential attachment of sugar residues to Dol-P and is topologically split across the ER membrane. The first seven reactions take place on the cytoplasmic side of ER, whereas the remaining seven occur in the ER lumen. First, glycosyltranferases catalyse the addition of two N-acetylglucosamine (GlcNAc) and five mannose (Man) residues to Dol-P using the nucleotide sugar donors, UDP-GlcNAc and GDP-Man. Subsequently, the $Man_5GlcNAc_2$-P-Dol intermediate must be flipped across the ER membrane for elongation and completion of LLO. $Man_5GlcNAc_2$-P-Dol is flipped to the lumenal side by an ATP-independent flippase (Rush and Waechter, 1995). The RFT1 protein of *Saccharomyces cerevisiae* was shown to be required for this translocation process (Helenius *et al*., 2002). The yeast strain *alg11* is deficient in GDP-Man-dependent mannosyltransferase, which is required for the synthesis of $Man_5GlcNAc_2$-P-Dol, and shows accumulation of $Man_3GlcNAc_2$-P-Dol on the cytoplasmic side of the ER (Cipollo *et al*., 2001).

Overexpression of RFT1 in *alg11* cells caused the accumulation of $Man_7GlcNAc_2$-P-Dol in the ER lumen suggesting that RFT1 is a potential candidate for an ER membrane flippase (Helenius *et al*., 2002). Once the $Man_5GlcNAc_2$-P-Dol intermediate is flipped to the luminal side of the ER, a further four mannose and three glucose (Glc) residues are added to make the complete LLO, $Glc_3Man_9GlcNAc_2$-P-Dol. Sugar donors for these reactions are Man-P-Dol and Glc-P-Dol. The complete oligosaccharide is transferred from dolichol to proteins by the OST complex and further modified as part of the CNX/CRT cycle (see 1.8 section). Additional modifications of the glycan take place in post-ER compartments such as the Golgi apparatus (Strasser *et al*., 2006).

Although many genes are involved in N-glycosylation, few mutants have been isolated in plants that would allow understanding of the molecular significance of the individual proteins taking part in this process. However, the use of chemical inhibitors such as tunicamycin has given a great insight into the process of N-glycosylation. Tunicamycin is a specific inhibitor of UDP-N-acetylglucosamine:dolichol phosphate N-acetylglucosamine-1-P transferase (GPT), the enzyme that catalyses the first glycosyltransferase reaction during LLO synthesis. Tunicamycin treatment is lethal for all eukaryotes, including plants (Zeng and Elbein, 1995). Sub-lethal doses of tunicamycin induce the expression of ER stress-related genes, particularly those involved in UPR. The first loss-of-function mutant of N-glycosylation identified in *A. thaliana* was *asparagine-linked glycosylation 3-2* (*alg3-2*). The ALG3 gene encodes for a1-3-mannosyltransferase, the enzyme responsible for the addition of the first Man residue after translocation of the LLO to the ER luminal face. Although *alg3-2* mutants show an enhanced UPR, they do not show any physiological phenotype, suggesting that the latter steps in N-glycosylation are not vital (Henquet *et al*., 2008). Treatment of *Cucumis sativus* (cucumber) with sub-lethal amounts of tunicamycin resulted in an increased expression of PR proteins, increased levels of salicylic acid and increased systemic acquired resistance (SAR) against the fungal pathogen, *Colletotrichum lagenarium* (Sticher and Metraux, 2000), pointing to a close relationship between N-glycosylation and defence responses. The effect of *AtPQL4* and *AtPQL6* mutation on both UPR and defence related genes is therefore in agreement with a possible function in N-glycosylation as suggested by its homology to *MPDU1* (see 1.4 section).

O-glycosylation comprises the linkage of glycans to amino acids containing a hydroxyl functional group like serine, threonine, tyrosine, hydroxyproline and hydroxylysine (Spiro *et al*., 2002). O-glycans are highly variable in structure as each sugar residue has 3 or 4

attachment sites for other sugar residues and they can also adopt different conformations. In addition, O-glycans can be long polysaccharide chains, namely glycosaminoglycans (GAGs) that consist of multiple disaccharide repeats such as N-acetylgalactosamine (GalNAc) or GlcNAc linked with glucuronic acid (GlcA) or galactose (Gal) residues (Wopereis *et al*., 2006). Few O-glycans contain Man residues and therefore require Man-P-Dol. This special form of O-glycosylation, named O-mannosylation, involves the attachment of Man residues to either serine or threonine residue of proteins (Spiro *et al*., 2002). To date few O-glycosylated proteins have been identified. Most of them are derived from *S. cerevisiae* and the best described being a mammalian skeletal muscle extracellular matrix protein, the α-dystroglycan (Worepeis *et al*., 2006).

C-mannosylation is another type of protein modification that occurs in the lumenal ER and involves the carbon-carbon linkage of a Man residue to the C-2 of the first tryptophan (Trp) residue of a consensus sequense Trp-x-x-Trp. (Spiro *et al*., 2002). The Man residue is derived from Man-P-Dol, as *lec15* mutants, deficient in Man-P-Dol synthase activity, show a decrease in C-mannosylation (Doucey *et al*., 1998). Few proteins containing C-mannosylation sites have been identified in mammals, with the most well described being the ribonuclease2 (RNase2) protein (Krieg *et al*., 1997, Doucey *et al*., 1998).

GPI anchoring is an additional type of glycosylation that enables tethering of proteins to the plasma membrane and is found in all eukaryotes. The first two steps of GPI synthesis occur at the cytoplasmic side of the ER. They involve the attachment of a GlcNAc residue to phosphatidylinositol (PI) and the subsequent deacetylation and acylation of the inositol ring of PI to produce the GlcN-acyl-PI intermediate. Re-orientation of the GlcN-acyl-PI in the ER membrane facilitates the attachment of additional Man residues derived from Man-P-Dol sugar donors. Further species-specific modifications take place on the lumenal side of ER. A transamidase transfers the mature GPI to nascent proteins with a GPI-attachment site at carboxyl terminus (Kinoshita and Inoue, 2000).

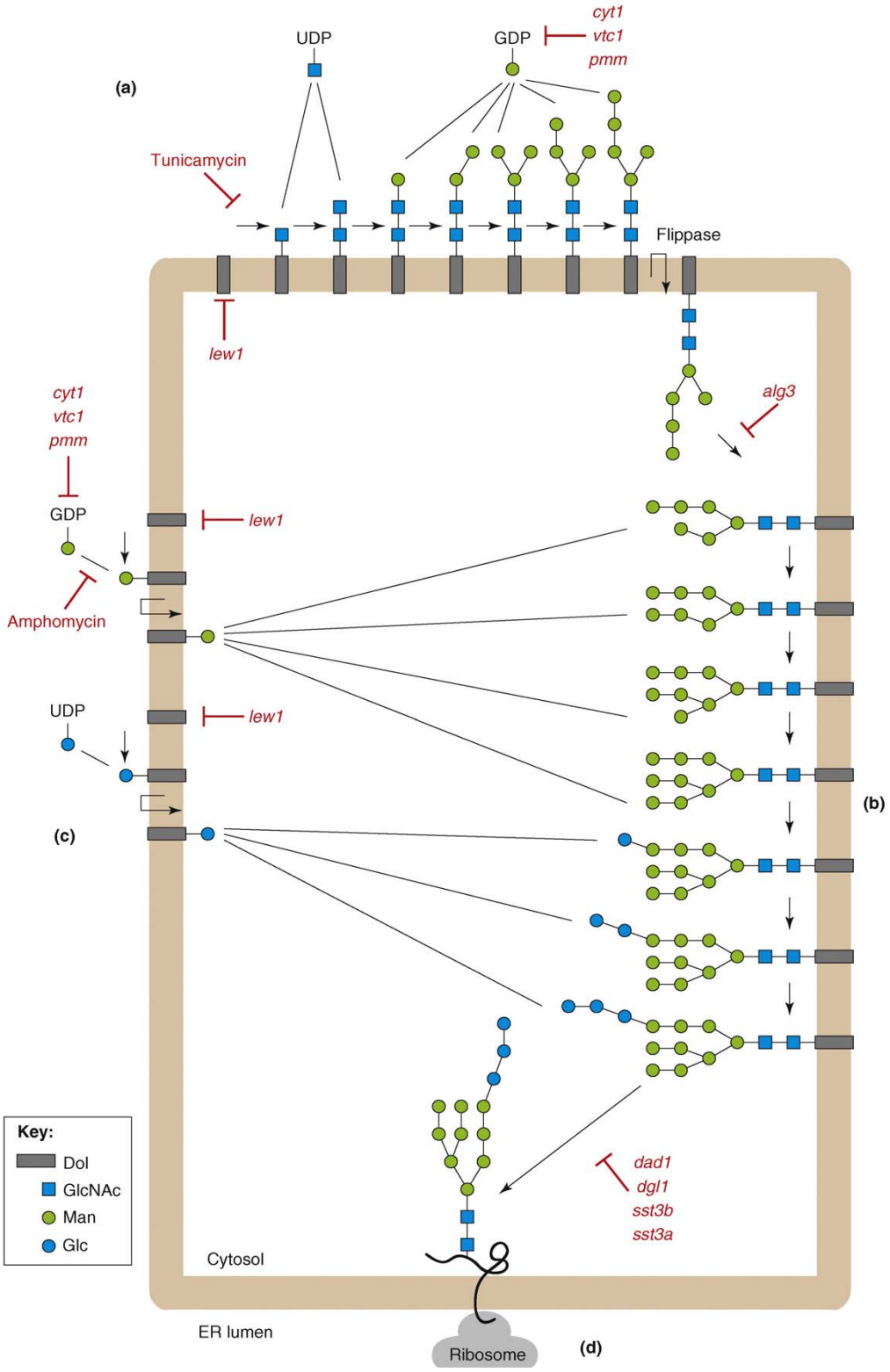

Figure 1.3: Lipid linked oligosaccharide biosynthesis in the ER.

N-glycosylation starts at the cytoplasmic side of ER membrane with **(a)** the attachment of two GlcNAc and five Man residues from nucleotide sugar donors to Dol-P generating the $Man_5GlcNAc_2$-P-Dol intermediate. **(b)** This intermediate is subsequently flipped across ER membrane and further four Man and 3 Glc residues are added to form the $Glc_3Man_9GlcNAc_2$-P-Dol. The Man and Glc residues are derived from Man-P-Dol and Glc-P-Dol sugar donors. **(d)** The complete glycan is transferred to protein as they are co-translationally translocated into the ER lumen. *A. thaliana* mutants and chemical inhibitors of individual steps are shown in red color. (Figure is taken from Pattison and Amtmann, 2009)

1.7 LEC35/MPDU1 and Man-P-Dol usage in plants

The MPDU1 protein, also known as LEC35, is implicated in all types of Man-P-Dol dependent glycosylation. The LEC35 gene was isolated from Chinese hamster ovary (CHO) cells through a screen using concanavalin (ConA), which binds high-mannose oligosaccharides (Kornfeld and Kornfeld, 1985), in combination with castanospermine (Cs) and swainsonine (Sw) that inhibit the Golgi-localised N-linked glycan processing enzymes. Cs inhibits glucosidase I and II whereas Sw inhibits mannosidase II (Elbein, 1987; Tulsiani *et al*., 1982). *lec35* mutants showed increased tolerance to both glycosylation inhibitors Cs and Sw suggesting that they could produce complex glycans via an alternative pathway (Lehramn and Zeng, 1989). The authors suggested that *lec35* mutants were defective in LLO composition and therefore by-passed the necessary activity of the three enzymes to produce complex glycans. In addition, high-pressure liquid chromatography (HPLC) analysis of LLOs incubated with GDP-[^{3}H]-Man showed an accumulation of $Man_5GlcNAc_2$-P-P-Dol at the expense of the mature LLO, $Glc_3Man_9GlcNAc_2$-P-P-Dol (Lehramn and Zheng, 1989). The accumulation of this LLO intermediate was not the consequence of a defective enzyme involved in Man-P-Dol synthesis, as Man-P-Dol synthetase and transferase activity was the same in mutant and wild type CHO-K1 cells (Anand *et al*., 2001). *lec35* mutants were also affected in glucose-dolichol-phosphate (GDP)-dependent LLO synthesis. Lack of glucosylated LLOs was not due to presence of incomplete mannosylation of LLOs, as in *lec15* mutants, which are defective in Man-P-Dol synthetase, glucosylation of the $Man_5GlcNAc_2$-P-P-Dol intermediate takes place producing $Glc_3Man_5GlcNAc_2$-P-P-Dol instead of $Glc_3Man_9GlcNAc_2$-P-P-Dol. Anand *et al*. (2001) also reported a defect of C-mannosylation of tryptophan in *lec35* mutants. *lec35* cells expressing the C-mannosylated RNase 2.4 exhibited a 7.4-fold decrease in mannosylation compared to wild type CHO-K1 cells. Moreover, mutations in the LEC35 gene resulted in a block of mannosylation of GPI during GPI synthesis. *lec35* mutants accumulate GlcN-acyl-PI that suggests an arrest in elongation of GPI at the first mannosylation step in the ER lumen (Camp *et al*., 1993). From the combined results, Anand *et al*. (2001) concluded that MPDU1/LEC35 has a role in utilisation of Man-P-Dol, but its exact mode of function has not yet been identified.

Man-P-Dol and Glc-P-Dol mediated glycosylation is essential for plant viability, as several mutants deficient in such processes resulted in gametic or embryonic lethality. However, the severity of the phenotype depends on the stage and location of glycosylation. As mentioned above, mutations occurring in later stages of N-glycosylation in the ER are not

lethal while those occurring in the first step of this process are. In addition, mutations that affect N-glycosylation in the Golgi are less severe than those occurring in the ER (Strasser *et al*., 2006). A possible explanation for the lethality associated with the inhibition of N-glycosylation is the saturation of chaperones and folding catalysts in the ER lumen that causes ER dysfunction due to inability of such proteins to respond to ER stress (Vitale and Ceriotti, 2004). Although it was speculated that *At*PQL4 and *At*PQL6 might have a potential role in N-glycosylation in the ER, no gametic and embryonic lethality was observed (Pattison, 2008).

1.8 ER Quality Control (ER QC)

Many proteins have to enter the secretory pathway in order to be secreted or targeted to a specific sub-cellular location. Such proteins are termed secretory proteins and can be secreted proteins or proteins residing in the plasma membrane or in the lumen of different organelles such as vacuoles (Sanderfoot and Raikhel, 2003). The secretory pathway, alternatively known as anterograde pathway, begins with the co-translational translocation of a protein into the ER, followed by its flow to the Golgi and subsequent sorting to its final destination (Bassham *et al*., 2008). The newly synthesized secretory proteins are subject to a quality control mechanism (QC) in the ER to adopt the correct conformation. ER QC involves retention of proteins that are not yet mature in the ER and targeting of misfolded proteins for degradation through the ER-associated degradation (ERAD) pathway (Vitale and Denecke, 2006). ER stress causes accumulation of non-native proteins in the ER that can form protein aggregates due to nonspecific interactions between hydrophobic residues that are exposed in the newly synthesized protein (Vitale and Boston, 2008).

Once the synthesized secretory protein enters the ER lumen, chaperones and other folding helper proteins bind to the nascent polypeptide chain to facilitate correct folding. The first folding helper is the enzyme signal peptidase that removes a N-terminal signal peptide present in the majority of secretory proteins (Vitale and Denecke, 2006). Subsequently, chaperones and co-chaperones bind to hydrophobic regions of proteins to prevent the formation of any aggregates (Liu and Howell, 2010). Several such folding proteins have been identified, with the most well described being the ER lumenal BiP. In *A. thaliana* three *BiP* genes have been found, named *BiP1*, *BiP2* and *BiP3*. BiP is responsible for several additional processes in the ER. For instance, it facilitates the movement of the

protein through the translocation pore in association with the Sec61 protein (Vitale and Denecke, 2006). Studies have reported that environmental stresses such as drought, heat and pathogen attack can cause ER stress that in turn results in the enhanced expression of all three *AtBiP* genes (Wang *et al*., 2005; Iwata *et al*., 2008).

Most of the proteins passing through the secretory pathway are modified by N-glycosylation. N-glycosylation ensures ER QC as the core $Glc_3Man_9GlcNAc_2$-P-P-Dol oligosaccharide is subject to further modifications inside the ER lumen by entering the calnexin/calreticulin cycle (Pattison and Amtmann, 2009). The CNX/CRT cycle depends on the de-glucosylation and re-glucosylation of the oligosaccharide by enzymes residing in the ER lumen. Figure 1.4 represents the CNX/CRT cycle including all the mutants identified in Arabidopsis to affect this process. Once the oligosaccharide is transferred to the protein, the two terminal glucose residues are removed by glucosidase I and II, respectively. The monoglucosylated oligosaccharide, $GlcMan_9GlcNAc_2$, binds to the two lectins CNX and CRT. CNX is an ER membrane protein, while CRT is a lumenal ER protein. Both lectins contain N-terminal regions forming β-sandwich domains that interact with the single glucose residue of the oligosaccharide of the proteins (Liu and Howell, 2010). Glucosidase II facilitates the release of the protein from the CNX/CRT cycle by removing the last glucose residue. However, if the protein has not adopted its native form, another ER resident protein, the UDP-glucose:glycoprotein glucosyltransferase (UGGT), will add a further glucose residue to the nonglucosylated oligosaccharide to allow further rounds of CNX/CRT cycle in order to control the folding status of the protein (Liu and Howell, 2010). The cycle is interrupted when the protein is correctly folded and the protein can then be exported to the Golgi (Pattison and Amtmann, 2009).

Mutations affecting proteins involved directly or indirectly in the CNX/CRT cycle have severe effects on plant fitness and phenotypes can range from being completely lethal to no obvious morphological phenotype (Pattison and Amtmann, 2009). For instance, the ER-localised protein, UDP-glucose/galactose transporter (*At*UTR) 1 in *A. thaliana* is responsible for the transport of UDP-glucose into the ER lumen. Mutations in the *At*UTR1 gene cause 50% decrease in UDP-glucose uptake suggesting that the protein is essential for the correct functioning of the CNX/CRT cycle (Reyes *et al*., 2006). In addition, a genetic screen for *Arabidopsis* mutants insensitive to the surrogate peptide elf18 for the elongation factor (EF)-TU, has identified several genes that provide a link between ER QC and pathogen response, including CRT3, UGGT and the ER retention receptor (ERD2) (Li *et al*., 2009; Nekrashov *et al*., 2009).

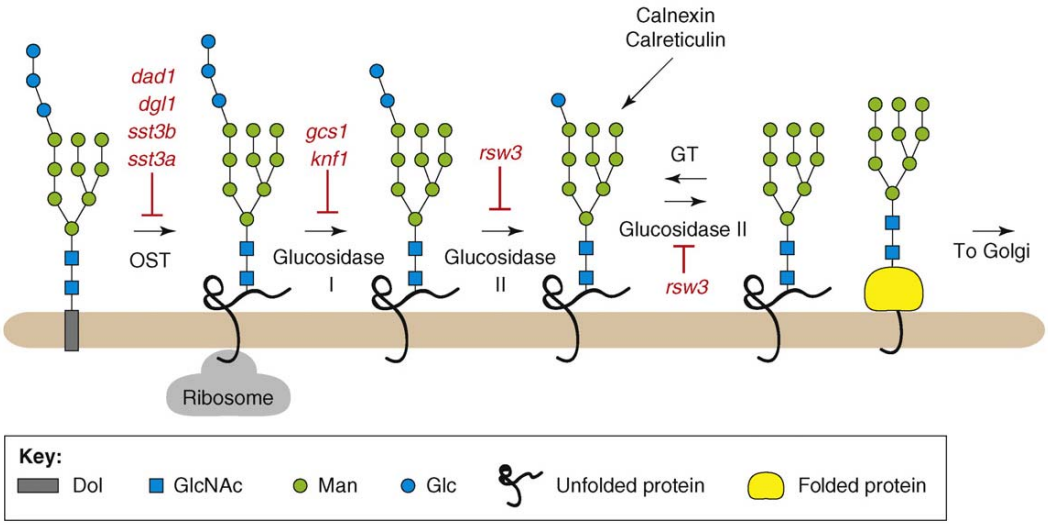

Figure 1.4: Calnexin/calreticullin cycle.

After transfer of the mature Glc3Man5GlcNAc2 oligosaccharide to protein, the newly produced glycoprotein enters the CNX/CRT cycle. The outermost and following glucose residue are removed by glucosidase I and II. The two lectins, CNX and CRT can bind the monoglucosylated oligosaccharide, promoting correct folding of the protein. After removal of the last glucose residue the protein can be exported to the Golgi. If it is still misfoded, it re-enters the CNX/CRT cycle by addition of a further glucose residue by UGGT (indicated as GT). *A. thaliana* mutants are shown in red color. (Figure is taken from publication by Pattison and Amtmann, 2009)

ER stress induces the UPR which in turn results in the enhanced expression of folding helpers to relieve the stress either by promoting correct folding or by eliminating defective proteins. UPR is not only stimulated by environmental stresses like pathogen attack, but also by normal developmental processes such as seed development that involves accumulation of storage bodies (Pattison and Amtmann, 2009). Studies in yeast have revealed that a key player in UPR is the BiP protein. Under normal conditions BiP is found to be associated with a RNA splicing factor, the inostol-required 1 (Ire1) protein (Liu and Howell, 2010). Upon accumulation of misfolded proteins free BiP decreases causing BiP dissociation from Ire1, which in turn activates a transcription factor that up-regulates expression of ER stress related genes (Travers *et al*., 2000; Ceriotti and Roberts, 2006). Such genes are not only chaperones and folding helpers, but also genes implicated in the secretory pathway or secretion (Travers *et al*., 2000). Microarray studies in *A. thaliana* showed a similar set of genes to be up-regulated during UPR, though down-regulation of proteins with signal peptides, especially cell wall proteins, was also evident (Martinez and Chrispeels, 2003). In addition, two ERAD genes, a putative ubiquitin and an AAA-type ATPase, were up-regulated suggesting a link between UPR and ERAD pathway.

As discussed before, N-glycosylation inhibition induces UPR that in turn up-regulates expression of BiP, CNX, CRT and other folding-related proteins (Ceriotti and Roberts, 2006). Many of the chaperones induced by UPR are also implicated in the ERAD pathway. The discrimination between native and misfolded proteins is facilitated by the CNX/CRT cycle. Permanently misfolded proteins remain in the ER lumen much longer than the folding intermediates and therefore the possibility to be trimmed by ER-localised mannosidase increases. This enzyme is responsible for the removal of the last Man residue from the nonglucosylated oligosaccharide. Hence, the re-glucosylation of the $Man_8GlcNAc_2$ is less probable than of the $Man_9GlcNAc_2$ causing the misfolded protein to be translocated to the cytosol (Ceriotti and Roberts, 2006). However, it is mostly unknown how defective proteins are recognised by folding factors (Liu and Howell, 2010). Studies have suggested that dislocation of these proteins occurs through the Sec61 complex. Translocation to the cytosol is dependent on ubiquitinylation of the defective protein that will allow proteasomal degradation to take place (Ceriotti and Roberts, 2006).

Not all defective proteins follow the ERAD pathway. Degradation of non-native proteins can be achieved in vacuoles through two different mechanisms, the Golgi-mediated pathway and autophagy (Vitale and Boston, 2008). The first mechanism entails the vesicular traffic of the protein through golgi and pre-vacuolar compartment, the subsequent sorting to the vacuole by a Vps 10 receptor and eventually the degradation by vacuolar proteases (Kruse *et al*., 2006). The alternative mechanism is based on autophagy. ER stress is shown to provoke the assembly of pre-autophagosomal structures (Yorimitsu *et al*., 2007). Studies in yeast have suggested that the autophagosome requires the early secretory pathway to supply membranes for its formation (Regiori *et al*., 2004). It has also been reported that ER fragments containing misfolded proteins are selectively recognised and transported to the vacuole within the autophagosome (Rose *et al*., 2006).

1.9 Objectives and thesis outline

The aim of this project is to give further insight into the function of two *At*PQL proteins, *At*PQL4 and *At*PQL6. This is achieved by investigating the sub-cellular localisation of the two proteins, the effect of overexpression on the localization of other membrane proteins and the phenotypic analysis of mutant lines for both genes under certain environmental conditions. The thesis contains three Results chapters (chapters 3-5). Chapter 2 provides details about the materials and methods used in this project.

Chapter 3 presents the sub-cellular localisation of the *At*PQL4 and *At*PQL6 proteins, using GFP-fusion constructs and confocal laser scanning microscopy of tobacco leaf cells. A previous study reported localization to the ER. Here, I confirm this finding by co-expressing the proteins with an ER marker protein. In addition, novel information on the sub-cellular localisation of a third protein from the same family, *At*PQL2, is also presented.

Chapter 4 presents new information on the molecular function of *At*PQL4 and *At*PQL6. Overexpression of the two *At*PQL proteins in tobacco leaves is shown to affect the targeting of secretory proteins. This was investigated by co-expressing GFP-*At*PQL proteins with a number of different fluorescent-tagged proteins. The implications of this observation for a possible function of *At*PQL4 and *At*PQL6 in the ER are discussed.

Chapter 5 describes the phenotypic analysis of mutant lines for *At*PQL4 and *At*PQL6 in a variety of environmental stresses. The observations at whole-plant level are discussed in the context of putative functions of the proteins at the (sub-)cellular level.

A general discussion of all the data presented in the thesis is provided in chapter 6. A possible function of the *At*PQL4 and *At*PQL6 proteins is proposed and ideas for future experiments are presented.

Chapter 2: Material and Methods

2.1 Materials

2.1.1 Chemicals

Except where otherwise stated, all chemicals used are from Sigma (Poole, UK) and Fischer-Scientific (Southampton, UK). Enzymes for molecular biology were from Invitrogen (Paisley, UK), Promega (Southampton, UK) and New England Biolabs (Hitchin, UK). Kits for DNA extraction were form Fischer-Scientific (Southampton, UK) and kits for gel extraction were from Qiagen (Crawley, UK). Custom primers were purchased from Invitrogen.

2.1.2 Plants

Arabidopsis thaliana ecotype Columbia (Col0) was the background for all mutants and transgenic lines. Six different *Arabidopsis thaliana* genotypes were used; wild-type Col0 (WT), *pql4-1*, *pql4-2*, *pql6-1*, *pql4-2/6-1* and *35S::AtPQL6-1*.

2.2 Plant Growth and Treatment

2.2.1 Growth on soil

To grow *A. thaliana* plants on soil, approximately 6 seeds were sown on moist compost (Levington F2, Fisons, Ipswich, UK) inside a standard circular plant pot (4 cm in diameter) and placed in a tray under propagator in darkness at 4°C for two days to allow stratification. The pots subsequently were placed in a controlled growth chamber (Sanyo Fitotron) in either long-day conditions (16 hours light, 8 hours darkness; light intensity 100-120 μmol m^{-2} sec^{-1}; temperature approximately 20°C/18°C day/night; relative humidity of 60%/70% day/night) or short-day conditions (9 hours light, 15 hours darkness; light intensity 120-150 μmol m^{-2} sec^{-1}; temperature approximately 20°C/18°C day/night; relative humidity of 60%/70% day/night). After one week, plants were transplanted in individual pots and the propagator was removed. Plants were watered every 4^{th} day until senescence. For seed collection, Aracon tubing was placed on top of the rosettes and

watering stopped once the first siliques became discoloured. The plants were allowed to first completely dry out before collecting the seeds.

2.2.2 Viral infection

Four seeds per genotype were sown on soil and placed in a controlled growth chamber in short-day conditions as described. After the emergence of the first true leaves, Arabidopsis seedlings were inoculated with CaMV isolate Cabb B-JI. 2µL of sterile water mixed with a small amount of cellite, used as an abrasive, and 0.1 µg of purified virus were pipetted onto the leaf. The leaf was rubbed using a small glass rod. Control plants were not infected. Three plants from each genotype were pooled to extract DNA at different time points as described below and quantified with qPCR (see below).

2.2.3 Growth on agar plates

A. thaliana seeds were surfaced sterilised. About 400 seeds were placed in 1.5 mL Eppendorf tube with 1mL 100% ethanol for one minute and mixed by inverting tube several times. The ethanol was discarded and 1 mL of sterilising solution (2.5% sodium hypochlorite and 0.01% Tween 20) was added into the tube and mixed by inverting several times. After incubation for five minutes, the bleach solution was replaced by 1 mL of double distilled water. Washing was repeated five times to ensure complete removal of bleach solution and the seeds kept in water. The tubes were wrapped in aluminium foil and placed in darkness at 4°C for two days to ensure stratification.

Different media were used for physiological experiments. For most of the experiments in this project, a full minimal medium (Control medium) was used (Table 2.1). To prepare the medium, reagents were mixed and diluted with double distilled water to the final concentration. 0.5x Muraskige and Skoog (MS) medium was also used where stated. 2.2 g of MS powder (Sigma, M5519) per litre was dissolved in double distilled water. Media were supplemented with sucrose to a concentration 1% and pH was adjusted to pH 5.6 with either 0.5 M of NaOH or using MES-TRIS buffer. To solidify the media, 1% Agar (Type A, Sigma) was added before autoclaving at 121°C for 20 minutes. Once the autoclaved medium had cooled to about 60°C, it was suspended into square plates (120 x 120 mm, Greiner) using titration pipettes.

Seeds were sown individually onto the solidified media using a sterile cut P200 pipette tip attached to a Gilson pipette. Generally, 6 seeds sown per plate containing 50 mL medium and spaced evenly into horizontal line approximately 15 mm form the top of the plate. The plates were sealed with 3M Micropore Tape (MidMeds Ltd, Nazeing, UK) and placed in controlled growth chamber (24 hours photoperiod; light intensity approximately 110 µmol m^{-2} sec^{-1}; temperature 20°C and relative humidity of 60%), except where otherwise stated.

Table 2.1: Final concentration of reagents used to prepare full minimal Control medium.

Reagents	Concentration
KNO_3	1.25 mM
$Ca(NO_3)_2$	0.5 mM
$MgSO_4$	0.5 mM
FeNaEDTA	42.5 µM
KH_2PO_4	0.625 mM
NaCl	2 mM
$CuSO_4$	0.16 µM
$ZnSO_4$	0.38 µM
$MnSO_4$	1.8 µM
H_3BO_3	45 µM
$(NH_4)_6Mo_7O_{24}$	0.015 µM
$CoCl_2$	0.01 µM

2.2.4 Stress treatments

Salt and Osmotic stress

Plants were grown on MS agar plates supplemented with 50 mM NaCl or 50 mM KCl to measure sensitivity to salt and osmotic stress, respectively.

Macronutrient depletion

Plants were grown on agar plates supplemented with varied strength of MS to measure sensitivity of seedlings to macronutrient depletion. 1/3, 1/10, 1/30, 1/100 and 1/300 MS dilutions were used. Four seeds of two different genotypes were sown on agar plate.

Sucrose starvation

Response of plants in varied carbon concentrations was measured by growing plants on MS agar plates supplemented with 0%, 0.5%, 1%, 3% and 4% of sucrose.

2.2.5 Analysis of growth and water content

From nine days of germination and onwards, plates were scanned to allow measurement of the roots using the EasyRhizo software (Armengaud *et al.,* 2000). Fourteen days post germination, shoots and roots were harvested to measure fresh weight and placed in foil at 60°C for three days to measure dry weight.

Water content was estimated according to the following formula:
W_{cont} (%)= 100-(DW/FW x 100)

Statistical analysis was performed using ANOVA test with SOFA Statistics version 0.9.25 (Paton-Simpson & Associates Ltd, Auckland, New Zealand).

2.2.6 Growth on liquid medium

Plants grown in liquid 0.5x MS medium prepared as described above. Sterile seeds were sown directly into either 6-well plates containing liquid medium. The plates were sealed with Micropore tape and placed in control growth chamber (24 hours photoperiod; light intensity approximately 110 μmol m^{-2} sec^{-1}; temperature 20°C and relative humidity of 60%).

2.3 DNA and RNA extraction, quantification

For the extraction of either DNA or RNA, plant material was placed into a 2 mL screwcap tube together with a grinding ball and placed directly into liquid nitrogen. Subsequently, the tubes were placed in a pre-cooled rack and the plant material ground using the Qiagen Tissue Lyser for 45-110 seconds depending on the amount of plant material, with a frequency of 28.6 Hz.

2.3.1 DNA extraction

DNA was extracted from *A. thaliana* using the Nucleospin® Plant II kit (Fischer-Scientific) according to the manufacturer's instructions, with an additional step of digestion with Proteinase K. After lysis step, 8 µL of Proteinase K (20µg/µL) were added into the tubes, followed by thorough vortexing. The tubes were incubated at room temperature for three hours. Proteinase K was inactivated by incubating the samples at 65°C for thirty minutes. DNA was twice eluted from the column in 50 µL of the supplied elution buffer. DNA quantity and purity was determined spectrophotometrically by preparing 1 to 50 dilutions of DNA and measuring the absorbance at 260 nm in an Eppendorf UVette® in the Eppendorf Biophotomoter Plus. Absorbance readings were compared to double distilled water. The purity of DNA was estimated from the A_{260}/A_{280} ratio.

2.3.2 RNA extraction

To prepare RNAse free water, 1 mL of DEPC (Diethyl pyrocarbonate, Fluka) was added to 1 L of double distilled water and stirred for approximately two hours. This water was subsequently autoclaved and used in all methods involving RNA.

RNA was extracted from *A. thaliana* by adding 1.4 mL of TRIzol solution (0.8M Guanidium thiocynate, 0.4 M Ammonium thiocynate, 0.1M NaAc pH 5.2, 5% Glycerol and 3% Phenol saturated in water pH4.5) to 100 mg of ground frozen plant material. The samples were mixed by vortexing for one minute and incubated at room temperature for five minutes. This was followed by centrifugation at 8000g for two minutes. The supernatant was transferred into new 2 mL Eppendorf tube and 300 µL of chloroform:isoamylalcohol (24:1) were added. The samples were mixed by vortexing for one minute, incubated at room temperature for two minutes and then centrifuged at 13000g at 4°C for ten minutes. The aqueous phase was carefully transferred into a fresh 1.5 mL

tube followed by adding isopropanol in a volume ratio of 1:1. The samples were mixed by inverting the tubes for several times and left at room temperature for 5 minutes to allow the precipitation of RNA. Subsequently, the samples were centrifuged at 13000g at 4°C for 10 minutes, washed with 1 mL of 70% ethanol and centrifuged at 13000g at 4°C for five minutes. The supernatant was removed and the pellet allowed to dry at air and resuspended in 50 µL of DEPC-treated water. The samples were placed at 42°C to ensure dissolving of dried RNA.

The RNA quantity and purity was measured spectrophotometrically in Eppendorf Biophotometer Plus. RNA was 50x diluted in DEPC-treated water and absorbance measured from 220 to 320 nm into an Eppendorf UVette®. RNA concentation was calculated following the formula: ($A_{260-230}$) x 40 x Dilution factor (ng/µL). The purity of RNA was estimated from the A_{260}/A_{280} ratio.

2.4 Polymerase Chain Reaction (PCR)

PCR was performed using the Gen Amp PCR System 9700 (Applied Biosystems). Primer sequences are shown in appendix A.

2.4.1 Standard PCR

Standard PCR was carried out using GoTaq DNA polymerase (Promega). Table 2.2 and 2.3 display the composition of the standard PCR mix prepared to a final volume of 25 mL and the cycling conditions. Template was genomic DNA. Aliquots of the mastermix were pipetteded into standard thin-wall PCR reaction tubes. Templates were added individually to each PCR tube.

2.4.2 Agarose gel electrophoresis and gel purification

PCR products were resolved by agarose gel electrophoresis. 15 µL of PCR product was loaded on a DNA agarose gel (1.5% agarose, 1x TAE containing 32µL/L ethidium bormide solution). 10 µL of DNA lambda ladder was loaded on each gel. DNA bands were separated at 100mV for 25-35 minutes and visualised under UV light using GelDoc 2000 scanner (Biorad).

PCR products were extracted from gels under UV light and purified using a QiaQuick gel extraction kit (Qiagen) according to manufacturer's instructions. DNA was eluted in 50µL elution buffer. DNA quantity and purity was determined spectrophotometrically as described above.

Table 2.2: Standard PCR reaction mix.

Component	**Volume (µL)**
5x Green *GoTaq* Buffer	5
$MgCl_2$ (25mM)	3
dNTP Mix (10mM of dATP, dCTP, dGTP and dTTP)	1
Forward Primer (10mM)	1
Reverse primer (10mM)	1
GoTaq (5U/µL)	0.2
Double distilled water	11.8
Template	2

Table 2.3: Cycling conditions of standard PCR.

Cycles	**Step**	**Temperature**	**Time (minutes)**
1	Denaturation	95°C	5
30	Denaturation	95°C	0.5
	Primer Annealing	60°C	0.5
	Extension	72°C	1
1	Final extension	72°C	5

2.4.3 Quantitative PCR (qPCR)

qPCR was performed in 96-well plates using Mx3000 (Stratagene) real-time PCR system and the Brilliant SYBR Green qPCR kit (Stratagene). Table 2.4 and 2.5 display the composition of the qPCR reaction mix prepared to a final volume of 12.5 mL and cycling conditions. The template was genomic DNA or DNA standards and nucleotide-free water. DNA standards were prepared from gel-extracted PRC products by performing standard PCR using the same primers as for qPCR. Purified PCR products were adjusted to 10 pg/μL and subsequently diluted to produce six different standards ranging from 1 pg/μL to 10^{-5} pg/μL.

At the end of the annealing step of every PCR cycle, SYBR green fluorescence was measured and the Ct (the number of cycles required to reach threshold fluorescence) was calculated using the machine software (MX3000). Plotting the Ct value of each dilution against the log initial template quantity created a standard curve. qPCR reactions were made in duplicates. To control and correct any errors occurring in each qPCR, the expression of the gene of interest should be tested relative to a stably expressed gene.

For viral infection experiments, the amount of virus DNA was estimated. The reference gene used was the *Arabidopsis* 18S ribosomal RNA gene. The *Arabidopsis* genome contains a fixed number of copies of the 18S rRNA gene and therefore 18S rRNA provides the most accurate measure of the amount of total DNA. CaMV DNA was quantified by Q-PCR, and for each sample, duplicates of reactions were performed. Table 2.6 displays the primers were used to amplify the CaMV Cabb B-JI gene and the *Arabidopsis* 18S ribosomal RNA gene.

Table 2.4: QPCR reaction mix.

Component	Volume per reaction (µL)
SYBR green qPCR Master mix	10
Forward Primer (10mM)	0.4
Reverse primer (10mM)	0.4
Double distilled water	4.2
Template	5

Table 2.5: Cycling conditions for qPCR.

	Cycles	Temperature	Time (minutes)
Amplification program	1	95°C	3
	40	95°C	0.10
		55°C	1
		72°C	1
Dissociation program	1	95°C	1
		55°C	0.30
		95°C	0.30

2.5 Molecular cloning procedures

2.5.1 Transformation of chemically competent *E.coli* cells

Aliquots of chemically competent *E.coli* (strain TOP10^{TM}, Invitrogen) cells were thawed on ice for five minutes and then 1 µL of plasmid was added and mixed by stirring for five seconds. The tubes were placed into liquid nitrogen for five minutes. This was followed by placing the tubes in a prewarmed water bath at 42°C for 45 seconds. Luria Bertani (LB) medium was added to each tube that was then incubated at 37°C for one hour by shaking at 200 rpm. Bacteria cells were harvested by centrifugation at 8000g for two minutes. The cells were resuspended into 100 µL of the supernatant and the whole volume was spread on LB agar plates (1% agar) under a flow hood using or autoclaved glass beads or a Drigalski spatula sterilised by ethanol flaming. The agar plates were supplemented with the appropriate antibiotics for selection of positive transformants as shown on Table 2.7. All the plates were incubated overnight at 37°C.

Table 2.6: Antibiotics used for selection of positive transformants.

Antibiotic	Final concentration (µg/mL)
Gentamycin	25
Kanamycin	50
Rifampicin	50
Spectinamycin	100

2.5.2 Plasmid minipreps

Single colonies picked with a sterile pipette tip and inoculated in 4 mL of LB medium containing the appropriate antibiotics. The cultures were grown overnight at 37°C by shaking at 200 rpm. Once cultures reach saturation they were transferred into 2 mL tubes and centrifuged at 4000g at 4°C fifteen seconds. The cell pellets were resuspended in 400 µL resuspension buffer (50 mM Tris-Cl, 10 mM EDTA, RNase A (10µg/ml), Lysozyme, pH 8 adjust) by vortexing. This was followed by adding 400 µL of lysis buffer (0.2 M NaOH, 1% SDS) and mixing by inverting the tubes for four times. The lysates were resuspend in 400 µL of neutralisation buffer (3M Potassium acetate, pH 5) and centrifuged

at 14000g at 4°C for ten minutes. 1 mL of the supernatant was transferred into fresh 2 mL tube and mixed with 1 mL of chloroform-isoamylchohol (24:1) by inverting the tubes for thirty seconds. The suspension was centrifuged at 14000g at 4°C for one minute and 950 µL of the supernatant was transferred into fresh 2 mL tubes. Isopropanol was added in a volume ratio of 1:1, the suspension was mixed and incubated at -20°C for twenty minutes. This was followed by centrifugation at 14000g at 4°C for fifteen minutes. The supernatant was transferred into a new tube containing 500 µL of 70% ethanol and centrifuged at 14000g at 4°C for five minutes. The DNA pellet was allowed to dry at air for ten minutes. The DNA pellet was dissolved in 100 µL of double distilled water by incubating them at 65°C for ten minutes.

2.5.3 Restriction digestion reactions

Plasmids were digested with restriction enzymes purchased from NEB or Promega. Table 2.8 shows the composition of the restriction digestion mix in a final volume of 20 µL. The mix was prepared with the appropriate reaction buffers for each enzyme and BSA where required. If necessary, the reaction was performed by using two enzymes into the same tube and choosing a reaction buffer to be compatible with both enzymes. The reactions were incubated at 37°C for approximately 1 hour. The samples were separated by agarose (1.5%) gel electrophoresis as described above.

Table 2.7: Composition of restriction digestion mix.

Component	Volume per reaction (µL)
Reaction buffer	5.1 µL
BSA (10µg/µL)	0.5 µL
Restriction enzyme	0.4 µL
Double distilled water	11 µL
Template	3 µL

2.5.4 Transformation of chemically competent *Agrobacterium tumefaciens* cells

Aliquots of chemically competent *A. tumefaciens* (strain GV3101) cells were transformed with binary plasmids using a thermal shock protocol. The cells were left to thaw at room temperature for five minutes and 5 μL of plasmid DNA was added. The cells were incubated first on ice and then on liquid nitrogen for five minutes. The tubes were then heated in a prewarmed water bath at 37°C for five minutes. 1 mL of liquid YEB medium was added into the tubes and the cells were incubated at 28°C for two hours while shaking at 200rpm. The cells were harvested by centrifugation at 8000g for two minutes and were suspended in 100 μL of supernatant. 10%, 30% and 60% of the suspensions were spread on LB or YEB agar plates containing gentamycin and rifampicin in addition the specific antibiotic for selection of the binary plasmid. The plates were sealed with parafilm and incubated at 28°C degrees for two days. Single colonies were picked from the plates with a sterile pipette tip and inoculated in 4 mL liquid LB medium supplemented with the same antibiotics as those used on the plates. The inoculums were incubated at 28°C overnight and used for plasmid extraction, restriction digest analysis, verification of correct transformation of agrobacteria with plasmid DNA, re-inocculation and then production of glycerol stocks, or for direct preparation of glycerol stocks as described below.

2.5.5 Bacterial glycerol stocks

For direct inoculation of transformed agrobacteria, glycerol stocks were produced. 590 mL of 4 mL overnight bacterial cultures were added into 2 mL screwcap tubes containing 900 mL of 40% glycerol under flow hood. The tubes were mixed by inversion and were snap frozen in liquid nitrogen. Stocks were stored at -80°C for long-term use. A sterile filter tip was used to scrape off some frozen bacterial stock for inoculation into liquid LB or YEB medium.

2.6 In vivo subcellular localisation and co-localisation of fusion proteins

The fluorescent fusion protein constructs 35S::*AtPQLs*::GFP used for *in vivo* subcellular localization were created by Dr Richard Pattison (University of Glasgow) using the

Gateway recombination system (Invitrogen). Vectors used for transient *A. tumefaciens* transformations were provided by Dr. Grefen and Prof. Blatt (University of Glasgow).

2.6.1 Creation of expression clones

Expression clones were created combining a gateway entry clone with an attR containing destination vector using the gateway LR-clonase II (Invitrogen). The LR-recombination reaction mix was made up to a final volume of 2.5 µL. 1 µL (=150 ng) of destination vector and mixed with 1 µL (=150 ng) of entry clone and 0.5 µL of LR-clonase II. The reaction was incubated at room temperature for one hour. 1 µL of the reaction was used to transform *E. coli* cells and positive transformants were verified by restriction digestion as described before. The destination vectors pH7YWG2 and pH7RWG2 were used to create YFP and RFP fusions respectively. Both vectors contain a cauliflower mosaic virus (CaMV) 35S promoter. The destination vector pUBC-Dest including fluorophores was used to create protein fusion constructs with either GFP or YFP driven by the *A. thaliana ubiquitin-10* gene promotor (Grefen *et al.,* 2010). Table 2.9 displays the expression clones created for this thesis.

Table 2.8: Expression clones created in this thesis using Gateway system.

Gene	Entry Clone	Destination vector	Expression clone
*At*PQL4	*pENTR 201 PQL4 NS*	*pH7RWG2*	*pH7YWG2 35S::At*PQL4-*RFP*
		pUBC-DEST	*pUB10::At*PQL4-*GFP*
*At*PQL6	*pENTR 201 PQL6 NS*	*pH7YWG2*	*pH7YWG2 35S::At*PQL6-*YFP*
		pUBC-DEST	*pUB10::At*PQL6-*GFP*

2.6.2 Transient expression of protein fusion constructs in *Nicotiana tabacum*

N. tabacum was used for transient expression of all the constructs using the agroinfiltration method. 4 mL *Agrobacterium* inoculations containing the appropriate construct and antibiotics were grown as described in general methods. Half amount of the cultures were added into 2 mL tubes and centrifuged at 13200g for two minutes. The supernatant was

removed, the other half of the culture was added and the centrifugation step was repeated. The bacteria cells were suspended in 2 mL of transformation buffer (10 mM MgCl2, 100 μM acetosyringone) and centrifuged at 8000g for two minutes. The washing step was repeated three times to remove any residual medium. This was followed by resuspension in 1 mL of transformation buffer to measure the OD_{600}. The final OD_{600} was 0.3 and 0.2 for subcellular localisation and co-localisation respectively. The cell suspensions were left at room temperature for approximately one hour. To infiltrate the *N. tabacum* plants, the underside of a young mature leaf was pierced with a fresh razor blade (without cutting through the tissue) and a 1 mL syringe used to inject the cells. The infiltrated areas of the leaf were marked and the plants were returned to the control growth room (16 hours light, 8 hours darkness; light intensity 100-120 μmol m^{-2} sec^{-1}; temperature approximately 26°C/18°C day/night; relative humidity of 60%/70% day/night) for two to three days before observation under the confocal microscope.

2.6.3 Transient expression of protein fusion constructs in *Arabidopsis*

A. thaliana seeds were surfaced sterilised, incubated at 4°C for two days to ensure stratification and then placed in control growth room under continuous light as described before. Seeds were incubated in six-well plates supplemented with 3 mL of 0.5x MS medium (pH 5.7) for three to four days to allow germination. The whole procedure was performed under the flow hood. *Agrobacterium* inoculations were prepared as described in general methods. Bacteria were pelleted by centrifugation at 4000g at 4°C for fifteen minutes and resuspended in 2 mL sterile transformation buffer (0.5x MS medium, 100 μM acetosyringone, 0.003% sylwet-77). This step was repeated twice and bacteria were finally resuspend in 1 mL of transformation buffer to measure the OD_{600}. A final OD_{600} of 0.1-0.2 was reached by diluting the bacteria in transformation buffer. The growth medium was removed from the six-well plates using 1 mL filter pipetting tip and replaced with 3 mL of *Agrobacterium* suspsension. The plates were resealed and transferred back to the control growth room for two to three days before confocal imaging.

2.6.4 Confocal laser scanning microscopy and analysis

Confocal imaging was performed on a Carl Zeiss CLSM-510-META-UV confocal laser-scanning microscope (Carl Zeiss, Inc., http://www.zeiss.co.uk). 20x lens and 40x immersion oil lenses were used. For visualizing GFP and YFP, an argon ion laser was used. Laser light of 514 nm was used to excite YFP. Reflected light was subsequently

reflected by a secondary NFT490 dichroic mirror and passed through a 530-600 nm bandpass filter to allow collection of fluorescence. For GFP visualization, excitation was at 488 nm and light was reflected by a secondary NFT 545 dichroic mirror. GFP fluorescence was collected as the light passed through a 505 long pass filter. In both cases, emitted light passed through a 635VIS dichroic mirror to allow collection of chloroplast autofluorescence using a META detector of a bandwidth of 621-700 nm.

For co-localisation experiments the settings were slightly altered to minimize potential problems caused by bleed through between the two fluorophores. Sequential acquisition of images in the yellow channel and then green channel was used. YFP fluorescence was collected using the same configuration as that for single expression of fusion proteins. However, for GFP fluorescence detection, excitation occurred at 458 nm and reflected light was collected using a 505-530 bandpass filter.

Control experiments were performed to test for bleed through between the fluorophores. For this purpose, single expression of GFP-tagged proteins were analysed using different confocal microscope configurations. GFP was excited at 458 nm, 488 nm or 514 using a range of light transmission from 1% to 30% and collecting fluorescence using GFP and/or YFP settings. In addition, single expression of YFP-tagged proteins was carried out. Measurements of fluorescence intensity from images (512x512) suggested that false YFP fluorescence was apparent in single expression of GFP-tagged protein as transmission exceeds 20%. However, YFP fluorescence detected in the co-expression experiments was 30.4-fold and 2.81-fold higher than the false YFP fluorescence detected when using 10% and 20% of transmission, respectively. Therefore, the transmission used to visualize GFP and YFP fluorescence in this thesis was from 3% to 10%.

Colocalisation events were evaluated using Zeiss LSM 510 AIM (v3.2) for analyzing line scans and IMAGEJ 1.43u software - particularly the Mander's/Pearson's coefficient plugin created by Tony Collins (Wrigth Cell Imaging Facility, Toronto, Canada) and Wayne Rasband (NIH, USA) – for creating scatter plots based on Pearson's coefficient (http://www.rsbweb.nih.gov/ij).

Chapter 3: Subcellular localisation of *At*PQL2, *At*PQL4 and *At*PQL6.

3.1 Introduction

In this chapter, I will present data for the subcellular localisation of three proteins of the *At*PQL family, *At*PQL2, *At*PQL4 and *At*PQL6. Previous studies have provided evidence for the ER localisation of *At*PQL4 and *At*PQL6 homologous proteins. However, no subcellular localisation data are available for *At*PQL2. The first part presents the subcellular localisation of the three proteins, and the second part presents supporting data showing co-localisation with an organelle marker.

To identify the subcellular localisation of the proteins *Agrobacterium*-mediated transformation was used. *At*PQL proteins fused to green fluorescent protein (GFP) at the C-terminus were transiently expressed in leaf epidermal cells of *N. tabacum*. Expression was under the control of the strong constitutive *35S* promoter (P_{35S}) of cauliflower mosaic virus (CaMV). Figure 3.1 displays a schematic representation of the expression cassette of the plasmids used to express the AtPQL proteins. Analysis of the localisation was carried out using confocal laser microscopy, 72 hours after transformation, when protein expression was expected to be at its maximum.

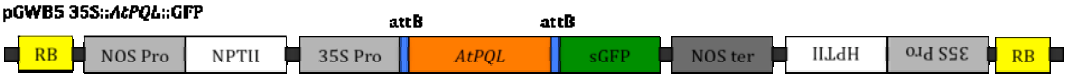

Figure 3.1: Expression cassette of palsmid containing the *At*PQL2, *At*PQL4 and *At*PQL6 gene.

The diagram shows the pGWB5 vector. The Gateway attB recombination sites and plant selectable markers NPTII and HPTII, which confer resistance to hygromycin and kanamycin respectively, are indicated. The position of the coding region relative to the CaMV *35S* promoter, sGFP tag and NOS terminator is also shown. (Figure is taken from PhD thesis by Pattison, 2008)

3.2 Results

3.2.1 Subcellular localisation of *At*PQL2

Confocal images of tobacco epidermal cells transformed with *At*PQL2-GFP fusion protein are presented in Figure 3.2. Frames a-c are projections of image stacks. Frame d is a single plain image and shows the bright field image for frames a-c. GFP fluorescence (shown in

green colour) is visible as a smooth line at the edge of the cell suggesting localisation of *At*PQL2 to the tonoplast. However, without a membrane marker it is difficult to distinguish between plasma membrane and tonoplast. One point, where separation of the plasma membrane from tonoplast appears to take place, is indicated by the arrow in frame b. The green spherical structures observed in frame b were chloroplasts, as indicated in frame c showing chloroplast autofluorescence. Autofluorescence mainly depends on the laser intensity used to visualise the fluorophore. In this particular case, high-intensity light was used to visualise *At*PQL2-GFP resulting in chloroplast fluorescence contributing to the GFP signal. *At*PQL2-GFP fluorescence was detected only in a small number of cells, although a number of various time points (36h, 48h, 72h, 84h) after infiltration were analysed and infiltration of tobacco leaves with *Agrobacterium* at various densities (OD_{600} nm) was tested.

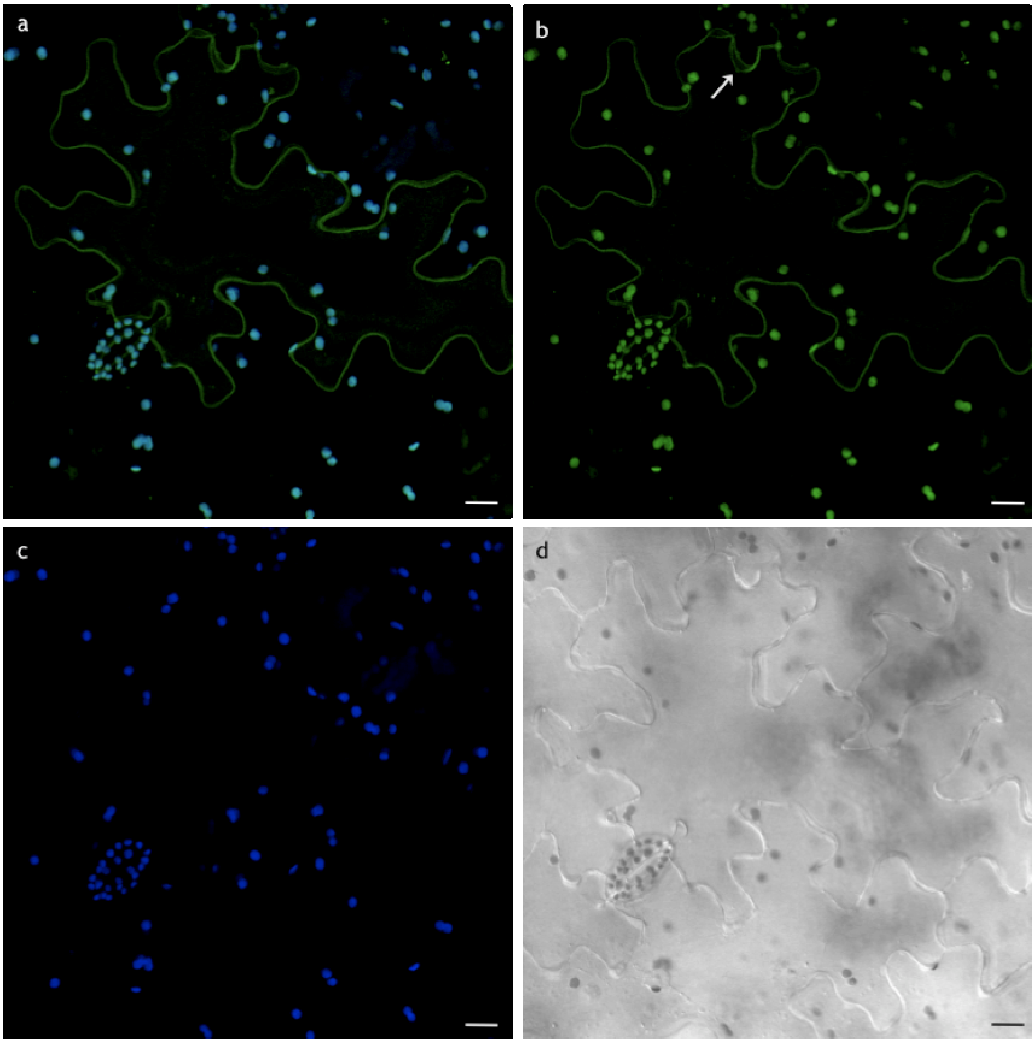

Figure 3. 2.: *At*PQL2 localises to the tonoplast.

Tobacco leaf epidermal cells expressing *At*PQL2-GFP fusion protein. Cells were transformed by agroinfiltration and analyzed by confocal microscopy 72 hours post transformation.
Frames a-c are z-stacks of 9 optical sections of 3.50 µm each and show composite fluorescence (a), GFP fluorescence (b) and chloroplast autofluorescence (c). Frame d is the single plane, bright-field image for a-c. GFP fluorescence labels the tonoplast (arrow).
Scale bar = 10µm

3.2.2 Sub-cellular localisation of *At*PQL4 and *At*PQL6.

Confocal images of tobacco epidermal cells expressing *At*PQL4-GFP and *At*PQL6-GFP fusion proteins are shown in Figures 3.3 and 3.4, respectively. In both figures, frames a-c are single plane images. Frames d-f represents projections of image stacks. The GFP fluorescence signal is shown in green colour in frame e, and frame g is the single plain bright-field image for frames d-f. In contrast to *At*PQL2-GFP, the fluorescence signal of *At*PQL4-GFP and *At*PQL6-GFP was detectable in approximately 50% of the transformed cells. GFP fluorescence was clearly visible in internal compartments forming net-like patterns within the cell (Figure 3.3c and 3.4c). GFP fluorescence also labeled the nuclear envelope that is continuous with the lattice-like network (see arrow in figures 3.3e and 3.4c). Additionally, fluorescence signal was distributed in long fast-moving strands, described as cytoplasmic ER (see arrow in Figures 3.3b and 3.4e). Fluorescence patterns were indicative of typical ER (Fluckiger *et al*., 2003, Sparkes *et al*., 2009) and provide evidence for ER localisation of the *At*PQL4 and *At*PQL6 proteins.

To exclude the possibility of mislocalisation due to overexpression under the control of the strong constitutive P_{35S} promoter, the coding sequences of *At*PQL4 and *At*PQL6 were also expressed as C-terminal fusions to YFP under the control of the *ubiquitin-10* (P_{UBQ10}) promoter that facilitates moderate expression of the transgene (Grefen *et al*., 2010). YFP fluorescence was again detected in typical ER-like patterns (data not shown). In addition, photobleaching experiments showed that both proteins appeared to be highly mobile when imaged during a time series (data not shown).

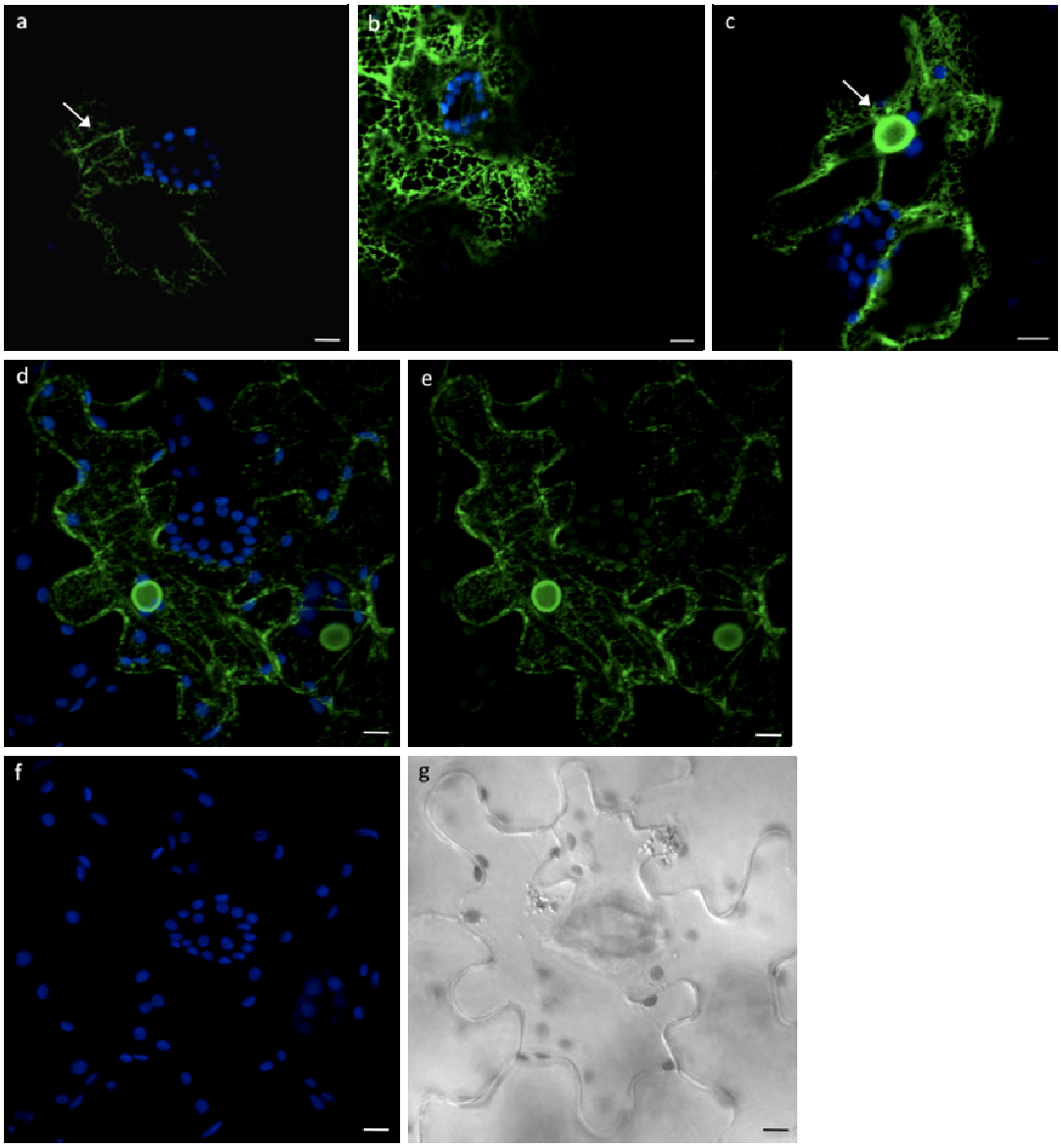

Figure 3.3: *At*PQL4 localises to the ER.

Tobacco leaf epidermal cells expressing *At*PQL4-GFP fusion protein. Cells were transformed by agroinfiltration and analyzed by confocal microscopy 72 hours post transformation.
Frames a-c are single plane images from different cells. Frames e-f are z-stacks of 8 optical sections of 3.50 µm and show composite fluorescence (d), GFP fluorescence (e) and chloroplast autofluorescence (f). Frame g is the single plane, bright-field image for d-f. GFP fluorescence labels the cortical ER (tubules and cisternae), cytoplasmic ER and nuclear envelope (arrows).
Scale bar = 10µm

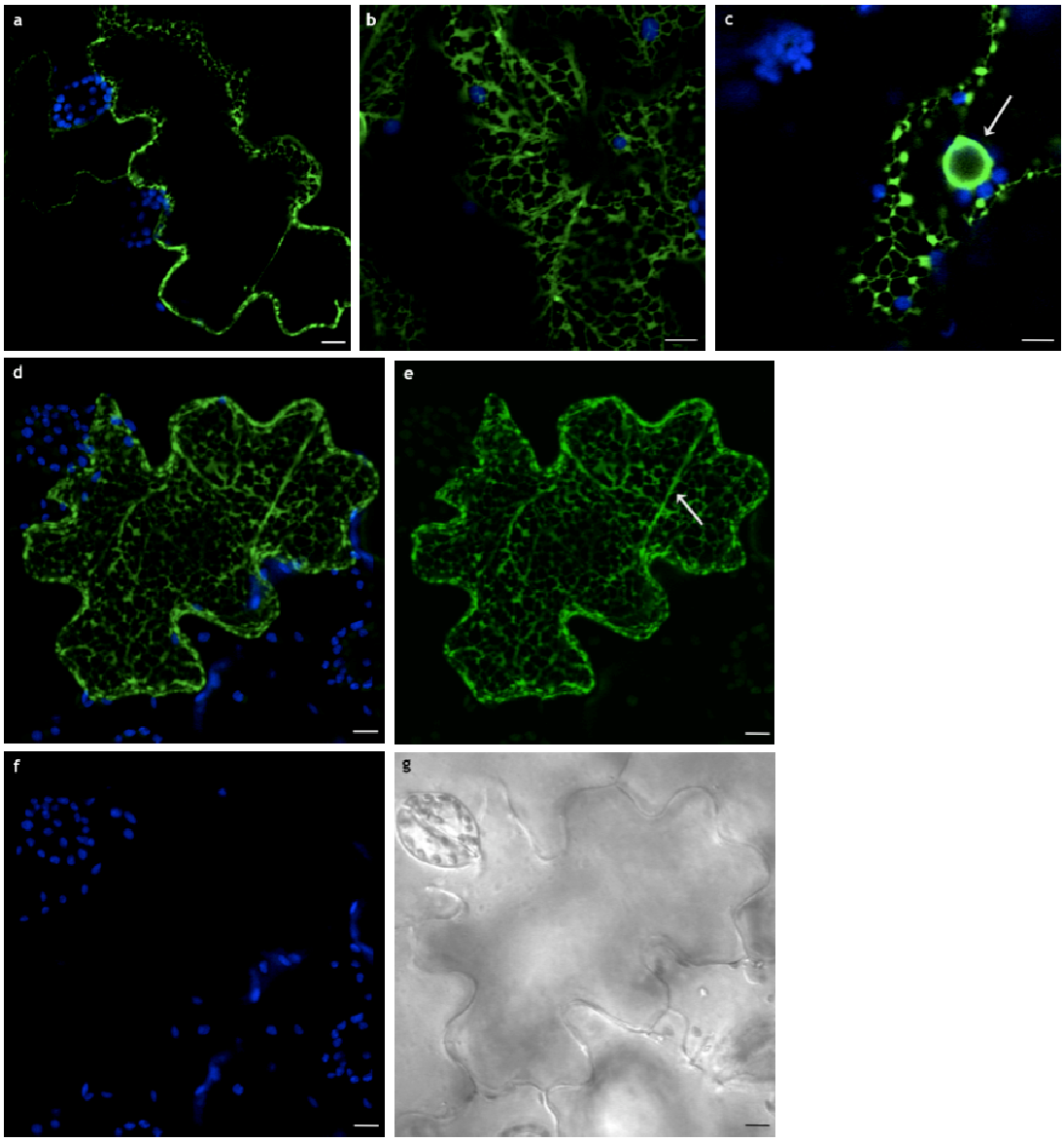

Figure 3.4: *At*PQL6 localises to the ER.

Tobacco leaf epidermal cells expressing *At*PQL6-GFP fusion protein. Cells were transformed by agroinfiltration and analyzed by confocal microscopy 72 hours post transformation.
Frames a-c are single plane images from different cells. Frames e-f are z-stacks of 12 optical sections of 3.50 µm and show composite fluorescence (d), GFP fluorescence (e) and chloroplast autofluorescence (f). Frame g is the single plane, bright-field image for d-f. GFP fluorescence labels the cortical ER (tubules and cisternae), cytoplasmic ER and nuclear envelope (arrows).
Scale bar = 10µm

3.2.3 Co-localisation of *At*PQL4 and *At*PQL6 with ER marker

To confirm the ER localisation patterns of *At*PQL4 and *At*PQL6, the fusion proteins were co-expressed with an ER lumenal marker protein. A construct in which the ER retention signal HDEL was fused to the C-terminus of the yellow fluorescent protein (YFP) was already available in the laboratory. Expression of fusion protein was driven by the strong constitutive P_{35S} promoter. Confocal images of tobacco cells expressing the YFP-HDEL fusion protein are shown in Figure 3.5. Frames a-c are projections of image stacks. Frame d is the single plain bright-field image for frames a-c. YFP fluorescence labelled the typical ER as has been reported in previous studies (Brandizzi *et al*., 2003; Sparkes *et al*., 2009).

For co-localisation experiments tobacco leaves were infiltrated with *Agrobacterium* containing the appropriate constructs at a ratio of 0.2 (OD_{600} nm) (see chapter 2, Molecular cloning procedures section). Figure 3.6 and 3.7 present co-localisation data for *At*PQL4-GFP and *At*PQL6-GFP with YFP-HDEL, respectively. Frames a-e are projections of image stacks. Frame f is the single plain bright-field image for frames a-e. Both GFP and YFP fluorescence signals produced network-like patterns (Figures 6(b,c) and 7(b,c)). Figures 3.6d and 3.7d show merged images that clearly show co-localisation of the two fluorescence signals and confirmed the ER localisation of the two AtPQL proteins. Quantification of the co-localisation events are shown in Figures 3.6g and 3.7g and was achieved by using fluorescence intensity analysis and Pearson's correlation analysis. Fluorescence intensity analysis was performed along a line scan (red arrows, Figure 3.6g and 3.7g). Fluorescence intensities were measured in arbitrary units and plotted against the distance from the origin of the line scan. The coefficient produced by the Pearson's correlation analysis provided evidence for the degree of the co-localisation between the two fluorophores. The value can range from -1 to 1, with 1 indicating complete positive correlation, 0 no correlation and -1 negative correlation (Bolte and Cordelières, 2006). *At*PQL4-GFP and YFP-HDEL co-expression resulted in complete colocalisation (Figure 3.6g). The GFP and YFP fluorescence signals displayed the same intensity patterns and completely overlapped along the line scan. Pearson's correlation analysis also suggested a high degree of co-localisation, with Pearson's coefficient of 0.948. Similarly, co-expression of *At*PQL6-GFP and YFP-HDEL resulted in high co-localisation (Figure 3.7g). Although GFP and YFP fluorescence intensities did differ at some points along the line scan, the two fluorescence signals generally overlapped. A high degree of co-localisation was also evident from the GFP/YFP scatter plot, with a Pearson's coefficient of 0.920.

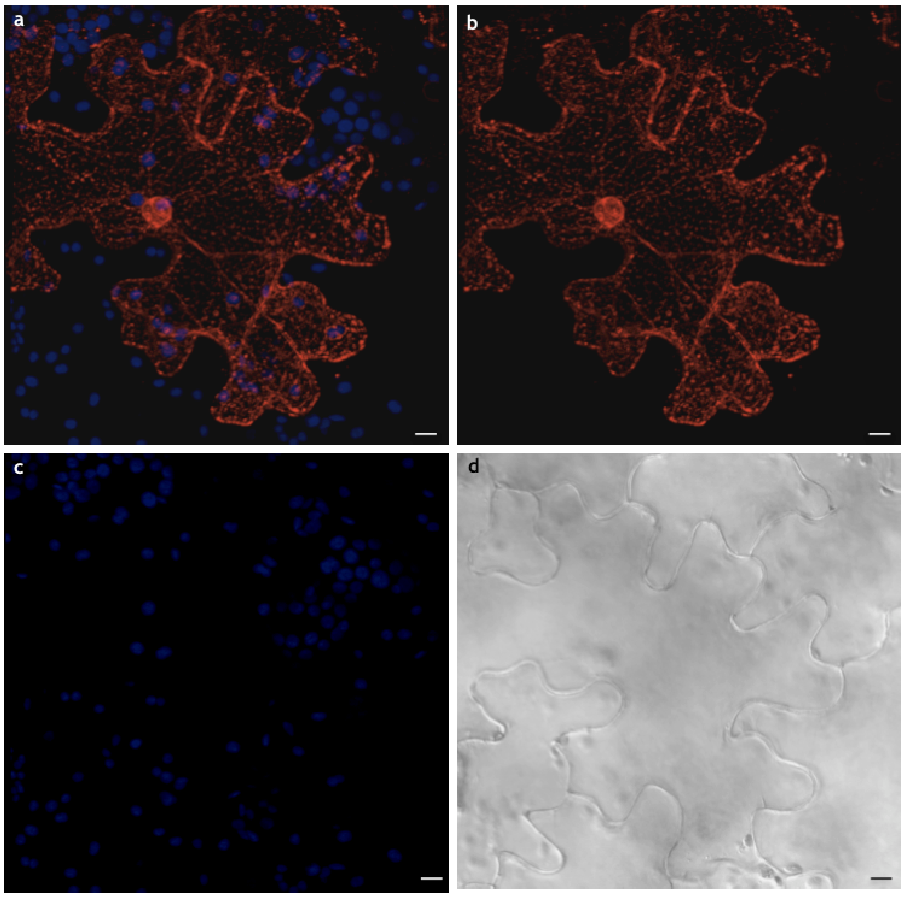

Figure 3.5: HDEL labels the ER.

Tobacco leaf epidermal cells expressing YFP-HDEL fusion protein. Cells were transformed by agroinfiltration and analyzed by confocal microscopy 72 hours post transformation.
Frames a-c are z-stacks of 25 optical sections of 1.15 µm and show composite fluorescence (a), YFP fluorescence (b) and chloroplast autofluorescence (c). Frame d is the single plane, bright-field image for a-c.
YFP fluorescence is distributed across tubular ER, cisternal ER and nuclear envelope.
Scale bar = 10µm

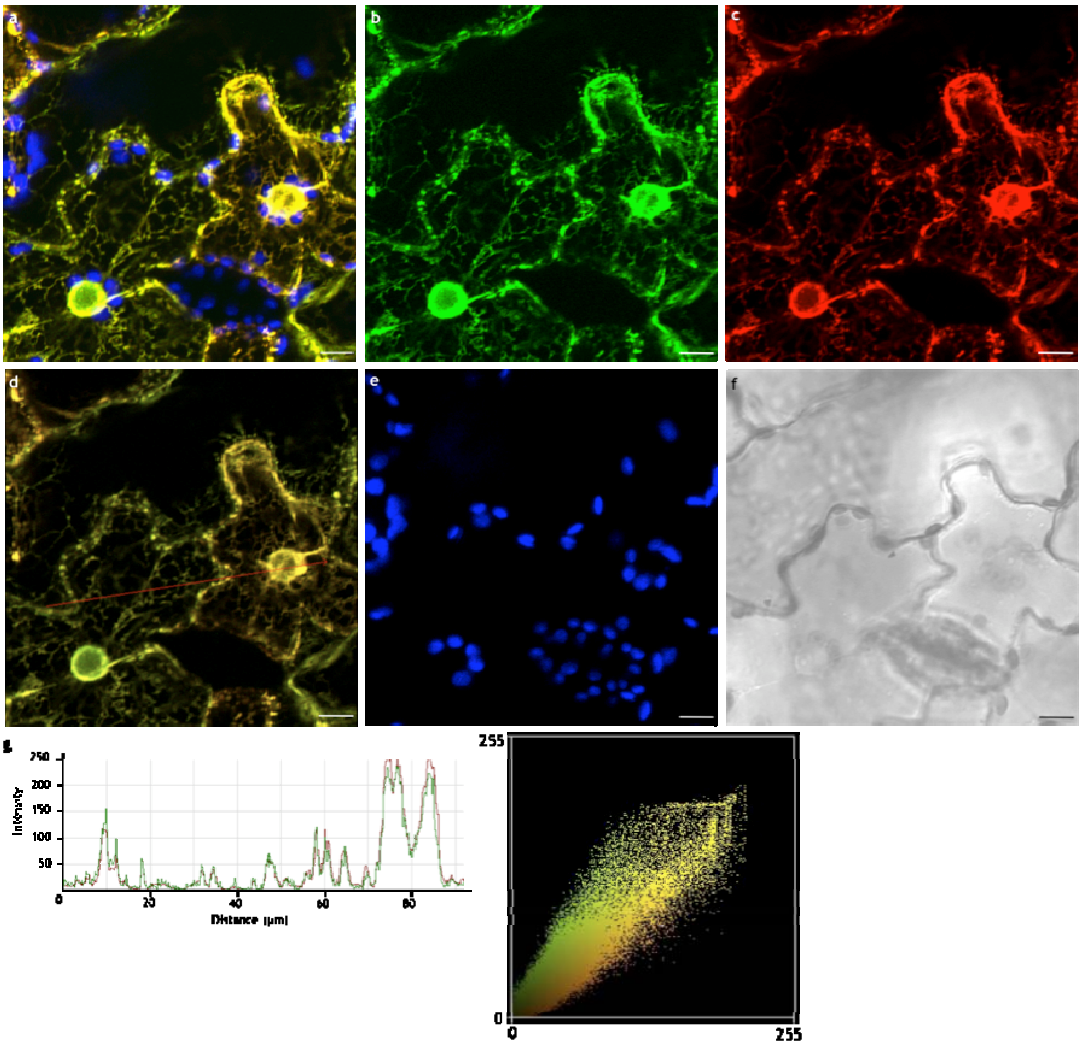

Figure 3.6: Co-localization of *At*PQL4 with ER marker.

Tobacco leaf epidermal cells co-expressing *At*PQL4-GFP and YFP-HDEL. Cells were transformed by agroinfiltration and analyzed by confocal microscopy 72 hours post transformation.
Frames a-e are z-stacks of 19 optical sections of 1.15 µm. Frames show (a) composite fluorescence, (b) GFP fluorescence, (c) YFP fluorescence, (d) GFP and YFP overlay (yellow color) and (e) chloroplast autofluorescence. Frame f is the single plane, bright-field image for a-e. In frame g fluorescence intensities of GFP (green line) and YFP (red line) are plotted against position on a line scan (red arrow). Fluorescence intensity is shown in arbitrary units. GFP/YFP scatter plot for frame d indicating strong positive correlation between two signals (P = 0.948). GFP and YFP co-localise to cortical ER and nuclear envelope.
Scale bar = 10µm

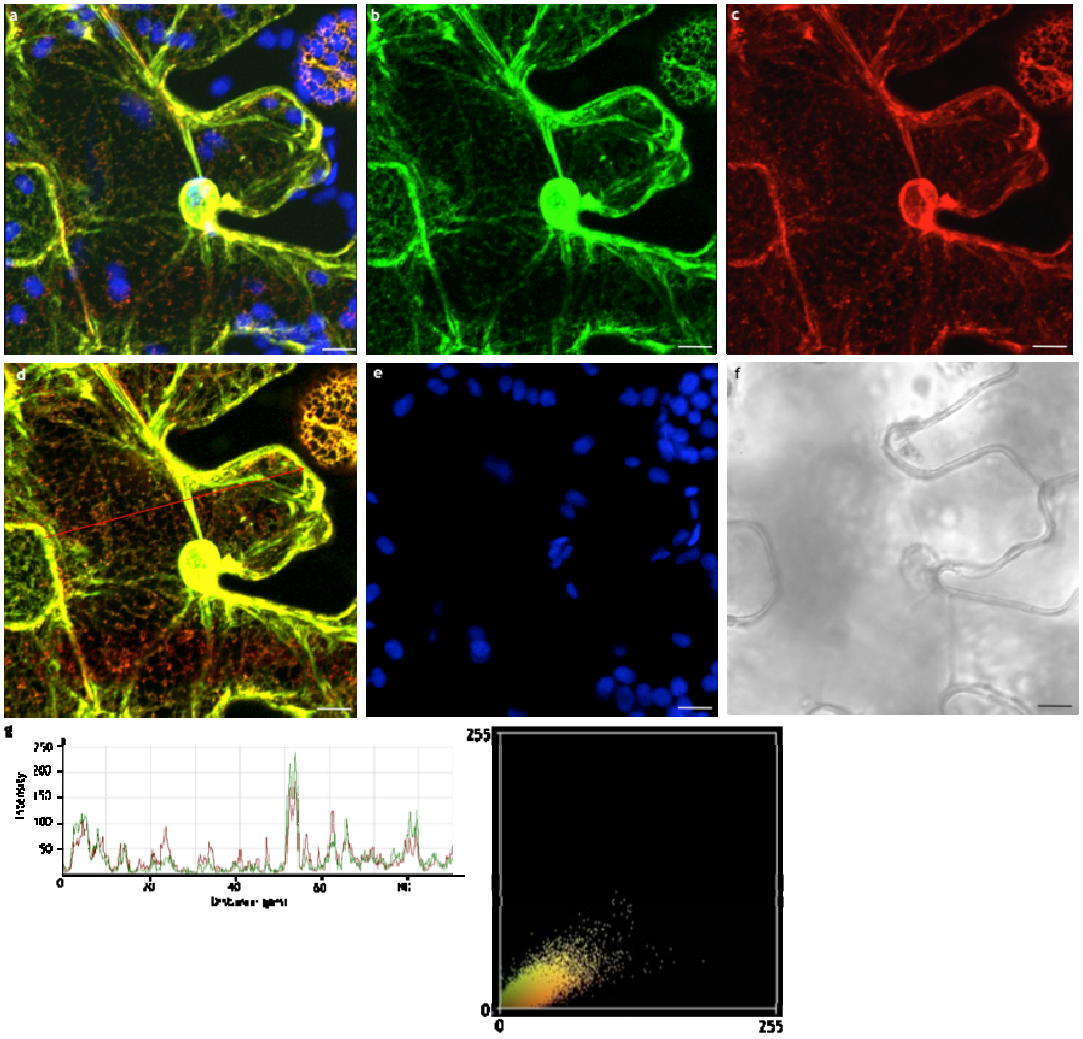

Figure 3.7: Co-localization of *At*PQL6 with ER marker.

Tobacco leaf epidermal cells co-expressing *At*PQL6-GFP and YFP-HDEL. Cells were transformed by agroinfiltration and analyzed by confocal microscopy 72 hours post transformation.
Frames a-e are z-stacks of 20 optical sections of 1.15 µm. Frames show (a) composite fluorescence, (b) GFP fluorescence, (c) YFP fluorescence, (d) GFP and YFP overlay (yellow color) and (e) chloroplast autofluorescence. Frame f is the single plane, bright-field image for a-e. In frame g fluorescence intensities of GFP (green line) and YFP (red line) are plotted against position on a line scan (red arrow). Fluorescence intensity is shown in arbitrary units. GFP/YFP scatter plot for frame d indicating strong positive correlation between two signals (P = 0.920). GFP and YFP co-localise to cortical ER, cytoplasmic ER and nuclear envelope.
Scale bar = 10µm

3.3 Discussion

3.3.1 Subcellular localisation of *At*PQL2 protein

The subcellular localisation data for *At*PQL2-GFP provide the first in vivo evidence for tonoplast localisation. The results are consistent with the previously detected tonoplast localisation of *At*PQL1, which is a close homologue of the *At*PQL2 (Pattison, 2008). To confirm the tonoplast localisation, co-localisation experiments using tonoplast marker proteins, such as TIP3;1 and TIP2, were carried out. Although the statistical analysis of colocalisation of *At*PQL2-GFP with TIP2-YFP suggested a high degree of colocalisation, this result was only obtained once as the detection of *At*PQL2-GFP fusion protein was very rare. The absence of fluorescence signal might be the result of the strong constitutive P_{35S} promoter. Overexpression of fusion proteins in combination with the *Agrobacterium*-mediated transformation might trigger post-transcriptional gene silencing (Johansen and Carrington, 2001; Mishiba *et al*., 2005). For this reason, experiments using gene silencing suppressors might facilitate the expression of *At*PQL2-GFP fusion protein. In addition, expression of fluorescent-tagged *At*PQL2 protein under the control of a weak or even better its native promoter could be more effective and might allow co-localisation data with fluorescent-tagged marker proteins. An equivocal tonoplast localisation of *At*PQL1 and *At*PQL2 argues against previously reported plasma membrane localisation of STM1, a GPCR protein from *S. pombe*, which is the closest homologue of these two proteins (see chapter 1). In line with its speculated function as a GPCR, STM1 was proposed to be localised in the plasma membrane with its N-terminus facing the extracellular space, where it can bind external ligands (Chung *et al*., 2001). It will therefore be worthwhile to co-express *At*PQL2 with a plasma marker protein to exclude the possibility of plasma membrane localisation.

3.3.2 Subcellular localisation of *At*PQL4 and *At*PQL6 proteins

Confocal microscopical analysis of *At*PQL4-GFP and *At*PQL6-GFP proteins showed in typical ER pattern. The term “typical ER” refers to nuclear envelope and cortical ER. The latter describes the interconnected membrane system formed by two distinct domains of ER: the cisternae and the tubules. Tubules can extend and fuse by three-way junctions forming polygonal networks. Loss of the high angle curvature of the polygon results in the formation of flattened membrane sheets, known as cisternae (Sparkes *et al*., 2009). The cortical ER is subject to dynamic modifications depending on the physiological conditions.

For instance, overexpression of GFP-tagged calnexin resulted in enlargment of cisternae (Runions *et al*., 2006). In addition, pathogen attacks induced cisternalisation. Takemoto *et al*. (2003) showed that upon inoculation of *A. thaliana* cotyledons with oomycete pathogens, more cisternae were formed. This shift to the cisternal form of the ER might be the consequence of increased production of proteins and lipids required for a defence response. Similar ER modifications have been observed under a range of stresses, such as temperature, radiation and water stress (Quader and Zachariadis, 2006). Moreover, the cortical ER network is in close proximity to the plasma membrane and is also continuous with the outer nuclear envelope. It was suggested that the outer nuclear envelope functions as a distinct ER domain that regulates the exchange of proteins between the nucleus and ER (Quader and Zachariadis, 2006). The outer nuclear envelope also controls the flow of membrane lipids required for the quick and proper reassembly of the nuclear envelope during the last stages of cell division (Staehelin, 1997; Quader and Zachariadis, 2006). The *At*PQL6-GFP fluorescence signal also stained another distinct domain of the ER, the cytoplasmic ER. The cytoplasmic ER describes the long fast-moving strands that extend the ER membrane to distant cellular locations such as the vacuole (Sparkes *et al*., 2009).

The ER localisation of *At*PQL4 and *At*PQL6 supports the notion that they might have a similar function as their closest characterised homolog MPDU1. The human MPDU1 is considered to be a chaperone required for utilisation of Man/Glc-P-Dol as sugar donors in glycosylation (Anand *et al*., 2001). Although experimental data confirming ER-localisation of MPDU1 have not been published, ER localisation is assumed, as Man/Glc-P-Dol is synthesised and utilised in the ER. ER localised fluorescence of both GFP-tagged *At*PQL proteins was additionally confirmed by co-localisation with YFP-HDEL fusion protein. The tetrapeptide Lys-Asp-Glu-Leu (KDEL) in mammals and His-Asp-Glu-Leu (HDEL) in the yeast *S. cerevisiae* have been shown to facilitate retention of proteins in the ER (Pelham, 1990). Reticuloplasmins, which are soluble proteins that function and reside in the luminal ER, carry the tetrapeptide H/KDEL at the C-terminus (Pagny *et al*., 1999, Frigerio *et al*., 2001). Reticuloplasmins escaping from ER are retrieved back to it by the action of a receptor that recognises the H/KDEL signal. In mammals, the receptor is distributed along the intermediate compartment between ER and Golgi apparatus and the early Golgi stacks (Griffith *et al*., 1994). The retrieval of reticuloplasmins from post-ER compartments has been suggested, as proteins residing in the ER were found to have undergone N-glycan modifications that occur in such compartments. For instance, addition of the KDEL signal to the lysosomal glycoprotein, cathepsin D, caused the protein to localise to the ER, but it also carried the N-acetylglucosamine-1-phosphate glycan that is

formed in the *cis*-Golgi compartment (Pelham, 1990). However, the distance over which ER retrieval occurs and the role of the HDEL/KDEL receptor in plants is under debate (Pagny *et al*., 2000; Frigerio *et al*., 2001). The results from the co-localisation experiments with YFP-HDEL provided evidence for the ER localisation of *At*PQL4 and *At*PQL6 proteins. However, the observed degree of co-localisation was surprising. The *At*PQLs are membrane proteins and would be expected to integrate into the ER membrane, whereas YFP-HDEL is a soluble protein residing in the ER lumen. Furthermore, while localisation of AtPQL4-GFP and *At*PQL6-GFP to typical ER is plausible, YFP-HDEL was expected to be constricted to discrete parts of the ER network.

It would be useful to perform co-expression of the *At*PQL4 and *At*PQL6 proteins with a marker protein that resides in the ER membrane. Such a marker could be the ER membrane-bound protein calnexin, a lectin-like protein promoting the correct folding of glycoproteins (Helenius, 1994). Moreover, beside the nuclear envelope that serves as a distinct ER domain (as explained above), there are several other functional domains within the ER network (Sparkes *et al*., 2009). For instance, ER exit sites (ERES) are defined as sites where anterograde protein transport from ER to Golgi takes place. Several proteins are involved in this process, such as the Sar1p guanosine triphosphatase (GTPase), Sec12 and the coat protein (COP)II components Sec24/Sec23 and Sec13/Sec31 (Hawes *et al*., 2008). Such proteins can be used as markers for ERES. Co-expression of *At*PQL4 and *At*PQL6 proteins with proteins that reside and function in discrete subdomains of the ER may provide further insights into the specific localisation and function of the two *At*PQL proteins. Finally, it would be reasonable to investigate the localisation of the *At*PQL proteins in *A. thaliana* to exclude any possibility of mislocalisation due to heterologous expression. Unfortunately, infiltration of Arabidopsis seedlings with fluorescent-tagged *At*PQL proteins was not successful. Despite using a range of *Agrobacterium* densities and observation by confocal laser scanning microscopy at different time points, the fluorescence signal to noise ratio in the seedlings was very low making subcellular localisation very difficult.

In conclusion, the results presented in this chapter provide new information on the subcellular localisation of the three *At*PQL proteins. They suggest localisation of *At*PQL2 to the tonoplast implying functional similarity with its homolog, *At*PQL1. In addition, they confirm localisation of *At*PQL4 and *At*PQL6 to the ER, supporting an involvement of these proteins in glycosylation and/or other ER.

Chapter 4: Effect of overexpressing *At*PQL4 and *At*PQL6 on the intracellular targeting of other proteins.

4.1 Introduction

The previous chapter presented evidence for the subcellular localisation of *At*PQL4 and *At*PQL6 proteins to the ER obtained by the co-localisation of either AtPQL protein with an ER marker protein. However, these experiments did not exclude the possibility of residual localisation to other membranes. To assess other subcellular locations, the plasma membrane protein AtSYP121, the tonoplast proteins *At*TIP2 (δ-TIP) and *At*TIP3;1 (α-TIP) and the glycoproteins EFR and FLS2 were obtained as fusion proteins with GFP or YFP. Transient *Agrobacterium*-mediated transformation of tobacco through leaf infiltration was used. Epidermal cells were analysed by using confocal laser scanning microscopy, 72 hours post transformation.

4.2 Results

4.2.1 Co-localisation with membrane marker proteins

*At*SYP121 is a member of the Soluble N-ethylmaleimide-Sensitive Fusion Protein Attachment Protein Receptor (SNARE) superfamily in *Arabidopsis*. *At*Syp121 resides at the plasma membrane where it functions in positioning of the Shaker channel KAT1 and in non-host resistance against barley powdery mildew fungi (Bassham & Blatt, 2008). In the plasma membrane of root cells *At*Syp121 forms a complex with KC1 and AKT1 (Honsbein *et al*., 2009). Confocal images of tobacco leaf epidermal cells transformed with SYP121-YFP fusion protein are presented in Figure 4.1. Frames a-c are projections of image stacks. Frame d is the single plain, bright-field image for frames a-c. YFP fluorescence (shown in red colour, frame b) was visible at the periphery of the cell. Fluorescent-tagged SYP121 protein was previously shown to localise to the plasma membrane in transient expression experiments (Uemura *et al*., 2004; Honsbein *et al*., 2009; Kato *et al*., 2010). High intensity laser light was required for detection of the YFP fluorescence signal, since expression under the control of P_{UBQ10} promoter was weak. Consequently, strong chloroplast autofluorescence is also seen (frame c).

Confocal images of tobacco epidermal cells co-expressing *At*PQL4-GFP or *At*PQL6-GFP with SYP121-YFP are shown in Figure 4.2 and 4.3, respectively. The frames a-e are projections of image stacks and frame f is the corresponding bright-field image. GFP fluorescence (shown in green colour) was localised at the ER, as expected (Figure 4.2b and 4.3b). Surprisingly, when co-expressed with *At*PQL4-GFP or *At*PQL6-GFP, YFP fluorescence (shown in red colour), deriving from SYP121-YFP, also labelled the ER network and the nuclear envelope (Figure 4.2c and 4.3c). Frame d displays an overlay of the two fluorescence signals, and regions where the two signals co-localise appear in yellow colour.

Fluorescence intensity analysis and Pearson's correlation analysis confirmed the co-localisation. In Figure 4.2, the GFP/YFP scatter plot indicates a good correlation of GFP and YFP fluorescence signals, with a Pearson's coefficient of 0.702. In addition, Figure 4.2g shows a high degree of co-localisation of the two fusion proteins at the nuclear envelope. Figure 4.2h also shows that the two fluorescence signals mostly overlapped. However, there were points along the line scan where they appear to be discrete. This might be due to the strong chloroplast autofluorescence signal that is shown in Figure 4.2c. Similar quantitative results were gained for the co-localisation experiments of *At*PQL6-GFP with SYP121-YFP (Figure 4.3g). As evident from the fluorescent intensity graph, the two fluorescence signals appeared to overlap along the greatest part of the line scan. Similarly, the GFP/YFP scatter plot showed a positive correlation of the two fluorescence signals, with a Pearson's coefficient of 0.720.

EFR-GFP and FLS2-GFP fusion proteins (provided by Zipfel, JIC) had previously been shown to localise to the plasma membrane when expressed in *Arabidopsis* roots. Unfortunately, it was not possible to express these proteins in tobacco. Despite several modifications of the protocol, very few cells expressed the fusion proteins and GFP fluorescence was very low.

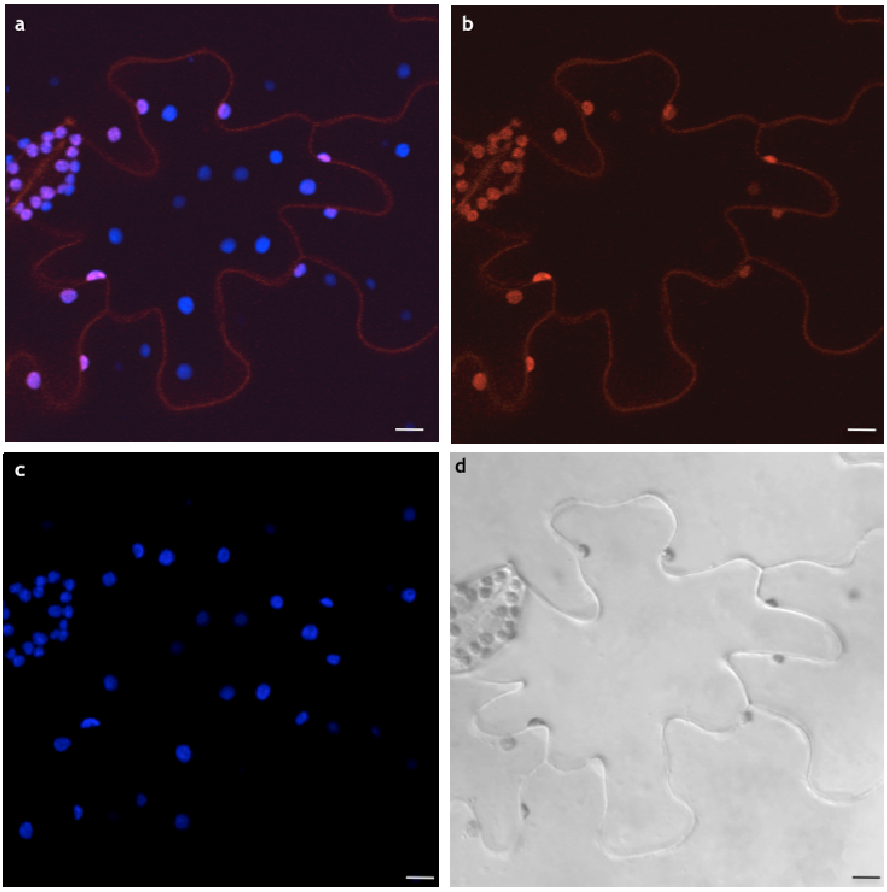

Figure 4.1: SYP121-YFP labels the plasma membrane.

Tobacco leaf epidermal cells expressing SYP121-YFP fusion protein. Cells were transformed by agroinfiltration and analyzed by confocal microscopy 72 hours post transformation.
Frames a-c are z-stacks of 15 optical sections of 1.46 µm. Frames show (a) composite fluorescence, (b) YFP fluorescence and (c) chloroplast autofluorescence. Frame d is the single plane, bright-field image for a-c. GFP fluorescence labels the plasma membrane.
Scale bar = 10µm

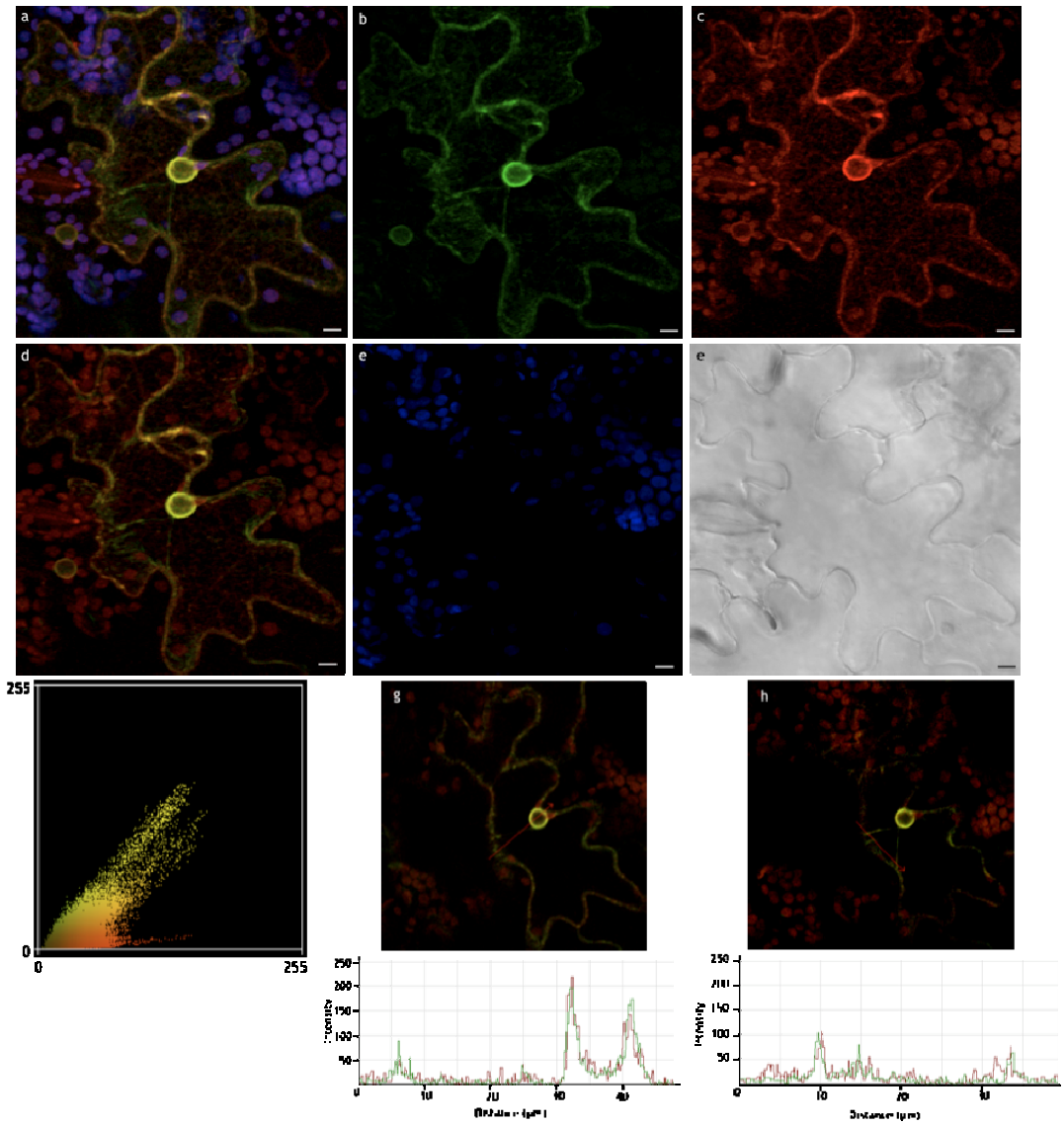

Figure 4.2: SYP121-YFP co-expressed with *At*PQL4-GFP localises to the ER.

Tobacco leaf epidermal cells co-expressing *At*PQL4-GFP and SYP121-YFP. Cells transformed by agroinfiltration and analyzed by confocal microscopy 72 hours post transformation.
Frames a-e are z-stacks of 20 optical sections of 1.46 µm. Frames show (a) composite fluorescence, (b) GFP fluorescence, (c) YFP fluorescence, (d) GFP and YFP overlay (yellow color) and (e) chloroplast autofluorescence. Frame f is the single plane, bright-field image for a-e. In frame g and h fluorescence intensities of GFP (green line) and YFP (red line) are plotted against position on a line scan (red arrows). Fluorescence intensity is shown in arbitrary units. GFP/YFP scatter plot for frame d indicating positive correlation between two signals (P = 0.702). GFP and YFP co-localise to cortical ER, cytoplasmic ER and nuclear envelope.
Scale bar = 10µm

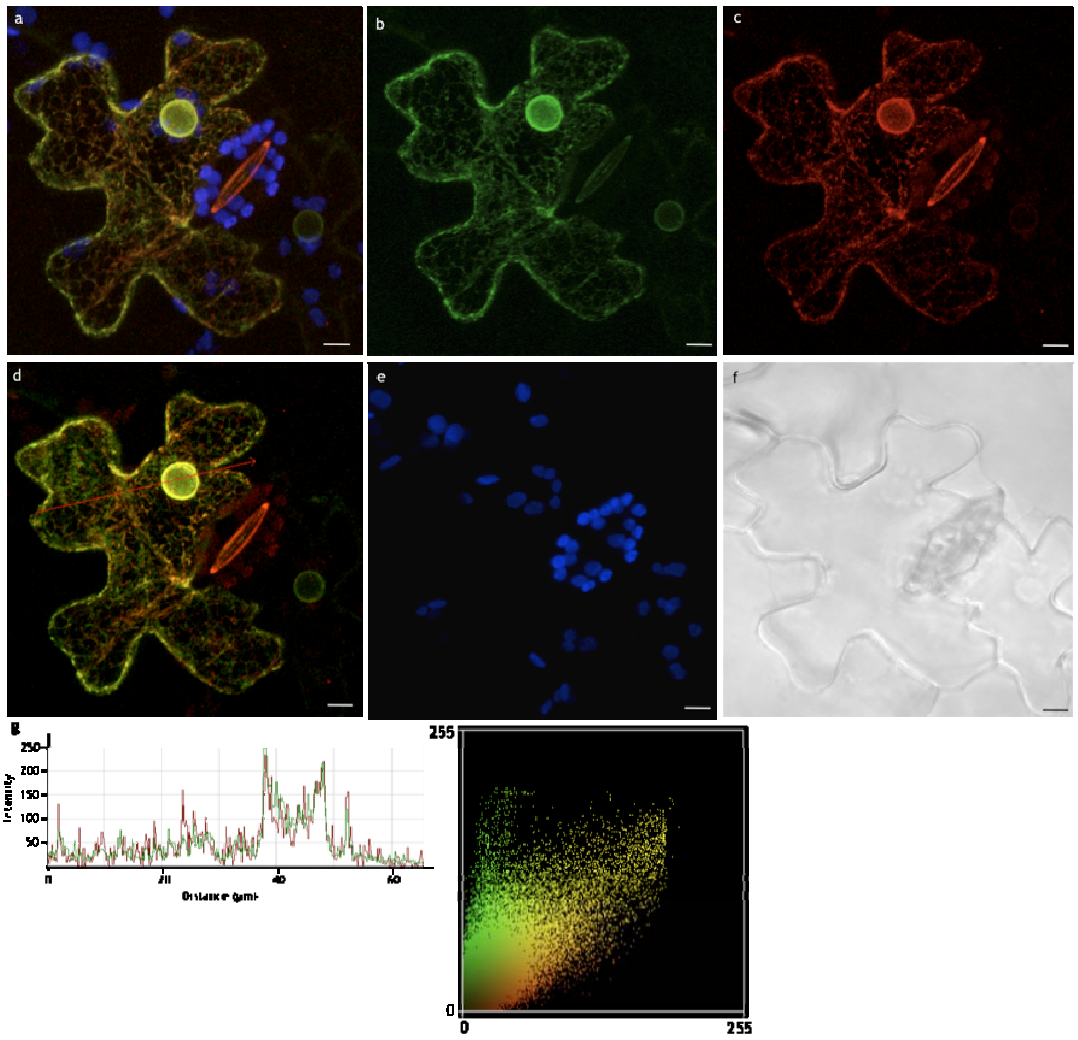

Figure 4.3: SYP121-YFP co-expressed with *At*PQL6-GFP localises to the ER.

Tobacco leaf epidermal cells co-expressing *At*PQL6-GFP and SYP121-YFP. Cells transformed by agroinfiltration and analyzed by confocal microscopy 72 hours post transformation.
Frames a-e are z-stacks of 26 optical sections of 1.46 µm. Frames show (a) composite fluorescence, (b) GFP fluorescence, (c) YFP fluorescence, (d) GFP and YFP overlay (yellow color) and (e) chloroplast autofluorescence. Frame f is the single plane, bright-field image for a-e. In frame g fluorescence intensities of GFP (green line) and YFP (red line) are plotted against position on a line scan (red arrow). Fluorescence intensity is shown in arbitrary units. GFP/YFP scatter plot for frame d indicating positive correlation between two signals (P = 0.720). GFP and YFP co-localises to cortical ER and nuclear envelope.
Scale bar = 10µm

4.2.2 Co-localisation with tonoplast marker proteins

Co-localisation of either *At*PQL4 or *At*PQL6 protein with SYP121 resulted in the ER retention of the latter. The question arises whether this phenomenon is specific for SYP121. Therefore, I performed colocalisation experiments expressing the two *At*PQL proteins with the tonoplast marker proteins, TIP2 and TIP3;1. Tonoplast intrinsic proteins (TIPs) function as aquaporins to regulate the transport of water and other molecules across the tonoplast (Jauh *et al*., 1999; Gattolin *et al*., 2009). YFP fusion constructs for these vacuolar markers were already available in the lab. Figure 4.4 show tobacco leaf epidermal cells overexpressing TIP2-YFP. Frames a-c are projections of image stacks and frame d represents the brightfield for a-c. In agreement with previous studies (Hunter *et al*., 2007), YFP fluorescence (shown in red colour) was found at the tonoplast (frame b). The YFP fluorescence also appeared in small spherical structures (see arrow), known as bulbs, which are a typical feature of tonoplast labeling. Little is known about the function of these structures, but a role as reservoir of membranes to facilitate vacuole expansion and/or as distinct vacuolar subregion, where hydrolytic activities occur, has been proposed (Saito *et al*., 2002; Hunter *et al*., 2007).

Tobacco cells co-expressing TIP2-YFP with either *At*PQL4-GFP or *At*PQL6-GFP are presented in Figures 4.5 and 4.6, respectively. Frames a-e are projections of image stacks. Frame f is the brightfield image for frames a-e. As shown before, *At*PQL4 and *At*PQL6 proteins are localised in ER. YFP fluorescence is also seen in a lattice-like network and the nuclear envelope suggesting ER localization for TIP2 when co-expressed with *At*PQL4 and *At*PQL6 (Figures 4.5c and 4.6c). Co-localisation (appearing in yellow color) of the fusion proteins is more obvious in the merged images (Figures 4.5d and 4.6d). Figure 4.5g shows the fluorescence intensity graph, in which the fluorescence signals derived from TIP2-YFP and PQL4-GFP follow the same pattern. The overall higher intensity of YFP fluorescence is due to the higher-intensity laser light required to excite TIP2-YFP. In addition, the GFP/YFP scatter plot indicates a positive correlation of *At*PQL4-GFP and TIP2-YFP, with a Pearson's coefficient of 0.755. The fluorescence intensity graph for the *At*PQL6-GFP and TIP2-YFP co-localisation event was more complex, but considerable overlap along the line scan of the two fluorescence signals was detected (Figure 4.6g). Positive correlation of GFP and YFP fluorescence signals is also evident in the GFP/YFP scatter plot, with a Pearson's coefficient of 0.850.

Colocalisation experiments of the two GFP-tagged *At*PQL proteins were also performed with TIP3;1-YFP (data not shown) and similar results were obtained, as TIP2. Thus, co-expression with PQL4 or PQL6 leads to ER retention of both tonoplast intrinsic proteins.

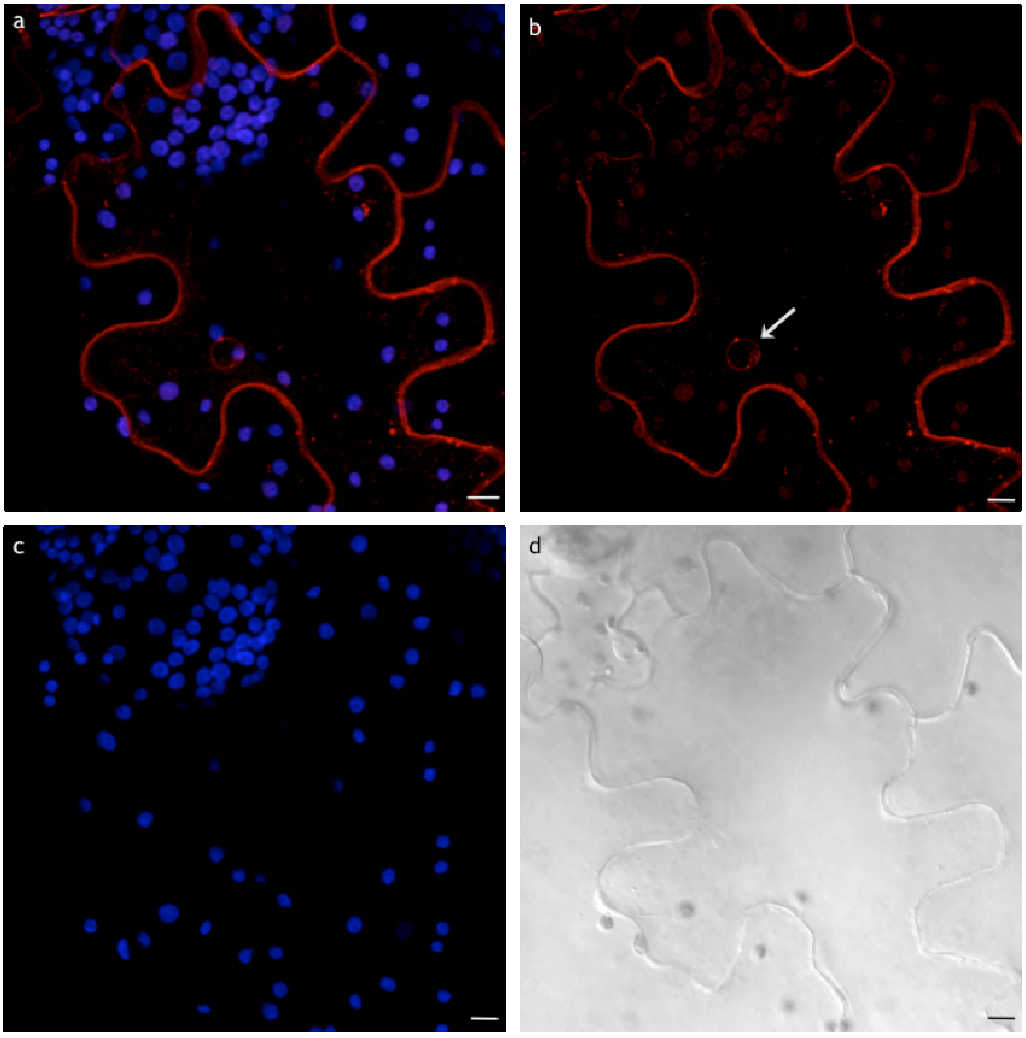

Figure 4.4: TIP2-YFP labels tonoplast.

Tobacco leaf epidermal cells expressing TIP2-YFP fusion protein. Cells were transformed by agroinfiltration and analyzed by confocal microscopy 72 hours post transformation.
Frames a-c are z-stacks of 30 optical sections of 1.46 µm and show (a) composite fluorescence, (b) YFP fluorescence and (c) chloroplast autofluorescence. Frame d is the single plane, brightfield image for a-c. YFP fluorescence labels the tonoplast.
Scale bar = 10µm

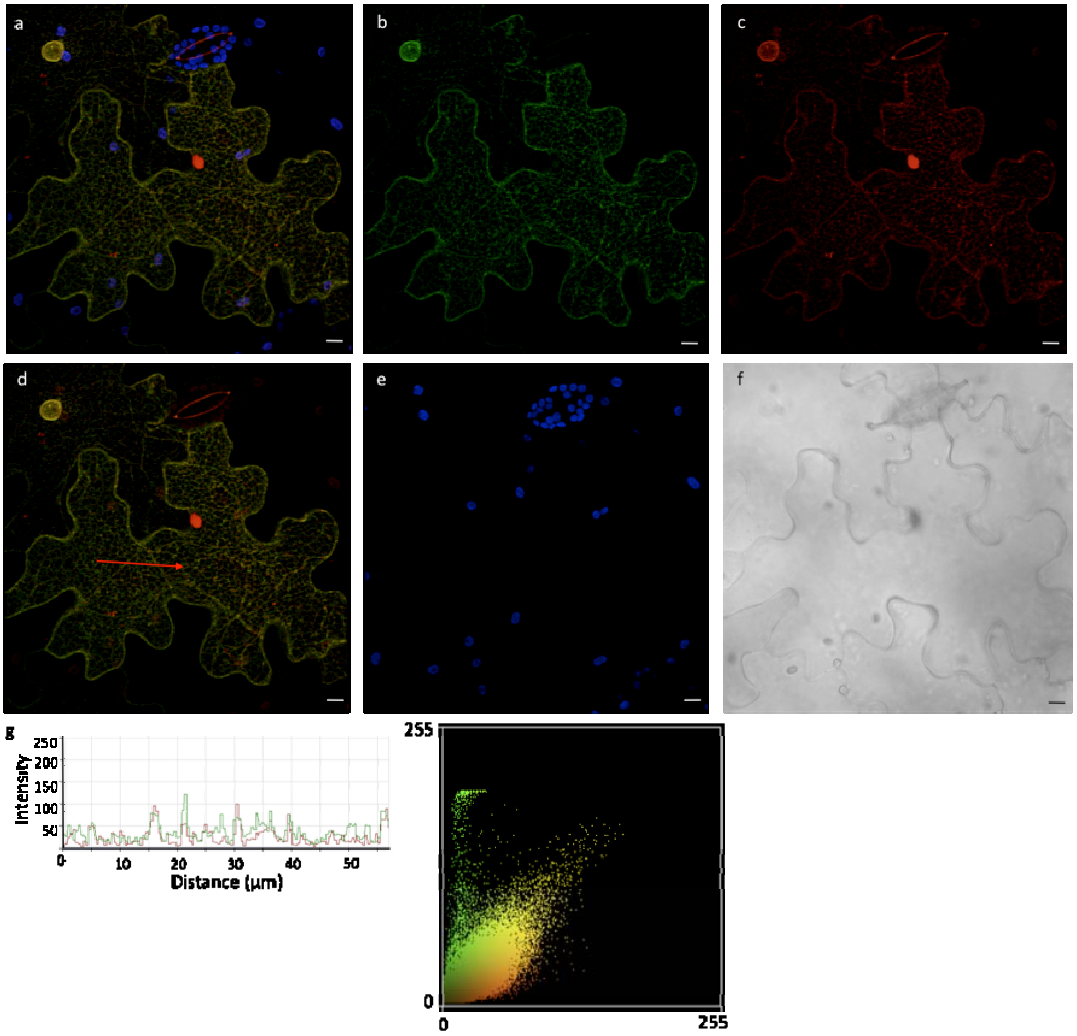

Figure 4.5: TIP2-YFP co-expressed with *At*PQL4-GFP localises to the ER.

Tobacco leaf epidermal cells co-expressing *At*PQL4-GFP and TIP2-YFP. Cells transformed by agroinfiltration and analyzed by confocal microscopy 72 hours post transformation.
Frames a-e are z-stacks of 20 optical sections of 1.46 µm. Frames show (a) composite fluorescence, (b) GFP fluorescence, (c) YFP fluorescence, (d) GFP and YFP overlay (yellow color) and (e) chloroplast autofluorescence. Frame f is the single plane, brightfield image for a-e. In frame g fluorescence intensities of GFP (green line) and YFP (red line) are plotted against position on a line scan (red arrows). Fluorescence intensity is shown in arbitrary units. GFP/YFP scatter plot for frame d indicating positive correlation between two signals (P = 0.745). GFP and YFP colocalises to cortical ER, cytoplasmic ER and nuclear envelope.
Scale bar = 10µm

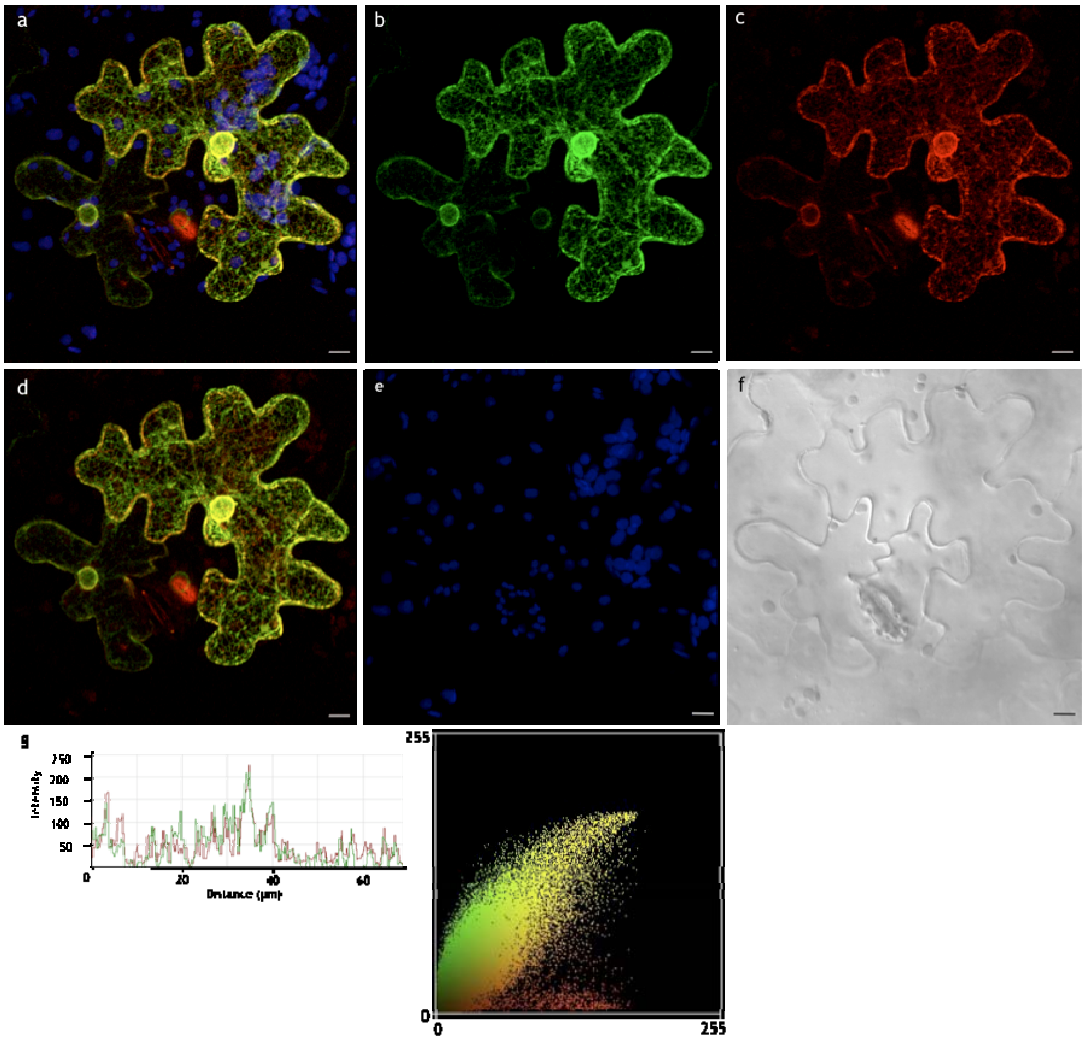

Figure 4.6: TIP2-YFP co-expressed with *At*PQL6-GFP localises to the ER.

Tobacco leaf epidermal cells co-expressing *At*PQL6-GFP and TIP2-YFP. Cells transformed by agroinfiltration and analyzed by confocal microscopy 72 hours post transformation.
Frames a-e are z-stacks of 22 optical sections of 1.46 µm. Frames show (a) composite fluorescence, (b) GFP fluorescence, (c) YFP fluorescence, (d) GFP and YFP overlay (yellow color) and (e) chloroplast autofluorescence. Frame f is the single plane, brightfield image for a-e. In frame g fluorescence intensities of GFP (green line) and YFP (red line) are plotted against position on a line scan (red arrows). Fluorescence intensity is shown in arbitrary units. GFP/YFP scatter plot for frame d indicating positive correlation between two signals (P = 0.850). GFP and YFP colocalises to cortical ER, cytoplasmic ER and nuclear envelope.
Scale bar = 10µm

4.3 Discussion

4.3.1 Co-localisation of *At*PQL4 and *At*PQL6 proteins with SYP121

SNARES are thought to have an important role in membrane trafficking facilitating the flow of proteins and other molecules across the endomembrane system. The SNARE SYP121 in *Arabisopsis* has been shown to be involved in K^+ channel trafficking. Studies using the dominant negative cytosolic Sp2 fragment showed that traffic of KAT1 to the plasma membrane is facilitated by SYP121 (Sutter *et al*., 2006b). Additionally, SYP121 promotes gating of other K^+ channels, such as the K^+ inward-rectifying channel AKT1. Honsbein *et al*. (2009) demonstrated that SYP121 directly and selectively interacts with KC1 to enable assembly of SYP121 with AKT1 forming a tripartite SNARE-K^+ complex at the plasma membrane. Root hair protoplasts of *Arabidopsis syp121*, *akt1* and *kc1* mutants showed a decrease in K^+ inward current and net K^+ uptake. These results imply a role of SYP121 in plant K^+ nutrition. Moreover, SYP121 forms a tetrameric complex with VAMP722 and SNAP33 to promote secretion of antifungal compounds at the site of penetration of powdery mildew fungi (Kwon *et al*., 2003). *Arabidopsis syp121* mutants have been shown to be more sensitive to the barley powdery mildew demonstrating a specific role of SYP121 in non-host resistance (Bassham and Blatt, 2008).

Co-expression of SYP121 with *At*PQL4 or *At*PQL6 resulted in its retention in the ER. Several reports in the literature have demonstrated occasional localisation of SYP121 to intracellular compartments beside the plasma membrane. Kato *et al*. (2010) reported that in stable transformed *Arabidopsis* seedlings grown under dark conditions, the GFP-SYP121 fusion protein localised to the vacuole. Also, studies using the GFP-tagged tobacco homolog of SYP121, *Nt*Syr1-GFP, showed localisation of the fusion protein in ER and other small internal compartments (Di Sansebastaino *et al*., 2006). With time progressing, these observations changed, and in later stages of expression the fusion protein was detected exclusively in the plasma membrane. However, the mislocalisation of SYP121-GFP reported here was evident at all time points tested (36h, 48h, 72h and 84h post transformation). To exclude that mislocalisation of SYP121 was due to heterologous expression, the *Arabidopsis* lines *35S:AtPQL4-1* and *35S:AtPQL6-1*, overexpressing *At*PQL4 and AtPQL6 proteins, respectively, were transformed with P_{UBQ10}-driven SYP121-YFP. Unfortunately, *Arabidopsis* infiltration posed many problems hindering detection of fluorescence (as discussed in chapter 3). To exclude the possibility that

overexpession of any ER resident proteins would result in the accumulation of SYP121 in the ER. SYP121-GFP was co-expressed with HDEL-YFP in tobacco leaf epidermal cells. As expected, localisation of SYP121 and HDEL in the plasma membrane and in the ER network, respectively (data not shown) could be clearly distinguished.

4.3.2 Co-localisation of *At*PQL4 and *At*PQL6 proteins with TIP2 and TIP3;1

The *At*PQL-mediated ER retention was not specific for SYP121. The same phenomenon was observed when *At*PQL4-GFP and *At*PQL6-GFP proteins were co-expressed with TIP2-YFP and TIP3;1-YFP fusion proteins. TIPs represent a distinct group of membrane intrinsic proteins (MIP) that are highly abundant in plant vacuoles, where they mediate the transport of water, proteins, gases and small uncharged molecules across the tonoplast (Gattolin *et al*., 2009). Studies have shown that different TIPs are associated with distinct types of vacuoles. For instance, TIP1 (γ-TIP) is related with lytic-type vacuoles, TIP3;1 with protein storage vacuoles containing seed-type storage proteins and TIP2 with vacuoles that store proteins synthesized in response to environmental and developmental cues (Jauh *et al*., 1998, Hunter *et al*., 2007). However, when co-expressed in the same cell they generally co-localise in the central vacuole (Gattolin *et al*., 2009).

Both TIP2 and TIP3;1 proteins showed fluorescence in typical net-like ER structures and nuclear envelope upon co-expression with the AtPQL proteins. Recently, Gattolin *et al*. (2010) demonstrated that TIP3;1 shows dual localisation to plasma membrane and tonoplast during seed maturation and germination. In addition to tonoplast and plasma membrane, ER-like structures were detected, but only during the first 24 hours suggesting that accumulation in the ER reflects the passage of the protein through this compartment. The authors speculated that the dual localisation of TIP3;1 might compensate for the low number of PIPs residing in the plasma membrane of seeds. As already pointed out, the ER retention of TIP proteins in cells overexpressing *At*PQL4 or *At*PQL6 was observed at various time points excluding the assumption that it was due to transient overload of ER.

The observation reported in this chapter indicates that both AtPQL4 and AtPQL6 determine the time of residence of plasma membrane and tonoplast proteins in the ER. Such a role is in accordance with the results from microarray experiments, which showed differential expression of typical ER-stress marker genes (e.g BiP) in *At*PQL4 and *At*PQL6 mutants (Pattison, 2008). To confirm a function of AtPQL4 and AtPQL6 in ER retention,

localisation of SYP121 and TIP proteins should now be monitored and quantified in *Arabidopsis* lines overexpressing *At*PQL4 and *At*PQL6.

4.3.3 Future experiments

One question arising from the co-localisation data is whether the overexpression of the *At*PQL4 and *At*PQL6 proteins causes an alteration in morphology of the internal compartments hindering the transport of proteins to their final destination? For instance, the decision when a protein enters the secretory pathway or is transported to the vacuole is taken in the Golgi (Hanton and Brandizzi, 2006). Any morphological abnormality of the Golgi might inhibit protein transfer resulting in a build up of proteins in the ER. Co-expression of the two AtPQL proteins with a typical Golgi marker protein, such as ST-YFP, should be carried out to address the effects of *At*PQL4 and *At*PQL6 overexpression on Golgi morphology and more specifically in the anterograde ER-to-Golgi traffic. In addition, one can imagine that overexpression of *At*PQL4 and *At*PQL6 may rescue mutants defective in the retrograde pathway, since ER retention will reduce the transport of proteins to the Golgi. For example, it would be worthwhile to overexpress both *At*PQL proteins in yeast *erd1Δ* and *erd2Δ* mutants defective in ER retention of proteins and monitor survival (Hardwick *et al*., 1990; Semenza *et al*., 1990). Chatre *et al*. (2005) reported that overexpression of the v-SNARE proteins, Sec22 and Memb11 in tobacco resulted in ER localisation of the Golgi marker proteins, ERD2 and ST and in ER retention of soluble cargo (sec-YFP) that was previously shown to be secreted to the apoplast. When co-expression of *At*PQL4-GFP or *At*PQL6-GFP with sec-YFP was attempted during this project, both fluorescence signals were detected in ER-like structures; however, sec-YFP alone was also found in the ER suggesting that the fusion construct contained an ER retention signal. Regeneration of the sec-YFP fusion protein without the ER retention signal is required before the experiments can be repeated.

Previous microarray experiments showed an upregulation of defence-related genes in *At*PQL4 and *At*PQL6 mutants (Pattison, 2008). Furthermore, AtPQL4 and AtPQL6 showed increased transcript levels in virus-infected plants. Since the human homolog MPDU1 is involved in ER glycosylation processes, it would be interesting to test whether overexpressing *At*PQL4 and *At*PQL6 proteins affects the targeting of FLS2 and EFR proteins. FLS2 and EFR are glycosylated plasma membrane proteins that specifically recognise pathogen effectors and elicit plant innate immune responses (Zipfel *et al*., 2006). Bacterial flagellin, ef-Tu or their peptide surrogates fls22 and elf18 are recognised by

FLS2 and EFR, respectively. Both proteins require transit through the ER to mature before reaching their final destination at the plasma membrane. Mutations in components involved in protein maturation resulted in less accumulation of EFR protein during the plant innate immune response (Zipfel *et al*., 2006; Li *et al*., 2009; Nekrasov *et al*., 2009). For instance, *carleticulin3* (*crt3*) mutants showed insensitivity to elf18, which inhibits seedling growth in wild type plants (Li *et al*., 2009). However, initial attempts during the course of this project to express EFR-GFP and FLS2-GFP fusion proteins in tobacco leaves did not yield any fluorescence signal, despite the infiltration at various ratios (OD_{600} nm) of *Agrobacterium* and observation at several time points after infiltration.

Analysis of EFR and FLS2 localisation in *At*PQL4 and *At*PQL6 *Arabidopsis* mutants, and growth assays of *At*PQL4 and *At*PQL6 mutants with fls22 and elf18 are currently underway. Since *At*PQL4 and *At*PQL6 have the same effect on ER retention of proteins when overexpressed, it will be of interest to see if *At*PQL4 and *At*PQL6 function by forming a complex. Use of bimolecular fluorescent complex formation (BiFC) technique will reveal any such interaction between the two *At*PQL proteins.

In summary, this chapter provided new information on the function of *At*PQL4 and *At*PQL6 proteins. Both *At*PQL proteins caused retention of the plasma membrane protein SYP121 and the tonoplast proteins TIP2 and TIP3;1 in the ER. From these and previous results, one can speculate that the two *At*PQL proteins might act as “chaperones” for proteins in the ER during glycosylation, folding and quality control.

Chapter 5: Phenotypic analysis of mutant lines for *At*PQL4 and *At*PQL6 genes.

5.1 Introduction

In this chapter I will describe further experiments to characterize the function of *At*PQL4 and *At*PQL6 proteins. To assess the function of the two *At*PQL proteins *in planta*, a variety of *A. thaliana* mutant lines and one overexpressor line were used. The homozygous knockout lines had been isolated from T-DNA insertion lines obtained from the SALK institute (Pattison, 2008). Two knockout mutant lines were used for *AtPQL4*. The first, *pql4-1*, has an insertion in the second exon, 224 bp 5' of the stop codon, whereas the second, *pql4-2*, has an insertion in the first exon, 109 bp 3' of the start codon. Neither of the mutant lines produces any mRNA for *AtPQL4* (Pattison, 2008). One knockdown mutant line was used for *At*PQL6, *pql6-1,* having an insertion in the fifth intron. A small amount of *At*PQL6 mRNA is still produced by this line (Pattison, 2008). The schematic diagram in Figure 1 represents the insertion site for each *A. thaliana* line. A double mutant line, *pql4-2/6-1*, and an overexpressor line for *At*PQL6, *35S::AtPQL6-1*, were also used.

Previous studies have found no obvious phenotype for the single knockout lines or the overexpressor line under a variety of stresses such as salt, heat and drought (Pattison, 2008). However, this might have been the result of functional redundancy between *At*PQL4 and *At*PQL6. Thus, I was interested in investigating the response of the double mutant in some of these stresses. Also, a number of additional experiments were carried out to search for physiological phenotypes. The rationale behind each experiment is described below.

5.1.1 Sensitivity to macronutrient depletion and salt stress

Depletion of macronutrients causes disturbance of ion homeostasis and depletion of essential metabolites, thus impacting on plant growth and development. Macronutrients such as nitrogen (N), phosphorus (P), sulphur (S) and magnesium (Mg) are essential for build-up of dry matter and energy, while potassium (K) and calcium (Ca) secure ion homeostasis by regulating ion transport and maintenance of water status (Amtmann and Blatt, 2008). Salinity causes ionic and osmotic stress with a detrimental effect on the fitness of the plant (Parida and Das, 2005). Because overexrepression of *At*PQL4 and

*At*PQL6 in tobacco leaves impacts on the targeting of plasma membrane proteins and tonoplast proteins (see chapter 4), one can speculate that the mutants are defective in ion and water transport and therefore show altered salt tolerance and/or sensitivity to macronutrient starvation.

5.1.2 Sensitivity to sugar starvation

Plant growth strongly depends on photosynthetic carbon fixation, and can be further enhanced by external sugar supply. Sugars are the principle substrates for energy generation via respiration and for biosynthesis of macromolecules such as proteins, lipids, DNA and RNA. Upon carbon starvation, cell viability is maintained by differential regulation of genes involved in transport facilitation, transcription, defence, metabolism and protein synthesis (Contento *et al*., 2004). Carbon starvation induces degradative pathways, such as autophagy to maintain cellular activities and compensate for the lack of carbohydrates (Rolland *et al*., 2006). Given the many implications of sucrose in plant fitness and its link to autophagy, it was of interest to investigate the growth of mutant lines in a range of sucrose concentrations.

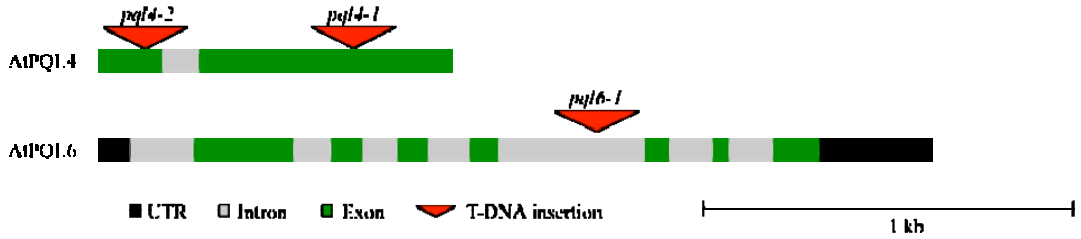

Figure 5.1: T-DNA insertion sites of SALK mutant lines used.

The diagram shows the *At*PQL4 and *At*PQL6 genes and the T-DNA insertions sites for *pql4-1*, *pql4-2* and *pql6-1* mutant lines (Figure taken from Pattison, 2008).

5.2 Results

5.2.1 Sensitivity to macronutrient starvation

To investigate differences in sensitivity to nutrient deficiency between the mutants and wild type, four seeds of each line were sown directly on agar plates supplemented with 1/3, 1/10, 1/30, 1/100 or 1/300 MS. Figure 5.2 shows representative images of these plants 9 days after germination. Dilution of the growth media clearly inhibited growth but no noticeable differences were seen between wild type and mutants.

Figure 5.3 shows the quantitative data for shoot and root fresh weight of the six genotypes used. The fresh weight was measured 14 days after germination. The shoot and root fresh weight of all lines decreased as the nutrient concentration decreased (Figure 5.3A and B). The shoot and root fresh weight of the double knockout mutant and overexpressor line was generally lower than of the wild type and the single knockout mutant lines, but this difference was not statistically significant. In higher concentrations, more variation between mutants and wild type was observed. Figures 5.3C and D presents the response to nutrient depletion within each line relative to the sufficient medium (1/3 MS). There is no obvious change in sensitivity among all the genotypes. To analyze further the sensitivity of the mutants in each condition, data were plotted relative to the wild type profile in each condition (Figures 5.3 E and F). Again, no significant difference was detected. The total root size (i.e. length of both main root and lateral roots) was measured 9 days after germination using EasyRhizo software (Armengaud *et al*., 2009). In all six genotypes the total root size decreased as the nutrient concentration decreased (data not shown). The mutant lines and overexpressor line did not show any significant difference in the sensitivity of root growth to nutrient deficiency compared to the wild type plants.

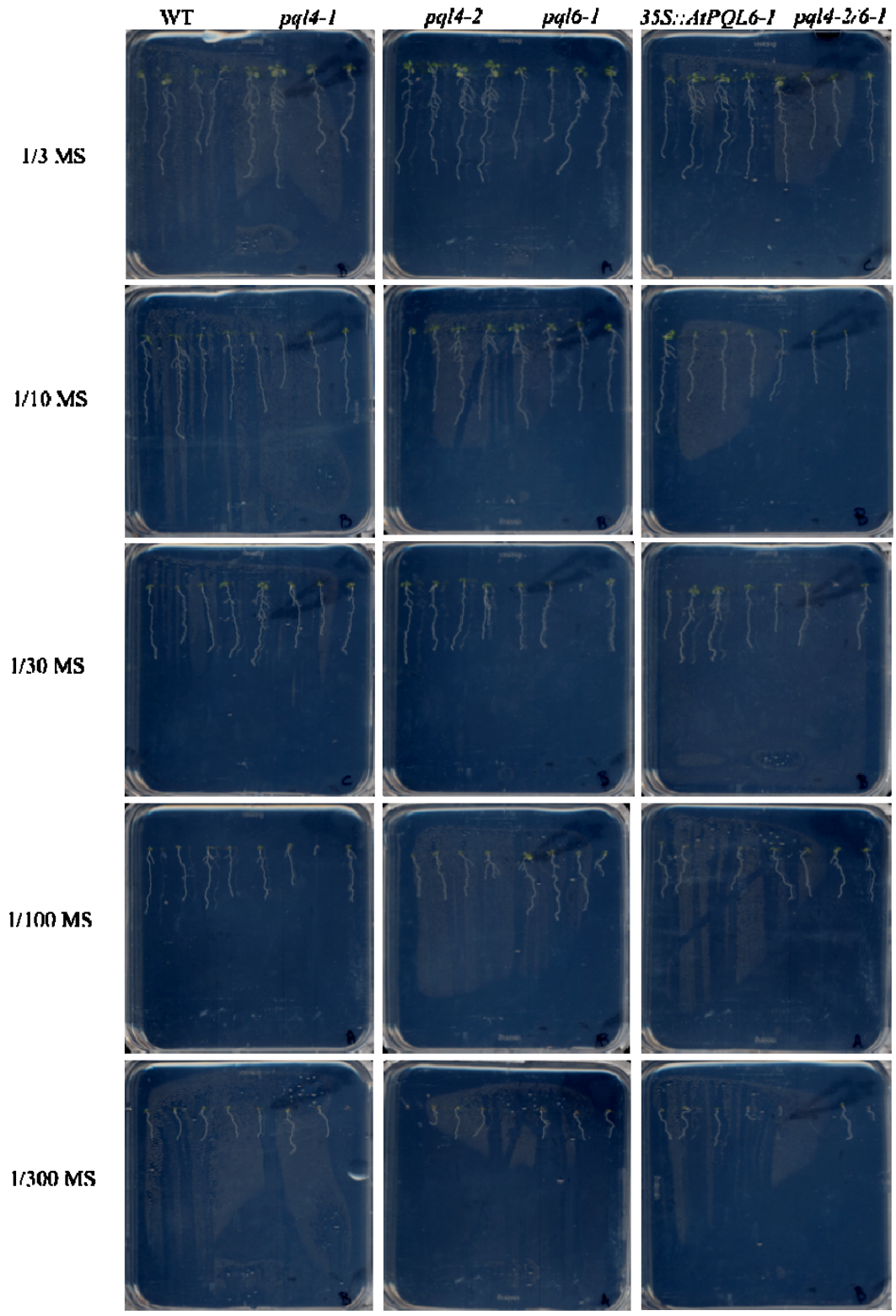

Figure 5.2: Effects of macronutrient starvation on *A. thaliana* (Col0) wild type, *AtPQL4* and *AtPQL6* mutants and *AtPQL6* overexpressor line.

Four seedlings each, of wild type or indicated *At*PQL line, grown on agar plates (120 x 120) containing media of various MS strength. Plants were grown under continuous light with intensity of approximately 120 μmol m^{-2} sec^{-1}. Photographs were taken 9 days after germination.

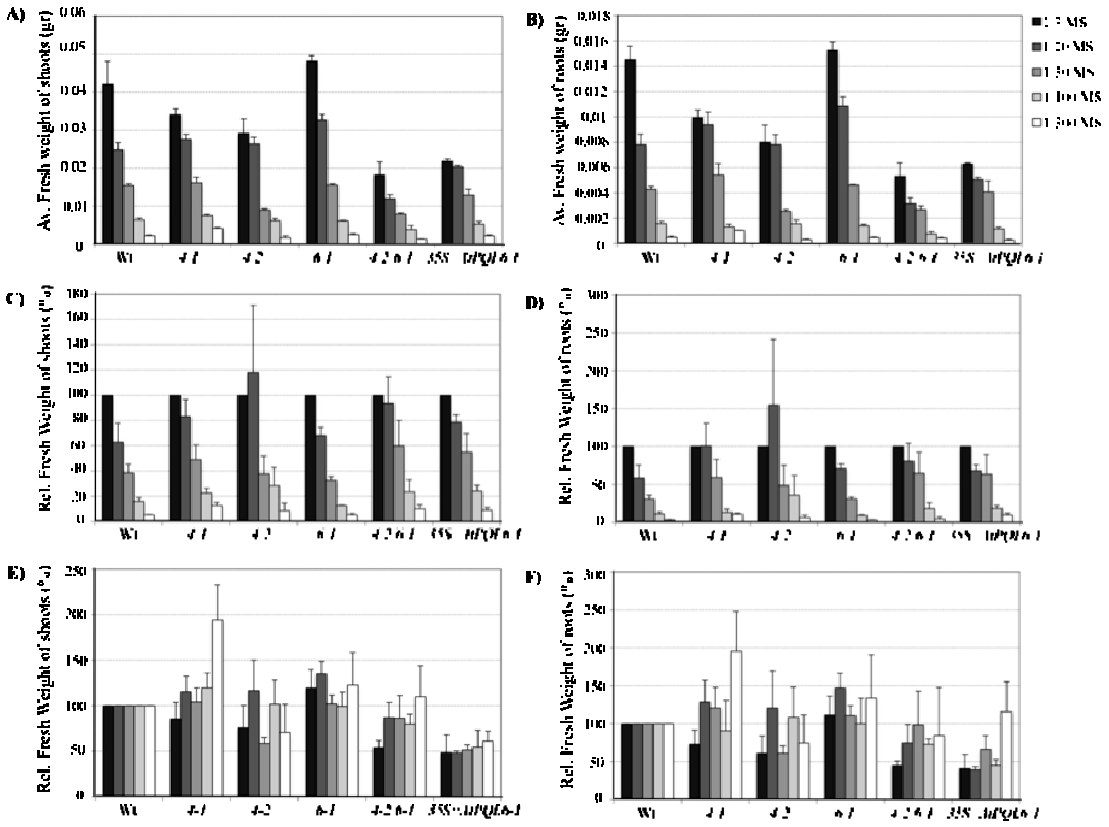

Figure 5.3: Quantification of sensitivity of *A. thaliana* (Col0) wild type, *AtPQL4* and *AtPQL6* mutants and *AtPQL6* overexpressor line to nutrient depletion.

Shoots and roots were harvested and weighed 14 days after germination. **A)**, **B)** Bars represent the average fresh weight of shoots and roots, respectively, of each line in each condition. Error bars represent ± standard error (n=12 plants). **C)**, **D)** Bars represent the average relative fresh weight of shoots and roots, respectively, of each line compared to sufficient medium in each condition. **E)**, **F)** Bars represent the average relative fresh weight of shoots and roots, respectively, of each line compared to wild type within each condition. Error bars represent ± standard error (n=3 replicates of 4 plants).

5.2.2 Sensitivity to salt and osmotic stress

To investigate the sensitivity to salt tolerance, six seeds of each mutant or wild type were sown on plates containing control medium and control medium supplemented with either 50 mM KCl or 50 mM NaCl. Figure 5.4 shows examples of scanned images taken from these plants, 9 days after germination. Inhibition of growth was observed on media supplemented with 50 mM KCl and 50 mM NaCl, with the latter exhibiting a stronger effect on growth. No obvious changes were seen between wild type and mutants.

The fresh weight of shoot and roots was measured 14 days after germination. Figure 5.4A and B show the average fresh weight of shoots and roots in each condition, respectively. The *pql4-1* knockout mutant did not show sensitivity on growth to salt and osmotic stress, while the growth of *pql4-2* knockout mutant was not strongly affected on 50mM KCl supplemented media. No significant difference was detected between the mutants and wild type. The growth response of the six lines compared to the control medium is shown in Figures 5.4C and D. The two *AtPQL4* knockout mutants were less sensitive to osmotic stress and the *pql4-1* was also less sensitive to salt stress. The response to salt and osmotic stress of each line within each condition relative to the wild type profile is presented in Figures 5.4E and F. No significant differences in the sensitivity to salt and osmotic stress were seen between the knockout and overexpressor lines comparing to wild type. Table 5.1 presents the percentage of water content of shoots and roots of each line within each condition. No differences in water content were observed between the mutant and wild type plants.

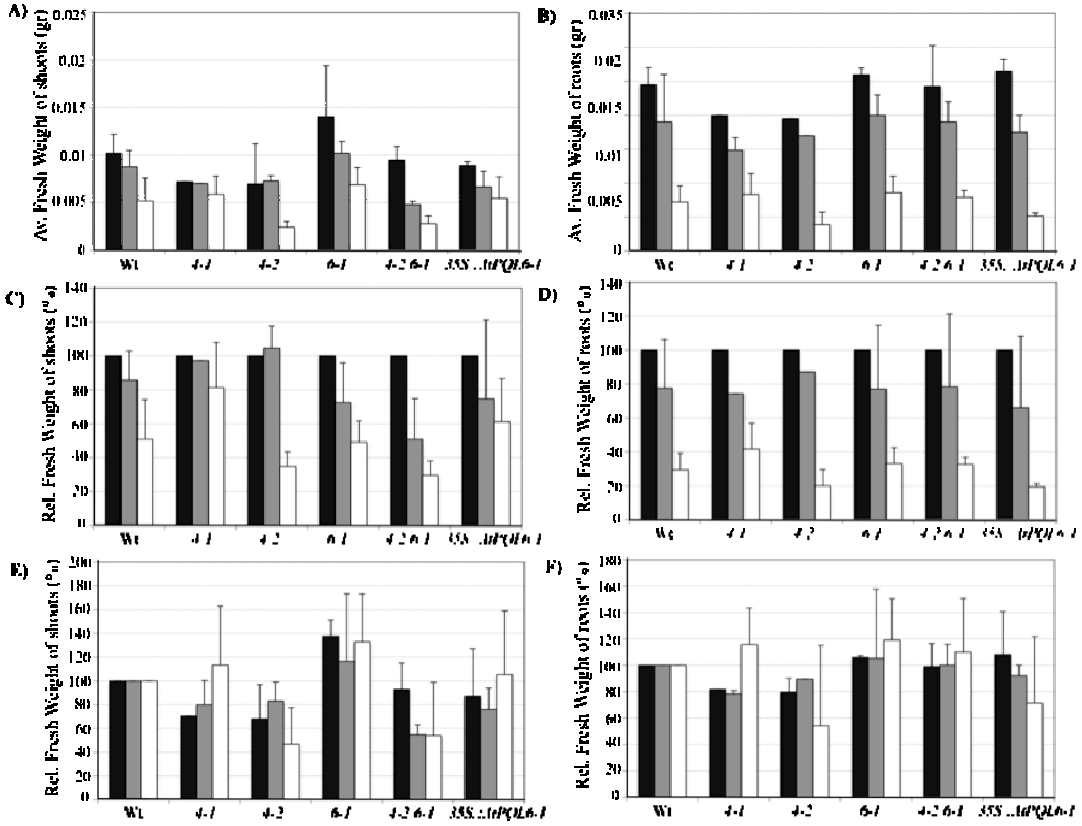

Figure 5.4: Quantification of sensitivity of *A. thaliana* (Col0) wild type, *AtPQL4* and *AtPQL6* mutants and *AtPQL6* overexpressor line to salt and osmotic stress.

Shoots and roots were harvested and weighed 14 days after germination. **A)**, **B)** Bars represent the average fresh weight of shoots and roots, respectively, of each line in each condition. Error bars represent ± standard error (n=12). **C)**, **D)** Bars represent the average relative fresh weight of shoots and roots, respectively, of each line compared to control medium in each condition. **E)**, **F)** Bars represent the average relative fresh weight of shoots and roots, respectively, of each line compared to wild type within each condition. Error bars represent ± standard error (n=2 replicates of 6 plants).

Table 5.1: Percentage of water content of shoots and roots of the wild type and *Arabidopsis* lines.

	Percentage of Water Content (%)											
	Shoots						**Roots**					
	Wt	*pql 4-1*	*pql 4-2*	*pql 6-1*	*pql 4-2/6-1*	*35S:: AtPQL 6-1*	Wt	*pql 4-1*	*pql 4-2*	*pql 6-1*	*pql 4-2/6-1*	*35S:: AtPQL 6-1*
Control Medium	98.9	95	97.3	96.6	97.7	93	93.9	96.7	95.4	95.7	98.1	98.2
+50 mM KCl	98.5	99.8	98.3	99.6	99.4	96.6	91.4	82.3	83	89.1	871.1	84.4
+50 mM NaCl	97.7	96.6	96.9	98.5	97.8	92.9	n/a	n/a	n/a	n/a	n/a	n/a

5.2.3 Sensitivity to sucrose starvation

The sensitivity of growth of the six lines to sucrose was determined by growing three seedlings on 0.5 MS media supplemented with 0 %, 0.5 %, 1 %, 3 % and 4 % of sucrose. Figure 5.5 shows example images of the six different genotypes taken 9 days after germination. No noticeable differences were detected between different concentrations of sucrose, and the mutant and wild type plants.

Figure 5.6 presents quantitative data for shoot and root fresh weight of the mutants and wild type. The fresh weight of shoots and roots was measured 14 days after germination. Inhibition of growth on medium without sucrose was detected for all mutants, except *pql4-1* (Figure 5.6A and B). In the other conditions, no significant change in growth was observed. Plants grown on media supplemented with 1% sucrose confirmed the growth pattern of the lines measured on sufficient medium in macronutrient starvation experiment, which contained 1% sucrose. The response to sucrose starvation in each line was therefore analysed relative to the 1% sucrose medium and is presented in Figure 5.6C and 5.6D. Again all the mutants, except *pql-4-1*, showed a higher sensitivity to low sucrose condition. Because differences vary among the six lines, sensitivity to sucrose starvation was investigated for each line relative to wild type within each condition (Figure 5.6E and 5.6F). The knockout and overexpressor lines showed stronger dependence on sucrose than wild type.

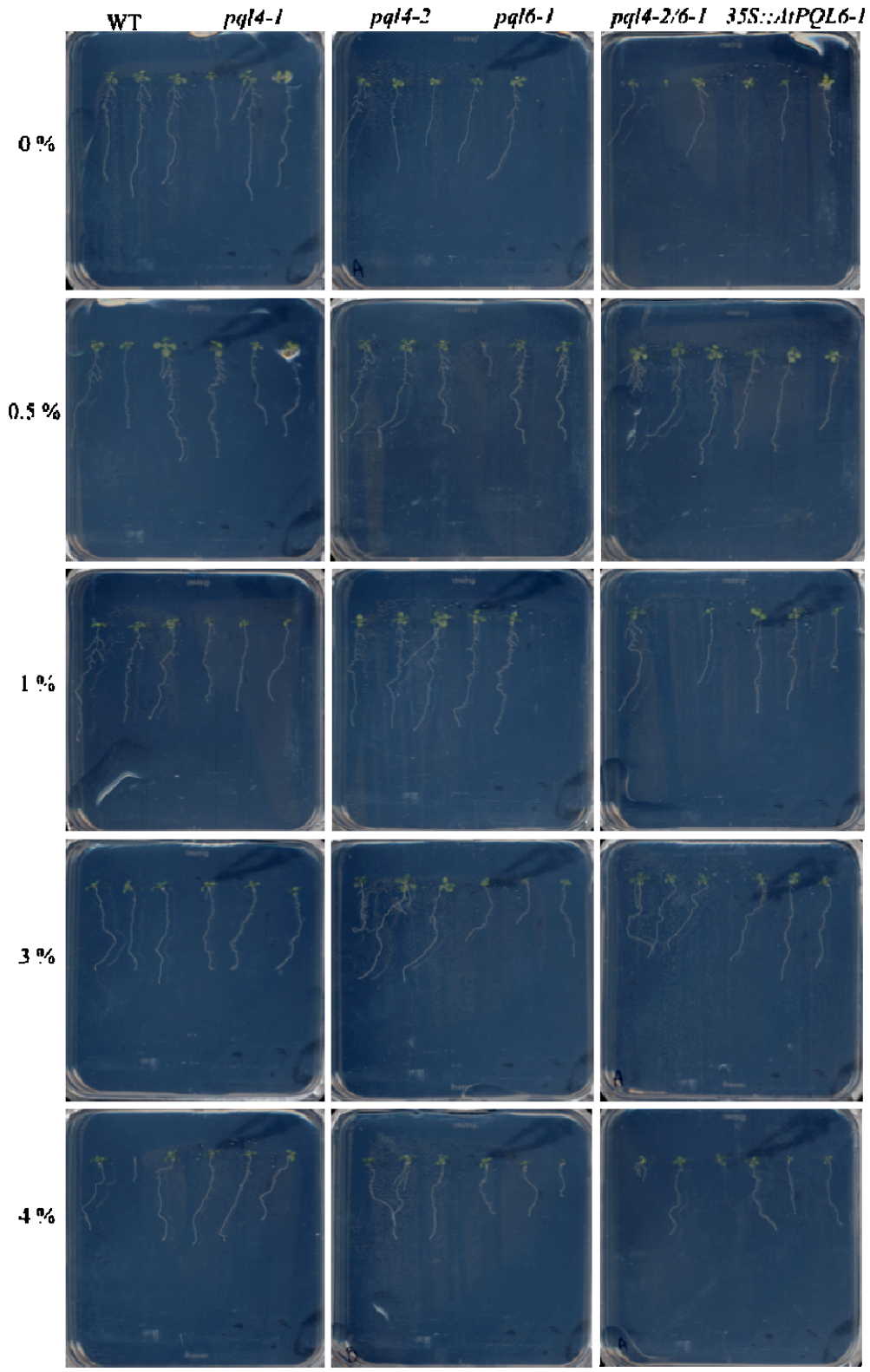

Figure 5.5: Effects of sucrose starvation on *A. thaliana* (Col0) wild type, *AtPQL4* and *AtPQL6* mutants and *AtPQL6* overexpressor line.

Three seedlings each, of wild type or indicated *At*PQL line, grown on agar plates (120 mm X 120 mm) containing 0.5 MS medium supplemented with different concentrations of sucrose (0 %, 0.5 %, 1 %, 3 % and 4 %). Plants were grown under continuous light with an intensity of approximately 120 µmol m^{-2} sec^{-1}. Photographs were taken 9 days after germination.

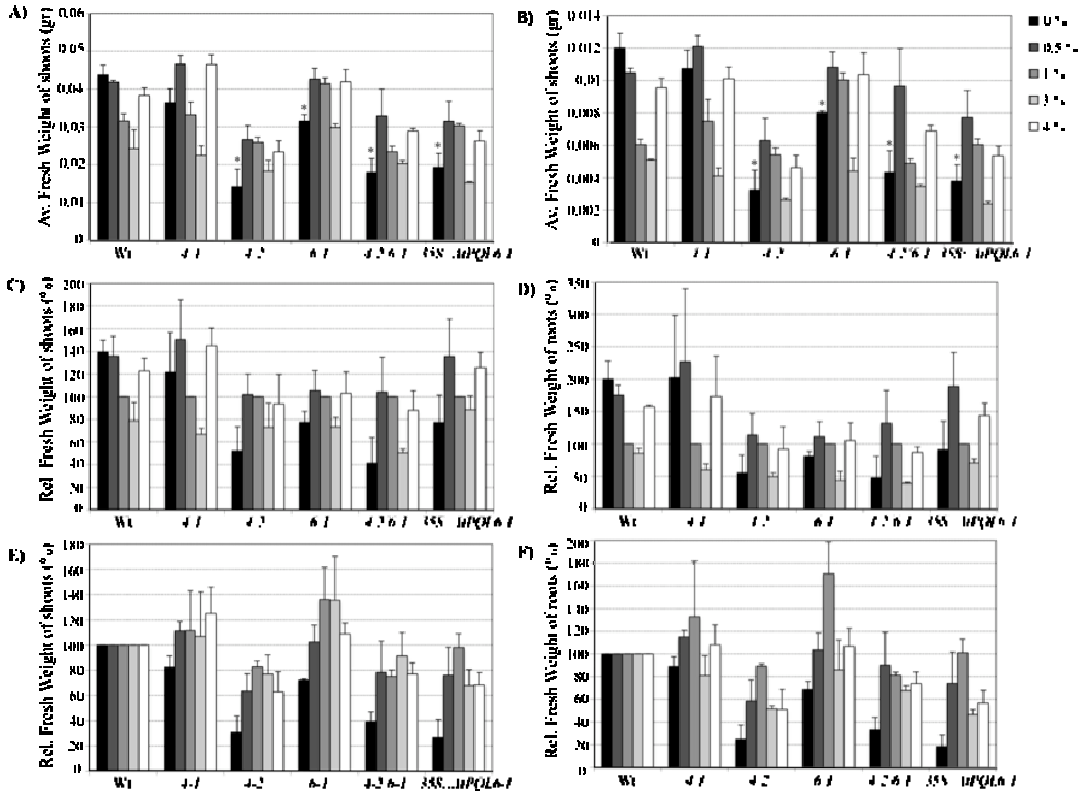

Figure 5.6: Quantification of sensitivity of *A. thaliana* (Col0) wild type, *AtPQL4* and *AtPQL6* mutants and *AtPQL6* overexpressor line to sucrose starvation.

Shoots and roots were harvested and weighed 14 days after germination. **A)**, **B)** Bars represent the average fresh weight of shoots and roots, respectively, of each line in each condition. **C)**, **D)** Bars represent the average relative fresh weight of shoots and roots, respectively, of each line compared to control medium in each condition. **E)**, **F)** Bars represent the average relative fresh weight of shoots and roots, respectively, of each line compared to wild type within each condition. Error bars represent ± standard error (n=3 replicates of 3 plants).

5.3 Discussion

In this study several mutant lines for *At*PQL4 and *At*PQL6 genes were used to facilitate functional characterization of the two proteins. If *At*PQL4 and *At*PQL6 are involved in Man/Glc-P-Dol dependent glycosylation, one could expect that mutations in these two genes will lead to gamete and embryo lethal phenotypes, as this type of glycosylation is essential for gametic transmission through pollen. As discussed in chapter 1, several mutants of genes with a role in Man/Glc-P-Dol synthesis showed embryo lethal phenotypes. Isolation of homozygous lines for AtPQL4 and AtPQL6 genes suggested that none of the mutations are gamete and embryo lethal. However, Pattison (2008) reported a small reduction in the gametic transmission of both *pql4-1* and *pql4-2*, which was consistent with observations for mutants affected in Man/Glc-P-Dol glycosylation (see chapter 1). Given the overlap in sub-cellular localisation of *At*PQL4 and *At*PQL6, it is likely that the lack of phenotype is the result of functional redundancy between the two proteins. However, *pql4-2/6-1* double mutants were also viable. In addition, *pql6-1* is not a null mutation, as small amount of transcript is still produced that might explain the lack of a strong phenotype for both the *pql6-1* and *pql4-2/6-1* mutants.

No obvious phenotype was observed at the whole plant level, when all mutants were tested in different condition with the exception of sucrose starvation. All mutant lines, except *pql4-1*, showed a significant reduction in growth on media without sucrose, as determined by shoot and root fresh weight measurements. Sucrose depletion leads to arrest in growth as protein, lipid and amino acid synthesis are reduced. Sugar catabolism is substituted by protein and lipid catabolism allowing cellular homeostasis to be maintained. Two degradative pathways, the selective ubiquitin proteasome-depedent pathway and the non-selective vacuolar autophagy, mediate protein breakdown (Yu, 1999; Roland *et al*., 2006). Rose *et al*. (2006) reported the up-regulation of autophagy genes (*At*ATG) when 4 day-old *A. thaliana* suspension-cultured cells were transferred to medium with no sucrose. Several studies have suggested an association between autophagy and ER function (Ishihara *et al*., 2001; Reggiori *et al*., 2004). For instance, ER stress caused by addition of dithiothreitol (DTT) and tunicamycin facilitated the formation of pre-autophagosomal structure (PAS) in *atg11Δ* cells defective in assembly of PAS. As discussed in chapter 1, ER stress stimulates UPR to relieve the stress by inducing genes involved in protein folding and ERAD pathway. Additionally, it is suggested that autophagy functions as a backup to the ERAD pathway if the latter is saturated by degradative substrates (Yorimitsu *et al*., 2007). It is known that proteins involved in folding processes are also implicated in preparing

misfolded proteins for degradation (Liu and Howell, 2010). Hence, one can speculate that the phenotype observed in sucrose-free medium might be the result of impaired flow of degradative proteins to autophagosomes inhibiting protein catabolism. This might be also consistent with the putative function of *At*PQL4 and *At*PQL6 proteins as folding helpers that was suggested by the co-localisation experiments (see chapter 4). Although several conditions reported to cause UPR were tested, it would be useful to investigate the effects of tunicamycin on the mutants as the former blocks the N-glycosylation process and triggers UPR (see chapter 1).

In conclusion, phenotypic analysis of mutants did not yield a great insight into the function of *At*PQL4 and *At*PQL6 proteins. However, the arrested growth of the mutants compared to wild type on sucrose-free media could possibly implicate a function for the two proteins in autophagy-related processes, which should be further investigated in the future.

Chapter 6: General Discussion

6.1 Introduction

The main objective of this thesis was the functional characterisation of two novel proteins, *At*PQL4 and *At*PQL6 from *At*PQL family from *A. thaliana*. This was achieved by following three different experimental approaches: 1) the subcellular localisation of the two *At*PQL proteins and functional characterisation 2) at a molecular cellular level and 3) at whole-plant level. Discussion of each of these approaches is made in chapters 3, 4 and 5, respectively. This chapter presents the overall information gained on *At*PQL4 and *At*PQL6 as well as suggests future experiments to answer questions that arose concerning the function of the two *At*PQLs. Figure 6.1 represents the overall information on the *At*PQL family, with a focus being on *At*PQL4 and *At*PQL6. The *At*PQL1, *At*PQL2 and *At*PQL3 showed high identity in amino acid sequence with the fission yeast plasma membrane protein STM1 (Pattison, 2008), which functions as a G-protein coupled receptor (Chung *et al*., 2001). Human MPDU1 is involved in Man-P-Dol dependent glycosylation processes, such as N-glycosylation (Anand *et al*., 2001; Kranz *et al*., 2001, Schenk *et al*., 2001) and shows high sequence identity with the *At*PQL4 and *At*PQL6 (Pattison, 2008). Overexpression of *At*PQL4 and *At*PQL6 proteins resulted in retention of membrane proteins in the ER. ERS1, a PQL protein from *S. cerevisiae*, was identified as a suppressor of the secretion of ER resident protein in *erd1Δ* mutants. Human CTNS is the closest homologue of *At*PQL5 (Pattison, 2008) and is involved in H^+-driven cystine transport from lysosomes to cytosol (Attard *et al*., 1999; Kalatzis *et al*., 2001). The hygromycin sensitive phenotype of *ers1Δ* yeast mutants was reversed by expression of CTNS (Gao *et al*., 2005).

The novel function of *At*PQL4 and *At*PQL6 in retaining plasma membrane and tonoplast proteins in the ER, discovered in this project, suggests that the previously observed phenotypes of MPDU1, ERS1 and CTNS are in fact different sides of the same "coin". For example, one could argue that the role of MPDU1 for N-glycosylation, the molecular basis of which has not yet been identified, is in fact linked to retaining proteins for a sufficient time in the ER membrane. This could concern either proteins to be glycosylated or the enzymes that act in different steps of N-glycosylation, or subsets of these in ER membrane associated functional complexes. A role of LEC35/MPDU1 as "chaperone" has indeed been proposed on the basis of the combined experimental data for this protein (Mark Lehrman, personal communication).

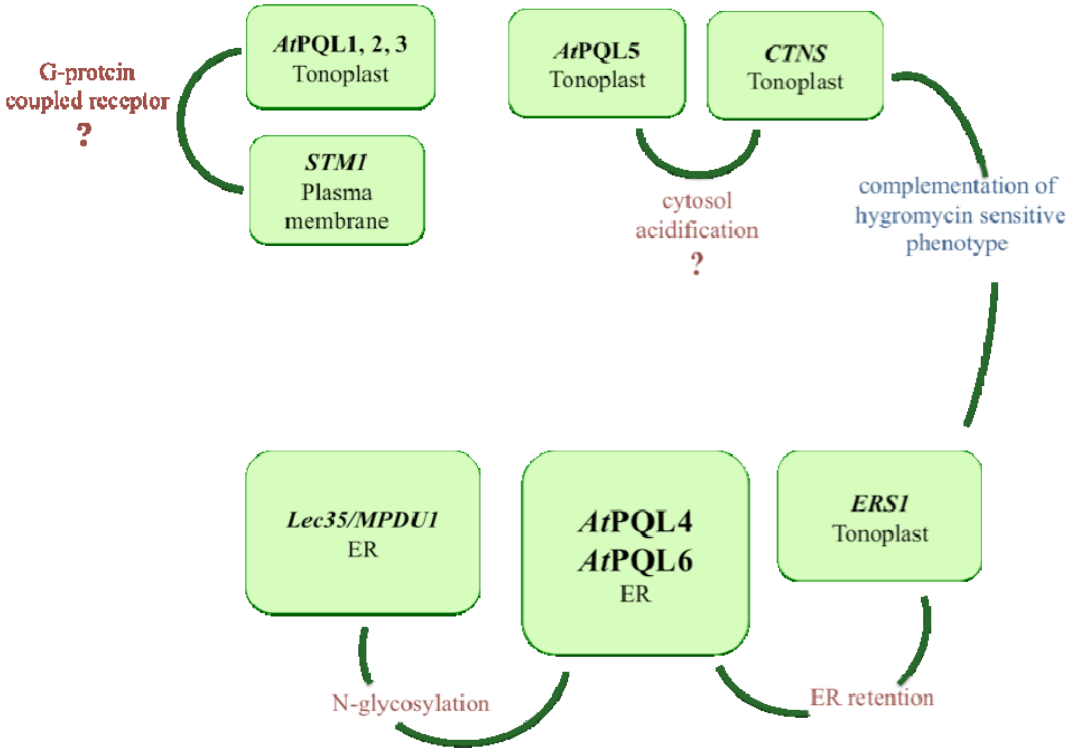

Figure 6.1: Information on the function of all the members of *At*PQL family.

The diagram shows all the members of *At*PQL family and their closest homologues. The sub-cellular localisation of each PQL protein is indicated. The proposed function is indicated with red color. Question marks indicate lack of information on the function of *At*PQL proteins.
*At*PQL1, 2 and 3 are localised to the tonoplast and show a high sequence identity with plasma membrane protein *STM1*, a putative G-protein coupled receptor. *At*PQL4 and *At*PQL6 are localised in the ER and show high sequence identity with the human protein MPDU1 that is involved in N-glycosylation. Overexpression of *At*PQL4 and *At*PQL6 resulted to ER retention of plasma membrane and tonoplast proteins. The tonoplast-localised protein ERS1 of *S.cerevisiae* was isolated as suppressor of *erd1Δ* yeast mutants defective in ER retention of proteins. Tonoplast *CTNS* protein is a proton-coupled cystine transporter and is the closest homologue of *At*PQL5, which localises to the tonoplast. *CTNS* complemented the hygromycin sensitive phenotype of *ers1Δ*.

6.2 Is there a functional homology with LEC35/MPDU1?

*At*PQL4 and *At*PQL6 are the closest homologues of the mammalian PQL protein LEC35/MPDU1. LEC35/MPDU1 is involved in all Man-P-Dol dependent glycosylation processes, such as N-glycosylation and GPI anchoring (Anand *et al*., 2001). The ER localisation of the two *At*PQL proteins is in agreement with a putative role in N-glycosylation. The differential regulation of ER stress-related genes in *At*PQL4 and *At*PQL6 mutant and overexpressor lines additionally argues in favor of N-glycosylation (Pattison, 2008).

A possible way to address the functional homology of *At*PQL4 and *At*PQL6 with LEC35/MPDU1 is to express the two *At*PQL proteins in *lec35* CHO cells and check for complementation. *lec35* mutants showed less sensitivity to a combination of glycosylation inhibitors than the wild type cells (Lehramn and Zeng, 1989). HPLC analysis of *lec35* mutants showed an accumulation of $Man_5GlcNAc_2$-P-P-Dol instead of the mature LLO, $Glc_3Man_9GlcNAc_2$-P-P-Dol (Lehramn and Zheng, 1989). Use of fluorophore-assisted carbohydrate electrophoresis (FACE) analysis will allow visualisation of LLOs from *At*PQL4 and *At*PQL6 mutants. FACE technique involves the cleavage of LLOs from dolichol with mild acid and the resolution of the removed LLOs on polyacrylamide gel according to size (Gao and Lehrman, 2002). If the two *At*PQL proteins are functional homologous to LEC35/MPDU1, an accumulation of the intermediate oligosaccharide is expected. Mutants defective in LLO synthesis showed a hypersensitive phenotype upon treatment with tunicamycin, which inhibits the first step of lipid-linked oligosaccharide (LLO) synthesis (see 1.6 section, Zhang *et al*., 2008). Phenotypic analysis of *At*PQL4 and *At*PQL6 mutants and overexpressors treated with tunicamycin should be carried out to check for increased sensitivity.

6.3 Do AtPQL4 and AtPQL6 have a “chaperone” role?

As shown in chapter 4, overexpression of *At*PQL4-GFP and *At*PQL6 fusions resulted in retention of plasma membrane and tonoplast proteins in the ER. These data indicate a potential role of *At*PQL4 and *At*PQL6 proteins in retaining proteins in the ER for sufficient time to allow ER quality control, including N-glycosylation, to take place. Several questions arose from these results and potential approaches to address such questions are discussed in chapter 4 (see 4.3.3 section). For instance, investigation of an altered

morphology of the ER resulting from overexpressing *At*PQL4 and *At*PQL6 should be undertaken, as it may cause disturbance of the ER exit sites (ERES) and prevent ER export of proteins. Complementation of yeast *erd1Δ*, *erd2Δ* and *ers1Δ* mutants defective in ER retention with *At*PQL4 and *At*PQL6 might also confirm a function as "chaperones". Although, Pattison (2008) did not observe complementation of the *ers1Δ* mutant hygromycin sensitive phenotype by any member of the *At*PQL family, it will be useful to repeat the same experiments, as he reported a lack of hygromycin phenotype of the *ers1Δ* mutants. Complementation of *ers1Δ* by *At*PQL4 and/or *At*PQL6 would argue in favor of an involvement in ER retention machinery, as *ers1Δ* was isolated in a screen for suppression of *erd1Δ* mutants defective in retention of ER lumenal proteins (Gao *et al*., 2005). If the chaperone function is valid, then a new mechanism of ER retention independent of the HDEL/KDEL signal might occur in plants. Such information could be valuable for the production of plant-made pharmaceuticals without having the plant-specific post-translational modifications that are immunogenic to humans (Gomord *et al*., 2010).

6.4 Are *At*PQL4 and *At*PQL6 essential for plant fitness?

A further indication of a "chaperone" role of *At*PQL4 and *At*PQL6 proteins derived from the observed reduced growth of *At*PQL4 and *At*PQL6 mutants in low sucrose. Carbon starvation is known to trigger degradative pathways to ensure protein catabolism and therefore cellular homeostasis by inducing unfolded protein response (UPR) (Reggiori *et al*., 2004; Rose *et al*., 2006). It is known that folding factors are also implicated in UPR to ensure ER quality control (Ceriotti and Roberts, 2006). It will be thus interesting to try a variety of stresses, such as tunicamycin and DTT that induce UPR in *At*PQL4 and *At*PQL6 mutants and check for hypersensitive phenotype.

One could expect that mutations on proteins having a role in protein folding, N-glycosylation and ER quality control processes will have a detrimental effect on plant fitness. The lack of embryo or gametic lethal phenotype might be the result of redundancy between *At*PQL4 and *At*PQL6. Epistatic complementation of the mutants might also explain the lack of a strong phenotype. Furthermore, *At*PQL6 mutant is a knock-down rather than knock-out mutant and thus produces a small level of transcript. Additionally, no information on the amount of protein produced from either *At*PQL4 or *At*PQL6 gene is available, at this stage. For this reason, it could be worthwhile to use the moss *Physcomitrella patens* as another system to establish the function of PQL proteins because

it is an easy and feasible system for targeted ‘knockout’ of genes by homologous recombination.

Appendix A

Table A-1: Primer sequences of *AtPQL4* and *AtPQL6*.

Gene	AGI	Primers		Amplicon size (bp)
AtPQL4	At5g59470	Forward Primer	CTAGGAATCGACTTGAGCTG	133
		Reverse Primer	GAAGCTTAACGGTCATTGAA	
AtPQL6	At4g07390	Forward Primer	GCATAAAGGTCTTCCCTTTT	173
		Reverse Primer	GATTAATCTGTCCAGCAAGC	

Table A-2: Other primer sequences.

Gene	Primers		Amplicon size (bp)
CaMV B-JI	Forward Primer	AGC GGT CAA AAT ATT GCT TA	141
	Reverse Primer	AAC TTA CCG TAT GCT AGA TTA CCT	
18S RNA	Forward Primer	CGT GAT CGA TGA ATG CTA CC	199
	Reverse Primer	GGG GTT TGT TGC ACG TAT TA	

Appendix B

CD is provided with supplementary images for Chapter 4

- Co-localisation of *At*PQL4-GFP with SYP121-YFP
- Co-localisation of *At*PQL6-GFP with SYP121-YFP
- Co-localisation of *At*PQL4-GFP with SYP121-YFP
- Co-localisation of *At*PQL6-GFP with SYP121-YFP

List of References

Amtmann, A. and Blatt, M. 2009. Regulation of macronutrient transport. New Phytologist 181: 35-52.

Armengaud, P., Zambaux, K., Hills, A., Sulpice, R., Pattison, R., Blatt, M. and Amtmann, A. 2009. EZ-Rhizo: integrated software for the fast and accurate measurement of root system architecture. Plant Journal 57: 945-56.

Attard, M., Jean, G., Forestier, L., Cherqui, S., van't Hoff, W., Broyer, M., Antignac, C. and Town, M. 1999. Severity of phenotype in cystinosis varies with mutations in the CTNS gene: predicted effect on the model of cystinosin. Human Molecular Genetics 8: 2507-2514.

Bassham, D.C., Brandizzi, F., Otegui, M.S. and Sanderfoot, A.A. 2008. The secretory system of Arabidopsis, in The Arabidopsis Book, (eds. Somerville CR and Meyerowitz EM, American Society of Plant Biologists), Rockville, MD doi 10.1199/tab.0116.

Bassham, D. C. and Blatt, M. R. 2008. SNAREs: Cogs and coordinators in signaling and development. Plant Physiology 147: 1504-1515.

Betts, M.R. and Russell, R.B. 2007. Amino acid properties and consequences of substitutions. in Bioinformatics for geneticists (eds, M.R. Barnes and I.C. Gray), John Wiley & Sons, West Sussex, pp. 311-340.

Bolte, S. and Cordelieres, F. P. 2006. A guided tour into subcellular colocalization analysis in light microscopy. Journal of Microscopy 224: 213-232.

Brandizzi, F., Hanton, S., daSilva, L. L. P., Boevink, P., Evans, D., Oparka, K., Denecke, J. and Hawes, C. 2003. ER quality control can lead to retrograde transport from the ER lumen to the cytosol and the nucleoplasm in plants. Plant Journal 34: 269-281.

Capitani, M. and Sallese, M. 2009. The KDEL receptor: New functions for an old protein. FEBS Letters 583: 3863-3871.

Ceriotti, A. and Roberts, L. M. 2006. Endoplasmic reticulum-associated protein degradation in plant cells. Plant Endoplasmic Reticulum 4: 75-98.

Chatre, L., Wattelet-Boyer, V., Melser, S., Maneta-Peyret, L., Brandizzi, F. and Moreau, P. 2009. A novel di-acidic motif facilitates ER export of the syntaxin SYP31. Journal of Experimental Botany 60: 3157-3165.

Chung, K. S., Won, M., Lee, S. B., Jang, Y. J., Hoe, K. L., Kim, D. U., Lee, J. W., Kim, K. W. and Yoo, H. S. 2001. Isolation of a novel gene from *Schizosaccharomyces pombe*: stm1(+) encoding a seven-transmembrane loop protein that may couple with the heterotrimeric G alpha 2 protein, Gpa2. Journal of Biological Chemistry 276: 40190-40201.

Cipollo, J. F., Trimble, R. B., Chi, J. H., Yan, Q. and Dean, N. 2001. The yeast ALG11 gene specifies addition of the terminal alpha 1,2-Man to the Man(5)GlcNAc(2)-PP-dolichol N-glycosylation intermediate formed on the cytosolic side of the endoplasmic reticulum. Journal of Biological Chemistry 276: 21828-21840.

Contento, A. L., Kim, S. J. and Bassham, D. C. 2004. Transcriptome profiling of the response of *Arabidopsis* suspension culture cells to Suc starvation. Plant Physiology 135: 2330-2347.

Cunillera, N., Arro, M., Fores, O., Manzano, D. and Ferrer, A. 2000. Characterization of dehydrodolichyl diphosphate synthase of *Arabidopsis thaliana*, a key enzyme in dolichol biosynthesis. Febs Letters 477: 170-174.

Di Sansebastiano, G.-P., Gigante, M., De Domenico, S., Piro, G. and Dalessandro, G. 2006. Sorting of GFP tagged NtSyr1, an ABA related syntaxin. Plant Signal Behaviour 1: 77-85.

Doucey, M. A., Hess, D., Cacan, R. and Hofsteenge, J. 1998. Protein C-mannosylation is enzyme-catalysed and uses dolichyl-phosahate-mannose as a precursor. Molecular Biology of the Cell 9: 291-300.

Elbein, A. D. 1987. Inhibitors of the biosynthesis and processing of N-linked oligosaccharide chains. Annual Review of Biochemistry 56: 497-534.

Fluckiger, R., De Caroli, M., Piro, G., Dalessandro, G., Neuhaus, J. and Di Sansebastiano, G. 2003. Vacuolar system distribution in Arabidopsis tissues, visualized using GFP fusion proteins. Journal of experimental botany 54: 1577-1584.

Frigerio, L., Pastres, A., Prada, A. and Vitale, A. 2001. Influence of KDEL on the fate of trimeric or assembly-defective phaseolin: Selective use of an alternative route to vacuoles. Plant Cell 13: 1109-1126.

Gao, X. D., Wang, J., Keppler-Rosse, S. and Dean, N. 2005. ERS1 encodes a functional homologue of the human lysosomal cystine transporter. FEBS Journal 272: 2497–2511.

Gattolin, S., Sorieul, M. and Frigerio, L. 2010. Tonoplast intrinsic proteins and vacuolar identity. Biochemical Society Transactions 38: 769-773.

Gattolin, S., Sorieul, M., Hunter, P. R., Khonsari, R. H. and Frigerio, L. 2009. In vivo imaging of the tonoplast intrinsic protein family in *Arabidopsis* roots. Bmc Plant Biology 9:133-141

Ghal, W.A., Thoene, J.G. and Schneider, J.A. 2002. Cystinosis. New England Journal of Medicine 347: 111-121.

Gomord, V., Fitchette, A. C., Menu-Bouaouiche, L., Saint-Jore-Dupas, C., Plasson, C., Michaud, D. and Faye, L. 2010. Plant-specific glycosylation patterns in the context of therapeutic protein production. Plant Biotechnology Journal 8: 564-587.

Grefen, C., Donald, N., Hashimoto, K., Kudla, J., Schumacher, K. and Blatt, M. R. 2010. A ubiquitin-10 promoter-based vector set for fluorescent protein tagging facilitates temporal stability and native protein distribution in transient and stable expression studies. Plant Journal 64: 355-365.

Griffiths, G., Ericsson, M., Krijnselocker, J., Nilsson, T., Goud, B., Soling, H. D., Tang, B. L., Wong, S. H. and Hong, W. J. 1994. Localisation of the Lys, Asp, Glu, Leu tetrapeptide receptor to the Golgi-complex and the itermediate compartment in mammalian cells. Journal of Cell Biology 127: 1557-1574.

Hammond, C., Braakman, I. and Helenius, A. 1994. Role of N-linked oligosaccharide recognition, glucose trimming, and calnexin in glycoprotein folding and quality control. Proceedings of the National Academy of Sciences of the United States of America 91: 913-917.

Hanton, S. L. and Brandizzi, F. 2006. Protein transport in the secretory pathway. Canadian Journal of Botany 84: 523-530.

Hardwick, K. G. 1990. ERD1, a yeast gene required for the retention of luminal endoplasmic reticulum proteins, affects glycoprotein processing in the Golgi apparatus. EMBO 9: 623-630.

Hardwick, K. G. and Pelham, H. R. B. 1990. ERS1 a 7 transmembrane domain protein from *Saccharomyces cerevisiae*. Nucleic Acids Research 18: 2177-2177.

Haws, C. 2008. The plant ER-Golgi interface. Traffic 9: 1571-1580.

Helenius, J. 2002. Translocation of lipid-linked oligosaccharides across the ER membrane requires Rft1 protein. Nature 415:447-450.

Honsbein, A., Sokolovski, S., Grefen, C., Campanoni, P., Pratelli, R., Paneque, M., Chen, Z. H., Johansson, I. and Blatt, M. R. 2009. A tripartite SNARE-K+ channel complex mediates in channel-dependent K+ nutrition in *Arabidopsis*. Plant Cell 21: 2859-2877.ou ei

Huang, J., Taylor, P., Chen, j.g., Uhrig, J.F., Schnell, D.J., Nakagawa, T., Korth, K.L. and Jones. A.M. 2006. The plastid protein THYLAKOID FORMATION1 and the plasma membrane G-protein GPA1 interact in a novel sugar-signaling mechanism in *Arabidopsis.* Plant Cell 18:1226-1238.

Hunter, P. R., Craddock, C. P., Di Benedetto, S., Roberts, L. M. and Frigerio, L. 2007. Fluorescent reporter proteins for the tonoplast and the vacuolar lumen identify a single vacuolar compartment in Arabidopsis cells(1 W). Plant Physiology 145: 1371-1382.

Ishihara, N., Hamasaki, M., Yokota, S., Suzuki, K., Kamada, Y., Kihara, A., Yoshimori, T., Noda, T. and Ohsumi, Y. 2001. Autophagosome requires specific early Sec proteins for its formation and NSF/SNARE for vacuolar fusion. Molecular Biology of the Cell 12: 3690-3702.

Iwata, Y., Fedoroff, N. V. and Koizumi, N. 2008. Arabidopsis bZIP60 is a proteolysis-activated transcription factor involved in the endoplasmic reticulum stress response. Plant Cell 20: 3107-3121.

Jauh, G. Y., Fischer, A. M., Grimes, H. D., Ryan, C. A. and Rogers, J. C. 1998. delta-Tonoplast intrinsic protein defines unique plant vacuole functions. Proceedings of the National Academy of Sciences of the United States of America 95: 12995-12999.

Jauh, G.Y., Phillips, T.E. and Rogers, J.C. 1999. Tonoplast intrinsic protein isoforms as markers for vacuolar functions. Plant Cell 11:1867-1882.

Johansen, L. K. and Carrington, J. C. 2001. Silencing on the spot. Induction and suppression of RNA silencing in the *Agrobacterium*-mediated transient expression system. Plant Physiology 126: 930-938.

Jonne, H. 2002. Translocation of lipid-linked oligosaccharides across the ER membrane requires Rft1 protein. Nature 415: 447-450.

Kalatzis, V., Cherqui, S., Antignac, C. and Gasnier, B. 2001. Cystinosin, the protein defective in cystinosis, is a H+-driven lysosomal cystine transporter. Embo Journal 20: 5940-5949.

Kalatzis, V., Nevo, N., Cherqui, S., Gasnier, B. and Antignac, C. 2004. Molecular pathogenesis of cystinosis: effect of CTNS mutations on the transport activity and subcellular localization of cystinosin. Human Molecular Genetics 13: 1361-1371.

Kato, N., Fujikawa, Y., Fuselier, T., Adamou-Dodo, R., Nishitani, A. and Sato, M. H. 2010. Luminescence detection of SNARE-SNARE interaction in *Arabidopsis* protoplasts. Plant Molecular Biology 72: 433-444.

Kinoshita, T. and Inoue, N. 2000. Dissecting and manipulating the pathway for glycosylphosphatidylinositol-anchor biosynthesis. Current Opinion in Chemical Biology 4: 632-638.

Koiwa, H., Li, F., McCully, M. G., Mendoza, I., Koizumi, N., Manabe, Y., Nakagawa, Y., Zhu, J. H., Rus, A., Pardo, J. M., Bressan, R. A. and Hasegawa, P. M. 2003. The STT3a subunit lsoform of the *Arabidopsis* oligosaccharyltransferase controls adaptive responses to salt/osmotic stress. Plant Cell 15: 2273-2284.

Kornfeld, R. and Kornfeld, S. 1985. Assembly of aspargine-linked oligosaccharides. Annual Review of Biochemistry 54: 631-664.

Kranz, C., Denecke, J., Lehrman, M. A., Ray, S., Kienz, P., Kreissel, G., Sagi, D., Peter-Katalinic, J., Freeze, H. H., Schmid, T., Jackowski-Dohrmann, S., Harms, E. and Marquardt, T. 2001. A mutation in the human MPDU1 gene causes congenital disorder of glycosylation type If (CDG-If). Journal of Clinical Investigation 108: 1613-1619.

Krieg, J., Glasner, W., Vicentini, A., Doucey, M. A., Loffler, A., Hess, D. and Hofsteenge, J. 1997. C-mannosylation of human RNase 2 is an intracellular process performed by a variety of cultured cells. Journal of Biological Chemistry 272: 26687-26692.

Kwon, C., Neu, C., Pajonk, S., Yun, H.S., Lipka, U., Humphry, M., Bau, S., Straus, M., Kwaaitaal, M., Rampelt, H., El Kasmi, F., Jurgens, G., Parker, J., Panstruga, R., Lipka, V. and Schulze-Lefert, P. 2008. Co-option of a default secretory pathway for plant immuneresponses. Nature 451: 835–840

Lehrman, M. A. and Zeng, Y. 1989. Pleiotropic resistance to glycoprotein processing inhibitors in Chinese-hamster ovary cells-The role of a novel mutation in the asparagine-linked glycosylation pathway. Journal of Biological Chemistry 264: 1584-1593.

Li, J., Zhao-Hui, C., Batoux, M., Nekrasov, V., Roux, M., Chinchilla, D., Zipfel, C. and Jones, J. D. G. 2009. Specific ER quality control components required for biogenesis of the plant innate immune receptor EFR. Proceedings of the National Academy of Sciences of the United States of America 106: 15973-15978.

Liu, J. X. and Howell, S. H. 2010. Endoplasmic Reticulum Protein Quality Control and Its Relationship to Environmental Stress Responses in Plants. Plant Cell 22: 2930-2942.

Martinez, I. M. and Chrispeels, M. J. 2003. Genomic analysis of the unfolded protein response in *Arabidopsis* shows its connection to important cellular processes. Plant Cell 15: 561-576.

Marty, F. 1999. Plant vacuoles. Plant Cell 11: 587-599.

Maurice, H. 2008. Identification of the gene encoding the {alpha}1,3-mannosyltransferase (ALG3) in *Arabidopsis* and characterisation of downstream N-glycan processing. Plant Cell 20: 1652-1664.

Mishiba, K., Nishihara, M., Nakatsuka, T., Abe, Y., Hirano, H., Yokoi, T., Kikuchi, A. and Yamamura, S. 2005. Consistent transcriptional silencing of 35S-driven transgenes in gentian. Plant Journal 44: 541-556.

Monika, A. 2001. Requirement of the Lec35 gene for all known classes of monosaccharide-P-Dolichol-depedent glycosyltransferase reactions in mammals. Molecular Biology of the Cell 12: 487-501.

Nekrasov, V., Li, J., Batoux, M., Roux, M., Chu, Z. H., Lacombe, S., Rougon, A., Bittel, P., Kiss-Papp, M., Chinchilla, D., van Esse, H. P., Jorda, L., Schwessinger, B., Nicaise, V., Thomma, B., Molina, A., Jones, J. D. G. and Zipfel, C. 2009. Control of the pattern-recognition receptor EFR by an ER protein complex in plant immunity. Embo Journal 28: 3428-3438.

Pagny, S., Lerouge, P., Faye, L. and Gomord, V. 1999. Signals and mechanisms for protein retention in the endoplasmic reticulum. Journal of Experimental Botany 50: 157-164.

Parida, A. K. and Das, A. B. 2005. Salt tolerance and salinity effects on plants: a review. Ecotoxicology and Environmental Safety 60: 324-349.

Pattison, R. J. 2008. Characterisation of the PQ-Loop repeat membrane protein family in Arabidopsis thaliana. PhD thesis, University of Glasgow.

Pattison, R. J. and Amtmann, A. 2009. N-glycan production in the endoplasmic reticulum of plants. Trends in Plant Science 14: 92-99.

Pelham, H. R. B. 1990. The retention signal for soluble proteins of the endoplasmic reticulum. Trends in Biochemical Sciences 15: 483-486.

Quader, H. and Zachariadis, M. 2006. The morphology and dynamics of the ER. Plant Endoplasmic Reticulum, in Plant Cell Monographs (ed, Robinson D.G.) Springer, Heidelberg- Germany, pp.1-23

Reggiori, F., Wang, C. W., Nair, U., Shintani, T., Abeliovich, H. and Klionsky, D. J. 2004. Early stages of the secretory pathway, but not endosomes, are required for cvt vesicle and autophagosome assembly in *Saccharomyces cerevisiae*. Molecular Biology of the Cell 15: 2189-2204.

Reyes, F., Marchant, L., Norambuena, L., Nilo, R., Silva, H. and Orellana, A. 2006. AtUTr1, a UDP-glucose/UDP-galactose transporter from *Arabidopsis thaliana*, is located in the endoplasmic reticulum and up-regulated by the unfolded protein response. Journal of Biological Chemistry 281: 9145-9151.

Rolland, F., Baena-Gonzalez, E. and Sheen, J. 2006. Sugar sensing and signaling in plants: Conserved and novel mechanisms. Annual Review of Plant Biology 57: 675-709.

Rose, T. L., Bonneau, L., Der, C., Marty-Mazars, D. and Marty, F. 2006. Starvation-induced expression of autophagy-related genes in *Arabidopsis*. Biology of the Cell 98: 53-67.

Roudier, F., Schindelman, G., DeSalle, R. and Benfey, P. N. 2002. The COBRA family of putative GPI-anchored proteins in *Arabidopsis*. A new fellowship in expansion. Plant Physiology 130: 538-548.

Runions, J., Brach, T., Kuhner, S. and Hawes, C. 2006. Photoactivation of GFP reveals protein dynamics within the endoplasmic reticulum membrane. Journal of Experimental Botany 57: 43-50.

Rush, J. S. and Waechter, C. J. 1995. Transmembrane movement of a water-soluble analog of mannosylphosphoryldolichol is mediated by an endoplasmic-reticulum protein. Journal of Cell Biology 130: 529-536.

Saito, C., Ueda, T., Abe, H., Wada, Y., Kuroiwa, T., Hisada, A., Furuya, M. and Nakano, A. 2002. A complex and mobile structure forms a distinct subregion within the continuous vacuolar membrane in young cotyledons of *Arabidopsis*. Plant Journal 29: 245-255.

Saito, K. 2004. Sulfur assimilatory metabolism. The long and smelling road. Plant Physiology 136: 2443-2450.

Sanderfoot, A.A. and Raikhel, N.V., 2002. The Secretory System of Arabidopsis, in The Arabidopsis Book, (eds. Somerville CR and Meyerowitz EM, American Society of Plant Biologists), Rockville, MD doi 10.1199/tab.0098

Semenza, J. C., Harwick, K. G., Dean, N. and Pelham, H. R. B. 1990. ERD2, a yeast gene required for the receptor-mediated retrieval of luminal ER proteins from the secretory pathway. Cell 61: 1349-1357.

Schenk, B., Fernandez, F. and Waechter, C. J. 2001. The ins(ide) and outs(ide) of dolichyl phosphate biosynthesis and recycling in the endoplasmic reticulum. Glycobiology 11: 61R-70R.

Schenk, B., Imbach, T., Frank, C. G., Grubenmann, C. E., Raymond, G. V., Hurvitz, H., Raas-Rotschild, A., Luder, A. S., Jaeken, J., Berger, E. G., Matthijs, G., Hennet, T. and Aebi, M. 2001. MPDU1 mutations underlie a novel human congenital disorder of glycosylation, designated type If. Journal of Clinical Investigation 108: 1687-1695.

Sparkes, I. A., Frigerio, L., Tolley, N. and Hawes, C. 2009. The plant endoplasmic reticulum: a cell-wide web. Biochemical Journal 423: 145-155.

Spiro, R. G. 2002. Protein glycosylation: nature, distribution, enzymatic formation, and disease implications of glycopeptide bonds. Glycobiology 12: 43R-56R.

Staehelin, L. A. 1997. The plant ER: A dynamic organelle composed of a large number of discrete functional domains. Plant Journal 11: 1151-1165.

Sticher, L. and Metraux, J. P. 2000. Inhibitors of N-linked glycosylation induce systemic acquired resistance in cucumber. Physiological and Molecular Plant Pathology 56: 245-252.

Strasser, R., Schoberer, J., Jin, C., Glossl, J., Mach, L. and Steinkellner, H. 2006. Molecular cloning and characterisation of *Arabidopsis thaliana* Golgi alpha- mannosidase II, a key enzyme in the formation of complex N-glycans in plants. Plant Journal 47: 827-827.

Sun-Wada, G. H., Wada, Y. and Futai, M. 2003. Lysosome and lysosome-related organelles responsible for specialized functions in higher organisms, with special emphasis on vacuolar-type proton ATPase. Cell Structure and Function 28: 455-463.

Sutter, J. U., Campanoni, P., Tyrrell, M. and Blatt, M. R. 2006. Selective mobility and sensitivity to SNAREs is exhibited by the *Arabidopsis* KAT1 K+ channel at the plasma membrane. Plant Cell 18: 935-954.

Swiezewska, E. and Danikiewicz, W. 2005. Polyisoprenoids: Structure, biosynthesis and function. Progress in Lipid Research 44: 235-258.

Takemoto, D., Jones, D. A. and Hardham, A. R. 2003. GFP-tagging of cell components reveals the dynamics of subcellular re-organization in response to infection of *Arabidopsis* by oomycete pathogens. Plant Journal 33: 775-792.

Travers, K. J., Patil, C. K., Wodicka, L., Lockhart, D. J., Weissman, J. S. and Walter, P. 2000. Functional and genomic analyses reveal an essential coordination between the unfolded protein response and ER-associated degradation. Cell 101: 249-258.

Tulsiani, D.R., Harris, T.M. and Touster, O. 1982. Swainsonine inhibits the biosynthesis of complex glycoproteins by inhibition of Golgi mannosidase II. Journal of Biological Chemistry 257: 7936-7939.

van Loon, L. C., Rep, M. and Pieterse, C. M. J. 2006. Significance of inducible defense-related proteins in infected plants. Annual Review of Phytopathology 44: 135-162.

Vitale, A. and Boston, R. S. 2008. Endoplasmic reticulum quality control and the unfolded protein response: Insights from plants. Traffic 9: 1581-1588.

Vitale, A. and Ceriotti, A. 2004. Protein quality control mechanisms and protein storage in the endoplasmic reticulum. A conflict of interests?. Plant Physiology 136: 3420-3426.

Vitale, A. and Denecke, J. 2006. The ER folding helpers: A connection between protein maturation, stress responses and plant development. Plant Endoplasmic Reticulum, in Plant Cell Monographs (ed, Robinson D.G.) Springer, Heidelberg- Germany, pp.45-74.

Wang, D., Weaver, N. D., Kesarwani, M. and Dong, X. N. 2005. Induction of protein secretory pathway is required for systemic acquired resistance. Science 308: 1036-1040.

Weiss, C. A., Huang, H. and Ma, H. 1993. Immunolocalisation of the G protein alpha-subunit encoded by GPA1 gene in *Arabidopsis*. Plant Cell 5: 1513-1528.

Wopereis, S., Lefeber, D. J., Morava, E. and Wevers, R. A. 2006. Mechanisms in protein O-glycan biosynthesis and clinical and molecular aspects of protein O-glycan biosynthesis defects: A review. Clinical Chemistry 52: 574-600.

Xiao-Dong, G. 2005. ERS1 encodes a functionalo homologue of the human lysosomal cystine transporter. FEBS Journal 272: 2497-2511.

Yorimitsu, T. and Klionsky, D. J. 2007. Endoplasmic reticulum stress - A new pathway to induce autophagy. Autophagy 3: 160-162.

Yu, S. M. 1999. Cellular and genetic responses of plants to sugar starvation. Plant Physiology 121: 687-693.

Zeng, Y. C. and Elbein, A. D. 1995. UDP-N-acetylglucosamine-1-phosphate transferase is amplified in tunicamycin-resistant soybean cells. European Journal of Biochemistry 233: 458-466.

Zhang, H., Ohyama, K., Boudet, J., Chen, Z., Yang, J., Zhang, M., Muranaka, T., Maurel, C., Zhu, J. K. and Gong, Z. 2008. Dolichol biosynthesis and its effects on the unfolded protein response and abiotic stress resistance in *Arabidopsis*. Plant Cell 20: 1879-1898.

Zipfel, C., Kunze, G., Chinchilla, D., Caniard, A., Jones, J. D. G., Boller, T. and Felix, G. 2006. Perception of the bacterial PAMP EF-Tu by the receptor EFR restricts *Agrobacterium*-mediated transformation. Cell 125: 749-760.